SIAM J. Applied Dynamical Systems
Vol. 19, No. 2, pp. 918–963

Intralayer Synchronization in Evolving Multiplex Hypernetworks: Analytical Approach*

Sarbendu Rakshit†, Bidesh K. Bera‡, Erik M. Bollt§, and Dibakar Ghosh†

Abstract. In this paper, we study intralayer synchronization of multiplex networks where nodes in each layer interact through diverse types of coupling functions associated with different time-varying network topologies, referred to as *multiplex hypernetworks*. Here, the intralayer connections are evolving with respect to time, and the interlayer connections are stagnant. In this context, an interesting and important problem is to analyze the stability of the intralayer synchronization in such temporal networks. We prove that if the dynamical multiplex hypernetwork for the time-average topology possesses intralayer synchronization, then each layer of the time-varying multiplex hypernetwork will also be synchronized for sufficiently fast switching. Then through master stability function formalism, we analytically derive necessary and sufficient stability conditions of intralayer synchronous states for such temporal architecture in terms of a time-average network. In this regard, we are able to decouple the transverse error component of the intralayer synchronization states for some special cases. Also, we extend our study for nonlinear intralayer coupling functions as well as multilayer hypernetwork architectures. Finally, the theoretical findings are verified numerically by taking the network of paradigmatic chaotic Rössler oscillators.

Key words. time-varying network, hypernetwork, multilayer network, synchronization, master stability function approach

AMS subject classifications. 37A60, 93D05, 93D20, 37D45, 37N20

DOI. 10.1137/18M1224441

1. Introduction.

In recent years, the research on complex networks has become an immensely active area with the emergence of scientific application over numerous disciplines [11, 3]. Single complex network architecture can capture the diverse class of subnetworks in which each subnetwork effects the other networks, and such network structures are called *multilayer networks*. The intralayer coupling mechanism for each layer may differ from the other layers and also from layer-layer interactions. When each layer has the same number of

*Received by the editors November 2, 2018; accepted for publication (in revised form) by I. Belykh February 5, 2020; published electronically April 23, 2020.
https://doi.org/10.1137/18M1224441
Funding: The third author's research was supported by the Army Research Office (USARO) (N68164-EG), the Office of Naval Research (ONR) (N00014-15-1-2093), and the Defense Advanced Research Projects Agency (DARPA). The fourth author's research was supported by SERB-DST (Department of Science and Technology), Government of India (project EMR/2016/001039).

†Physics and Applied Mathematics Unit, Indian Statistical Institute, Kolkata, West Bengal, 700108, India (sarbendu.math@gmail.com, diba.ghosh@gmail.com).
‡Department of Mathematics, Indian Institute of Technology Ropar, Punjab - 140001, India, and Physics and Applied Mathematics Unit, Indian Statistical Institute, Kolkata, West Bengal, 700108, India (bideshbera18@gmail.com).
§Department of Mathematics, Department of Electrical and Computer Engineering, and Department of Physics, Clarkson University, Potsdam, NY 13699 (ebollt@clarkson.edu).

nodes and interlayer connections have one-one correspondence, that is, connecting only the replica nodes of each layer, then the network structure is called a multiplex network. Recently, such networks [10, 29] have become a rapidly growing research topic, since it elegantly furnishes a representation of many realistic systems, such as social networks [54], mobility networks [14], neural networks [2], subway networks [16], air transportation networks [15], etc., that are appropriately described by this multiplex framework. At the same time, multiplex networks are also supported to describe the several spontaneous processes, such as spreading of epidemics [47, 21, 13, 46], diffusion processes [20], percolation [12, 8], evolutionary game dynamics [55], etc. Various type of interactions can be systematically organized into a different class of network structures. When a set of nodes interacts with the other classes of nodes within the same network through various types of interactions, such network architecture is called *hypernetworks* [50]. Such structural network formation gives us a framework to analyze the various complex phenomena, which include transportation networks [30], power grids and computer communication networks [12], social interaction networks [31], neuronal networks [4, 27], and coordinated motion of schools of fish [33, 1].

The study of synchronization in large-scale complex networks has become an extremely active area across numerous theoretical and applied scientific fields. Different types of synchronization phenomena [44, 42], such as interlayer synchronization [48], intralayer synchronization [17] in multiplex networks, and cluster synchronization [9] in multilayer networks, are studied. To analyze the stability of the synchronization state in static multilayer networks, a general method has recently been proposed in [5]. A few studies [50, 43, 26] have been performed on the hypernetwork (i.e., networks with multiple kinds of couplings between nodes of the same type) in the monolayer situation. Instead, the case of networks formed by nodes of different types (where all the nodes of the same type form a "group") has been studied in [51]. In both of the mentioned cases of different couplings types and different nodes types, a dimensionality reduction was obtained, which led to a master stability function (MSF) solution of the stability problem, similar to the original approach in [36]. With the help of this approach, Sorrentino [50] analytically and numerically investigated the stability of the global synchronization state in a static monolayer hypernetwork consisting of different types of network Laplacians. In the case of [26], the dimensionality reduction was obtained by using simultaneous block diagonalization of matrices. By this dimensional reduction, necessary and sufficient conditions for the stability of the synchronous solution can be easily obtained. However, all of these synchronization phenomena were usually studied in completely time-static networks, which means the underlying interaction topology is time-invariant. The time-varying features are ubiquitous in many natural and real-life networks [56, 32, 34, 49, 45], where the links between the nodes are created, destroyed, or rewired over various time-scales [25].

Reference [52] provides a new fast switching stability criterion, which gives sufficient conditions for a temporal network to behave in unison and thus contributes a new insight about the stability analysis of a time-varying network. Let there be a new description of connectivity, the time-average graph Laplacian; then its spectral property employed with master stability formalism accurately predicts synchronization. The connection graph stability method [6, 7] also analyzes the stability of synchronization for time-varying networks. This method is rooted explicitly in graph theory, based on the total length of all paths through edges on the network connection graph. In our previous studies [42, 43], we have assumed that for sufficiently

fast switching, the time-varying system exhibits a stable synchronous solution whenever it is stable in the corresponding time-average system. In those previous works, the analytical studies were restricted to only the simple scalar diffusive types of interaction functions, but the coexistence of the different types of coupling functions was not discussed.

The stability of synchronization was analyzed stochastically for a group of dynamic agents that communicate via a moving neighborhood network [41] by introducing the concept of a "long-time expected communication network." It was shown that if the long-time expected network supports synchronization, the stochastic network will also synchronize when the agents communicate sufficiently fast within the network. Porfiri, Stilwell, and Bollt [40] studied the synchronization in a stochastic time-varying network, and it could be possible even if the network is not always connected but the expected network is connected for sufficiently fast switching. Global synchronization was also studied in coupled chaotic systems with randomly intermittent coupling [39] using partial averaging techniques and stochastic Lyapunov stability theory for sufficiently small switching periods. The theoretical findings of the fast switching stability criterion are also experimentally verified in coupled Chua's circuits with master-slave configuration [38]. If the blinking system switches fast enough, then a solution of the blinking system closely follows the solution of the average system for a finite time interval. Afterward, they drift apart [22]. The explicit bounds of that time interval that relate the probability, the switching frequency, the precision, and the length of the time interval to each other can also be found. In a follow-up paper, the asymptotical properties of general blinking systems with identically distributed independent random switching variables were also studied [23]. The unexpected windows of synchronization for moderate switching frequencies were noticed in [28], in which synchronization in the switching network becomes stable even though it is unstable in the average network for fast switching. Later, the stability of the global synchronization for nonfast switching networks was studied in [37, 18].

Inspired by the above facts, we study the intralayer synchronization in time-varying multiplex hypernetworks. Here each link corresponding to the intralayer interaction function is allowed to switch stochastically with respect to time with a certain rewiring frequency, while the layer-layer connectivity is stagnant over time. Through the fast switching stability criterion, we first prove the stability of the intralayer synchronization for time-average multiplex hypernetworks, implying the stability of the corresponding time-varying network. Through the master stability function theory, we derive necessary and sufficient conditions for the intralayer synchronization state, and correspondingly we enunciate the validity of the time-average system. Moreover, the master stability equations can be decoupled if only one of the time-average Laplacian matrices commutes with all other matrices. We show that the spectrum of the time-average intralayer graph Laplacian precisely predicts the stability of the intralayer synchronization. We also extend the stability theory for intralayer synchronization for multilayer hypernetworks and also for nonlinear intralayer coupling functions. To verify our analytical findings, we use a paradigmatic chaotic system, namely the Rössler oscillator as the node dynamics in each layer, and we explore the parameter regions for intralayer synchronization.

2. Background materials.

In this section, we give some preliminaries that are essential for this work, especially on basic graph theory on hypernetworks, the master stability function

approach for a static network, and the notion of the fast switching stability criterion of a time-varying system.

We denote the set $\{k, k+1, \ldots, N\}$ by $\mathbf{N}_k$, where $k, N \in \mathbb{N}$. For a square matrix A, A^{tr} and A^* respectively denote the transpose and Hermitian of that matrix.

Here $\otimes$ denotes the matrix Kronecker product. A few standard properties of the Kronecker product for square matrices are utilized here, stated as follows [19]:

1. $(A \otimes B)(C \otimes D) = (AC) \otimes (BD)$,
2. $(A \otimes B)^{tr} = A^{tr} \otimes B^{tr}$,
3. $(A \otimes B)^{-1} = A^{-1} \otimes B^{-1}$.

Throughout our manuscript, $O_{p\times q}$ denotes $p \times q$ zero matrix, and I_p is the $p \times p$ identity matrix.

2.1. Graph theoretical characterization. Various types of interactions can be systematically organized into classes of network structures. Mathematically, a complex network is a pair $\mathscr{G} = (X, E)$, where X is the set of vertices and E denotes the set of edges connecting the vertices, using classical graph theory.

A multilayer network is a pair $\mathscr{M} = (\mathscr{G}, \mathscr{C})$, where $\mathscr{G} = \{\mathscr{G}_\beta = (X_\beta, E_\beta) : \beta \in \{1, 2, \ldots, L\}\}$ is a family of graphs each representing a layer and $\mathscr{C} = \{E_{\beta_1\beta_1} \subseteq X_{\beta_1} \times X_{\beta_2} : \beta_1, \beta_2 \in \{1, 2, \ldots, L\}, \beta_1 \neq \beta_2\}$ is the set of interconnections between nodes of nonidentical layers $\mathscr{G}_{\beta_1}$ and $\mathscr{G}_{\beta_2}$. The elements of E_β are intralayer connections, and elements of $\mathscr{C}$ are called crossed layers, where all elements of $E_{\beta_1\beta_2}$ are the interlayer connections. A multiplex network is a special type of multilayer network, in which each layer has the same number of nodes and interlayer connections of a given node that connect only to its counterpart nodes in the rest of the layers. In other words, for a multiplex network $|X_1| = |X_2| = \cdots = |X_L| = N$ and $E_{\beta_1\beta_2} = \{(v_i^{[\beta_1]}, v_i^{[\beta_2]}), i \in \mathbf{N}_1 : v_i^{[\beta_1]} \in X_{\beta_1},\ v_i^{[\beta_2]} \in X_{\beta_2}\}$, $|\cdot|$ denotes the cardinality of a set.

Consider a family of networks $\mathscr{G}^{[\alpha]} = (X, E^{[\alpha]})$, $\alpha = 1, 2, \ldots, M$, where X is the fixed set of nodes for each α, and $E^{[\alpha]} \subseteq X \times X$ is a nonempty set of edges. If $E = \{E^{[\alpha]} : \alpha = 1, 2, \ldots, M\}$ is the family of links, then a hypernetwork is a pair $\mathscr{H} = (X, E)$. Here each $E^{[\alpha]}$ corresponds to the various modes of interaction. We call each of these a *tier*.

Definition 2.1. *A multilayer hypernetwork is an ordered pair $\mathscr{M}_\mathscr{H} = (\mathscr{G}, \mathscr{C})$, where $\mathscr{G} = \{\mathscr{G}_\beta = (X_\beta, E_\beta) : \beta \in \{1, 2, \ldots, L\}\}$ are the family of graphs, each representing a layer, in which $E_\beta = \{E_\beta^{[\alpha]} : \alpha \in \{1, 2, \ldots, M\}\}$ are the family of hyperlinks for each tier α. $\mathscr{C} = \{E_{\beta_1\beta_2} \subseteq X_{\beta_1} \times X_{\beta_2} : \beta_1, \beta_2 \in \{1, 2, \ldots, L\},\ \beta_1 \neq \beta_2\}$ is the set of interlayer connections between nodes of nonidentical layers $\mathscr{G}_{\beta_1}$ and $\mathscr{G}_{\beta_2}$.*

A complex network $\mathscr{G} = (X, E)$ is described as time-varying if $\mathscr{G} = \mathscr{G}(t)$ depends explicitly on time t, i.e., both $X = X(t)$ and $E = E(t)$ are functions of time. This includes the case in which the switching between the edges $E(t)$ varies as the graph evolves, where the set of nodes, X, is time-invariant. The time-varying networks are therefore characterized by the adjacency matrices that undergo such abrupt changes. Such a time-varying network $\mathscr{G}(t) = (X, E(t))$ will be described as jointly connected if the union of its frozen time networks $(X, \cup_t E(t))$ constitutes a connected graph. For complete synchronization to occur, the underlying temporal network should be jointly connected.

Our underlying network is a multiplex temporal hypernetwork, where each tier $E_\beta^{[\alpha]}(t)$ of

the network is a function of time, but the interlayer connection $\mathscr{C}$ is time-invariant.

Definition 2.2. *The time-stamped multilayer hypernetwork $\mathscr{M}_{\mathscr{H}}(t)$ is jointly connected if the union of its frozen-time projected network $\left(\cup_{\beta=1}^{L} X_\beta\ ,\ \cup_t \cup_{\alpha=1}^{M} \cup_{\beta=1}^{L} E_\beta^{[\alpha]}(t) \cup \mathscr{C}\right)$ constitutes a connected graph.*

To achieve complete intralayer synchronization, it should be jointly connected. In a frozen time, any tier $\left(X, E^{[\alpha]}\right)$ may have one or more disconnected components, but the frozen-time projected network should be connected.

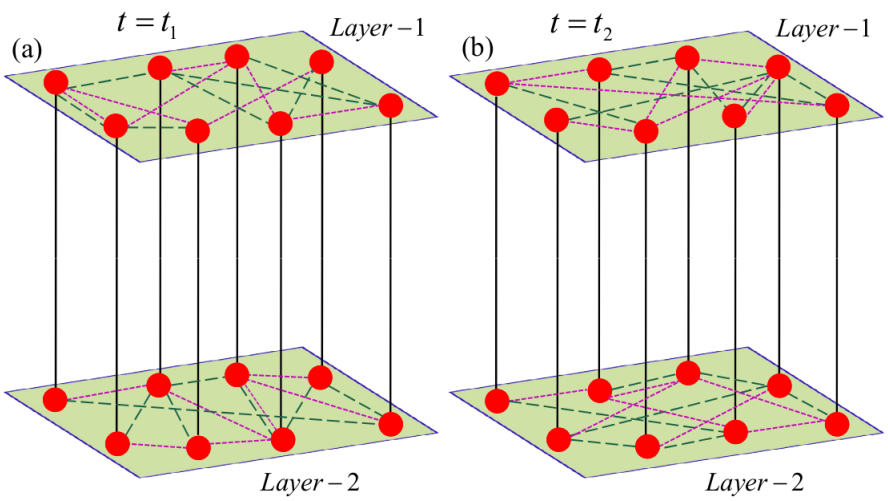

Figure 1. *Schematic of time-varying interactions in a hypernetwork with a multiplex formation at two different time instants:* (a) t_1 *and* (b) t_2. *Each node is represented by a red solid circle. The green dashed and magenta dotted lines denote the different types of interactions of the hypernetwork, while the interlayer connections between the layer are denoted by solid black lines.*

The schematic diagram (Figure 1) represents the time-varying interaction in a hypernetwork with the multiplex structure of two layers consisting of $N = 8$ nodes and $M = 2$ interaction types in each layer. Two different types of interacting tiers are shown for two particular instances of times $t = t_1$ and $t = t_2$ in Figures 1(a) and 1(b), respectively. Here the links of one tier are denoted by the green dashed lines and the other one by magenta dotted lines, whereas the interlayer connections between the layers are represented by black solid lines.

2.2. Review of master stability function approach. From the dynamical system's perspective, an important question arises on when a synchronization state of a network of coupled oscillators is stable, regarding the coupling strength. The MSF approach [36] analyzes the stability of the synchronization state of primarily identically coupled oscillators. Also, the stability condition for synchronization using the MSF approach in the coupled nearly identical systems has been extended [53]. This approach assumes that all the coupled oscillators are identical and the synchronization manifold is invariant, to guarantee the existence of a synchronous solution. Here the coupling function for each link is same and should vanish after achieving the synchronization, to make the specific stability diagram.

Consider a network consisting of N identical oscillators, where $\mathbf{x}_i$ is the d-dimensional state vector of the ith node, with its autonomous evolution $\dot{\mathbf{x}}_i = F(\mathbf{x}_i)$. We assume that the dynamics of the entire network can be written as

$$\dot{\mathbf{x}}_i = F(\mathbf{x}_i) - \epsilon \sum_{j=1}^{N} \mathscr{L}_{ij} B \mathbf{x}_j, \tag{2.1}$$

where ϵ is the coupling strength, $B \in \mathbb{R}^{d\times d}$ determines through which variables the N oscillators are coupled, and $\mathscr{L}$ is the network Laplacian.

When complete synchronization occurs, all the oscillators evolve synchronously with $\mathbf{x}_i = \mathbf{x}_0$. Perturbation to the ith oscillator from its synchronization manifold is by $\delta\mathbf{x}_i$. Letting $\delta\mathbf{x} = [\delta\mathbf{x}_1^{tr}, \delta\mathbf{x}_2^{tr}, \ldots, \delta\mathbf{x}_N^{tr}]^{tr}$, the variational equation of (2.1) near its synchronization manifold $\mathbf{x}_0(t)$ can be written as

$$\delta\dot{\mathbf{x}} = \big[I_N \otimes JF(\mathbf{x}_0) - \epsilon\, \mathscr{L} \otimes B\big]\delta\mathbf{x}. \tag{2.2}$$

The synchronous state is said to be locally stable if for any small perturbation $\delta\mathbf{x}_i$ each oscillator asymptotically converges to the synchronization manifold, i.e., $\mathbf{x}_i \to \mathbf{x}_0$ as $t \to \infty$, which implies that $\delta\mathbf{x}_i \to 0$ as $t \to \infty$ for $i \in \mathbf{N}_1$. In other words, the trivial equilibrium point of (2.2) is asymptotically stable. However, (2.2) contains information regarding the parallel component of the synchronization error vector, as well as the transverse components, while the synchronization solution will be asymptotically stable only if the latter components are damp-out, and conversely. Therefore, to analyze the stability of the synchronous solution, we should concentrate on the stability of the variations $\delta\mathbf{x}_i$ which are transverse to the synchronization manifold. So we have to separate out the parallel component from (2.2).

The Laplacian matrix $\mathscr{L}$ is a real valued square matrix; furthermore, for the bidirectional coupling, it is symmetric. As we know, every square matrix is unitarily triangularizable by its basis of eigenvectors. So there exists a matrix $P \in M_N(\mathbb{C})$ such that $U = P^{-1}\mathscr{L}P$ is a triangular matrix, where the columns of P are the orthonormal eigenvectors of $\mathscr{L}$ and $P^*P = PP^* = I_N$. The principal diagonal elements $\{\gamma_1, \gamma_2, \ldots, \gamma_N\}$ of U are the eigenvalues of $\mathscr{L}$. In the context of synchronization, it is assumed that the underlying network is connected as a minimal condition of synchronizability. Hence, exactly one eigenvalue of $\mathscr{L}$ is zero (say, $\gamma_1 = 0$) and the other eigenvalues $\gamma_i \in \mathbb{C}$ for all $i \in \mathbf{N}_2$.

Now consider the Schur transformation

$$\xi(t) = (P \otimes I_d)^{-1}\delta\mathbf{x}(t). \tag{2.3}$$

Applying (2.2), we have

$$\dot{\xi}(t) = \big[I_N \otimes JF(\mathbf{x}_0) - \epsilon\, U \otimes B)\big]\xi(t). \tag{2.4}$$

For the block diagonal structure of $I_N \otimes JF(\mathbf{x}_0)$ and the block triangular form of $U \otimes B$, the stability of (2.4) is equivalent to the stability of the following N uncoupled systems:

$$\dot{\xi}_i(t) = \big[JF(\mathbf{x}_0) - \epsilon\gamma_i B)\big]\xi_i(t), \quad i \in \mathbf{N}_1. \tag{2.5}$$

For $i = 1$, the variational equation becomes $\dot{\xi}_1(t) = JF(\mathbf{x}_0)\ \xi_1(t)$. But it is the linearized equation of the synchronization dynamics $\dot{\mathbf{x}}_0 = F(\mathbf{x}_0)$. Thus it evolves along the parallel to the synchronization solution, which we want to eliminate. For $i \in \mathbf{N}_2$, the variational equation (2.5) evolves transversally to the synchronization manifold. This dimensionality reduction allows us to easily calculate the Lyapunov exponents of the decoupled transverse error systems for the stability of the synchronization state.

The synchronization state will be stable if all the eigenmodes are stable for the given coupling strength. Then the maximum Lyapunov exponent Λ_{max} of the transverse variational equations reveals the stability of the synchronization state. If $\Lambda_{max}(\epsilon) > 0$ for some coupling strength ϵ, then the system (2.5) diverges, which indicates that the system (2.4) is asynchronous. By increasing ϵ, if Λ_{max} becomes negative, then we will get stable synchronization. Now we can associate a function $\Lambda_{max}(\epsilon) : \mathbb{R} \to \mathbb{R}$ with transverse eigendirections (2.5) as a function of the coupling strength ϵ, which returns the maximum Lyapunov exponent among all transverse directions. That is why this stability analysis was coined as the *master stability function approach* [36]. Hence, by the MSF approach, the coupling strengths for which the dynamical network evolves synchronously can be computed for a *static network*.

2.3. Review of the fast switching stability criterion. For a temporal network, the underlying Laplacian matrix changes with respect to time. Therefore, its eigenvalues and corresponding eigenvectors are functions of time. So the span of the basis of eigenvectors changes whenever the Laplacian matrix changes. However, to eliminate the parallel error component from the entire error dynamics, we should project the error components to a unique space. So the Schur transformation (2.3) and the MSF cannot be applied directly in the case of a time-varying network. To compromise with this difficulty, Stilwell, Bollt, and Roberson [52] introduced the fast switching stability criterion for time-varying networks. To get an overview of the stability of temporal graphs, we briefly review some of these details.

Fast switching indicates that the time-scale of the network evolution is faster than the time-scale of the coupled oscillators. The stability analysis of this paper is based on the fast switching stability technique. It provides new insights about the stability of dynamical systems when the underlying network is time-varying. Before describing this technique, we need the following preliminary lemma, which was proved in [52].

Lemma 2.3. *If there exists a time-average matrix $\bar{E}$ of the matrix valued function $E(t)$ such that*

$$\frac{1}{T}\int_t^{t+T} E(\tau)\ d\tau = \bar{E} \qquad \forall\ \ t \in \mathbb{R}^+ \ \ \textit{and for some constant } T,$$

then for sufficiently fast switching, the system

$$\dot{\mathbf{z}}(t) = \big[A(t) + E(t)\big]\ \mathbf{z}(t), \quad \mathbf{z}(t_0) = \mathbf{z}_0,\ t \geq t_0, \tag{2.6}$$

will be uniformly asymptotically stable whenever the time-average system

$$\dot{\mathbf{x}}(t) = \big[A(t) + \bar{E}\big]\ \mathbf{x}(t), \quad \mathbf{x}(t_0) = \mathbf{x}_0,\ t \geq t_0, \tag{2.7}$$

is also uniformly asymptotically stable.

Here $\mathbf{z}_0$ and $\mathbf{x}_0$ are two independent different initial conditions from the basin of attraction of the asymptotically stable state of systems (2.6) and (2.7), respectively. However, this lemma works for any constant time t, but for sufficiently large time T, it depends on $A(t)$ and how fast $E(t)$ is switching. The stability of the frozen time system does not guarantee the stability of the switched system, but this lemma shows that the switched time-varying system can be asymptotically stable if for sufficiently fast switching, the time-average system is asymptotically stable.

Now consider a temporal network of N identical coupled oscillators

$$\dot{\mathbf{x}}_i(t) = F(\mathbf{x}_i(t)) - \epsilon \sum_{j=1}^{N} \mathscr{L}_{ij}(t)\ B\ \mathbf{x}_j(t), \tag{2.8}$$

where $i \in \mathbf{N}_1$ and $\mathscr{L}(t)$ is the time-varying graph Laplacian.

For sufficiently fast switching, the time-average Laplacian matrix $\bar{\mathscr{L}}$ satisfies

$$\bar{\mathscr{L}} = \frac{1}{T}\int_t^{t+T} \mathscr{L}(\tau)\ d\tau$$

for some constant T. The matrix $\bar{\mathscr{L}}$ has the same inherent zero-row sum property from the parent Laplacian $\mathscr{L}(t)$. But $\bar{\mathscr{L}}$ may not necessarily describe any particular network; rather it is just the term by term time-average of the time-varying graph Laplacian $\mathscr{L}(t)$.

The real square matrix $\bar{\mathscr{L}}$ can be unitarily triangularizable. Then we can construct a unitary matrix P with each column representing the orthonormal eigenvectors of $\bar{\mathscr{L}}$, such that

$$P^{-1}\bar{\mathscr{L}}P = \bar{U} = \begin{bmatrix} 0 & \bar{U}_1 \\ O_{N-1\times 1} & \bar{U}_2 \end{bmatrix} \text{ is the Schur transformation of } \bar{\mathscr{L}}.$$

Here $\bar{U}_2 \in M_{N-1}(\mathbb{C})$ is an upper triangular matrix with principal diagonal elements as $N-1$ eigenvalues of $\bar{\mathscr{L}}$ excluding 0. The equation of motion of the coupled system incorporating the above average Laplacian will be obtained from (2.8) just by replacing $\mathscr{L}(t)$ by $\bar{\mathscr{L}}$. Considering the Schur transformation and using the unitary matrix P, the equation of the error system transverse to the synchronization manifold can be written as

$$\dot{\eta}(t) = \left[I_{N-1} \otimes F(\mathbf{x_0}(t)) - \epsilon \bar{U}_2 \otimes B\right]\ \eta(t). \tag{2.9}$$

By considering the same Schur transformation applied to (2.8), the equation of motion of the transverse error system becomes

$$\dot{\xi}(t) = \left[I_{N-1} \otimes F(\mathbf{x_0}(t)) - \epsilon U_2(t) \otimes B\right]\ \xi(t), \tag{2.10}$$

$$\text{where } P^{-1}\mathscr{L}(t)P = \begin{bmatrix} 0 & U_1(t) \\ O_{N-1\times 1} & U_2(t) \end{bmatrix} \text{ is the Schur transformation of } \mathscr{L}(t).$$

Now it is easy to produce

$$\bar{U}_1 = \frac{1}{T}\int_t^{t+T} U_1(\tau)\ d\tau.$$

Thus, by applying Lemma 2.3, we can conclude that if the time-average system has an asymptotically stable synchronization manifold, then the time-varying network also possesses an asymptotically stale synchronous solution for sufficiently fast switching. This fast switching stability criterion will be used to assess the local stability of the intralayer synchronization state.

3. Mathematical model. We now consider a coupled multiplex dynamical network, where different types of interactions are simultaneously present in each layer. With this network architecture, here for the first time, we rigorously analyze the stability of the intralayer synchronization state. In each layer, individual dynamical systems are coupled through more than one distinct connection, each of which corresponds to different types of interactions. We start by considering two layers, each composed of N nodes of d-dimensional identical dynamical systems. In each layer, N nodes are interacting through M different tiers of connections, which represent different kinds of couplings among themselves. The states of the layers are represented by the vectors $\mathbf{x} = \{\mathbf{x}_1, \mathbf{x}_2, \ldots, \mathbf{x}_N\}$ and $\mathbf{y} = \{\mathbf{y}_1, \mathbf{y}_2, \ldots, \mathbf{y}_N\}$ with $\mathbf{x}_i, \mathbf{y}_i \in \mathbb{R}^d$. Then the mathematical form of the general time-varying multiplex hypernetwork can be represented as

$$\begin{aligned}\dot{\mathbf{x}}_i &= F_1(\mathbf{x}_i) - \sum_{\alpha=1}^{M} \epsilon_\alpha \sum_{j=1}^{N} \mathscr{L}_{ij}^{[1,\alpha]}(t) G_\alpha^{[1]}(\mathbf{x}_j) + \lambda H_1(\mathbf{x}_i, \mathbf{y}_i),\\ \dot{\mathbf{y}}_i &= F_2(\mathbf{y}_i) - \sum_{\alpha=1}^{M} \epsilon_\alpha \sum_{j=1}^{N} \mathscr{L}_{ij}^{[2,\alpha]}(t) G_\alpha^{[2]}(\mathbf{y}_j) + \lambda H_2(\mathbf{y}_i, \mathbf{x}_i),\end{aligned} \tag{3.1}$$

where $i \in \mathbf{N}_1$. Here $F_{1,2} : \mathbb{R}^d \to \mathbb{R}^d$ and $H_{1,2} : \mathbb{R}^d \times \mathbb{R}^d \to \mathbb{R}^d$ are the continuously differentiable functions which respectively represent the autonomous evolution of the uncoupled oscillator and the output vectorial function between the layers. The individual dynamics within the same layer are identical but are different for nodes in different layers. Here $H_l(\mathbf{x}, \mathbf{y})$ is different from $H_l(\mathbf{y}, \mathbf{x})$ for $l = 1, 2$. $G_\alpha^{[l]} : \mathbb{R}^d \to \mathbb{R}^d$ is the vector field of the output vectorial function within the layers for tier α in layer-l. It is clear that the intralayer coupling functions corresponding to tier α differ for the two different layers. ϵ_α is the intralayer coupling strength for tier α, which determines how the information is distributed between nodes through different coupling configurations. The parameter λ, interlayer coupling strength, controls the interaction between the two layers.

The time-varying intralayer network configuration corresponding to the graph $\big(X_l, E_l^{[\alpha]}(t)\big)$ is encoded by the $N \times N$ adjacency matrix $\mathscr{A}^{[l,\alpha]}(t)$ which describes the interconnections between individual oscillators for tier α in the lth layer. Here $\mathscr{A}_{ij}^{[l,\alpha]}(t) = 1$ if $(v_i, v_j) \in E_l^{[\alpha]}(t)$, i.e., the ith node and the jth node of the layer-l are connected in tier α at time t and zero otherwise. $\mathscr{L}^{[l,\alpha]}(t)$ is the corresponding zero-row sum graph Laplacian, obtained from the adjacent matrices $\mathscr{A}^{[l,\alpha]}(t)$. The diagonal element $\mathscr{L}_{ii}^{[l,\alpha]}(t)$ is the sum of the nondiagonal elements in the ith row of $\mathscr{A}^{[l,\alpha]}(t)$, and the off-diagonal elements are the negatives of the corresponding elements in $\mathscr{A}^{[l,\alpha]}(t)$, i.e., $\mathscr{L}_{ij}^{[l,\alpha]}(t) = -\mathscr{A}_{ij}^{[l,\alpha]}(t)$ if $i \neq j$ and $\mathscr{L}_{ii}^{[l,\alpha]}(t) = \sum_{j=1}^{N} \mathscr{A}_{ij}^{[l,\alpha]}(t)$.

Now the intralayer links of the network $\big(X_l, E_l^{[\alpha]}(t)\big)$ vary over time by rewiring the entire network stochastically and independently, with a rewiring frequency f. Particularly, at any

time t and integration time step dt, we rewire each tier in the two layers independently, by constructing a new network with probability fdt. Large f indicates very fast switching of links, implying that the networks change rapidly, whereas small f implies that the two layers are almost static, as the links have a very low probability of change. Each of these successively created networks will be structurally equivalent due to the choice of fixed parameter values throughout the procedure. We are assuming that the intralayer network topologies corresponding to tier α for both of the two layers are exactly identical. However, at a particular time instant, their adjacency matrices will not generally be equal due to the time-varying connectivity nature of the edges for each tier. On the other side, the interlayer connections are complete multiplex structured and static over time. We assert this as a sufficiently generalized model as a multiplex hypernetwork, which allows enough connectionism for intralayer synchronization, and also admit a complete rigorous analysis.

In this paper, our principal contribution is to show, for temporal (sufficiently fast) intralayer network topologies, that each layer can synchronize if in the time-average network, each layer possesses stable complete synchronization.

4. Main results. In complete intralayer synchronization, each individual layer converges on the same time evolution, which occurs when individual oscillator in each layer of a multiplex networks is appropriately coupled. At the intralayer synchronization state, let layer-1 evolve synchronously with $\mathbf{x}_i = \mathbf{x}_0$ and layer-2 with $\mathbf{y}_i = \mathbf{y}_0$ for all $i \in \mathbf{N}_1$. The dynamics of the synchronization solution $\big(\mathbf{x}_0(t), \mathbf{y}_0(t)\big)$ can be written as

$$\begin{aligned} \dot{\mathbf{x}}_0 &= F_1(\mathbf{x}_0) + \lambda H_1(\mathbf{x}_0, \mathbf{y}_0), \\ \dot{\mathbf{y}}_0 &= F_2(\mathbf{y}_0) + \lambda H_2(\mathbf{y}_0, \mathbf{x}_0). \end{aligned} \tag{4.1}$$

Definition 4.1. *The multiplex network* (3.1) *is said to achieve the complete intralayer synchronization state if the two solutions* $\mathbf{x}_0(t), \mathbf{y}_0(t) \in \mathbb{R}^d$ *satisfy the equation of motion* (4.1) *such that for all* $i \in \mathbf{N}_1$,

$$\|\mathbf{x}_i(t) - \mathbf{x}_0(t)\| \to 0 \quad \textit{and} \quad \|\mathbf{y}_i(t) - \mathbf{y}_0(t)\| \to 0 \quad \textit{as} \quad t \to \infty.$$

Consequently, the intralayer synchronization manifold can be defined as

$$\mathcal{S} = \big\{(\mathbf{x}_0(t), \mathbf{y}_0(t)) \subset \mathbb{R}^{2d} \ : \ \mathbf{x}_i(t) = \mathbf{x}_0(t), \ \mathbf{y}_i(t) = \mathbf{y}_0(t), \quad i = 1, 2, \ldots, N \text{ and } t \in \mathbb{R}^+\big\}.$$

Its evolution equation is dominated by (4.1). The intralayer synchronization can be observed physically if this manifold is stable with respect to the perturbations in the transverse subspace. Now we delve into the stability of $\mathcal{S}$ for the temporal multiplex hypernetwork (3.1).

Perturb the ith node in layer-1 from its synchronization manifold $\mathbf{x}_0$ with an amount $\delta\mathbf{x}_i(t)$ and the ith node in the layer-2 with an amount $\delta\mathbf{y}_i(t)$. So the current state of the ith node in each layer is $\mathbf{x}_i(t) = \mathbf{x}_0(t) + \delta\mathbf{x}_i(t)$, $\mathbf{y}_i(t) = \mathbf{y}_0(t) + \delta\mathbf{y}_i(t)$ for $i \in \mathbf{N}_1$. Linearizing each oscillator of (3.1) about the synchronous trajectory $(\mathbf{x}_0, \mathbf{y}_0)$, the dynamics of the error system

in vectorial form yield

$$
\begin{aligned}
\delta\dot{\mathbf{x}} &= I_N \otimes JF_1(\mathbf{x}_0)\delta\mathbf{x} - \sum_{\alpha=1}^{M} \epsilon_\alpha \mathscr{L}^{[1,\alpha]}(t) \otimes JG_\alpha^{[1]}(\mathbf{x}_0)\delta\mathbf{x} \\
&\quad + \lambda\Big[I_N \otimes JH_1(\mathbf{x}_0,\mathbf{y}_0)\delta\mathbf{x} + I_N \otimes DH_1(\mathbf{x}_0,\mathbf{y}_0)\delta\mathbf{y}\Big], \\
\delta\dot{\mathbf{y}} &= I_N \otimes JF_2(\mathbf{y}_0)\delta\mathbf{y} - \sum_{\alpha=1}^{M} \epsilon_\alpha \mathscr{L}^{[2,\alpha]}(t) \otimes JG_\alpha^{[2]}(\mathbf{y}_0)\delta\mathbf{y} \\
&\quad + \lambda\Big[I_N \otimes JH_2(\mathbf{y}_0,\mathbf{x}_0)\delta\mathbf{y} + I_N \otimes DH_2(\mathbf{y}_0,\mathbf{x}_0)\delta\mathbf{x}\Big],
\end{aligned} \tag{4.2}
$$

where $\delta\mathbf{x}(t) = \big[\delta\mathbf{x}_1(t)^{tr}, \delta\mathbf{x}_2(t)^{tr}, \ldots, \delta\mathbf{x}_N(t)^{tr}\big]^{tr}$ and $\delta\mathbf{y}(t) = \big[\delta\mathbf{y}_1(t)^{tr}, \delta\mathbf{y}_2(t)^{tr}, \ldots, \delta\mathbf{y}_N(t)^{tr}\big]^{tr}$. Here J and D are the Jacobian operators with respect to the first and second variables, respectively, i.e., $JH(\mathbf{x}_0,\mathbf{y}_0) = \frac{\partial H(\mathbf{x},\mathbf{y})}{\partial \mathbf{x}}|_{(\mathbf{x},\mathbf{y})=(\mathbf{x}_0,\mathbf{y}_0)}$ and $DH(\mathbf{x}_0,\mathbf{y}_0) = \frac{\partial H(\mathbf{x},\mathbf{y})}{\partial \mathbf{y}}|_{(\mathbf{x},\mathbf{y})=(\mathbf{x}_0,\mathbf{y}_0)}$.

Now consider that each time-varying intralayer network topology possesses a static time-average network for sufficiently fast rewiring. Since the network topologies of tier α in both of the layers are the same, their time-averaged Laplacian matrices will match. Then there exists a constant T such that

$$
\frac{1}{T}\int_t^{t+T} \mathscr{L}^{[l,\alpha]}(\tau)\, d\tau = \bar{\mathscr{L}}^{[\alpha]} \quad \text{for} \quad l = 1,2 \text{ and } \alpha = 1,2,\ldots,M.
$$

These time-average Laplacian matrices are the indicator of the intralayer synchronization state. All of them are zero-row sum real square matrices. Their spectrum will be used to analyze the stability of the error system (4.2). By assuming these average matrices are connected, exactly one eigenvalue $\gamma_1^{[\alpha]}$ is zero, and the other eigenvalues $\gamma_i^{[\alpha]} \in \mathbb{C}$, $i \in \mathbf{N}_2$. Also, $\bar{\mathscr{L}}^{[\alpha]}$ can be unitarily triangularized by $V^{[\alpha]}$, where $V^{[\alpha]}$ is a unitary matrix. Its ith column is the eigenvector of $\bar{\mathscr{L}}^{[\alpha]}$ corresponding to the eigenvalue $\gamma_i^{[\alpha]}$, and all columns form orthogonal bases of $\mathbb{C}^N$. Without loss of any generality, consider the first column of $V^{[\alpha]}$ to be $\big(\frac{1}{\sqrt{N}}, \frac{1}{\sqrt{N}}, \ldots, \frac{1}{\sqrt{N}}\big)^{tr}$ corresponding to the eigenvalue zero. Then there exists an upper triangular matrix $\bar{U}^{[\alpha]}$ over the field $\mathbb{C}$ such that $\bar{U}^{[\alpha]} = {V^{[\alpha]}}^{-1} \bar{\mathscr{L}}^{[\alpha]} V^{[\alpha]}$ with its principal diagonal elements being the eigenvalues of $\bar{\mathscr{L}}^{[\alpha]}$.

Theorem 4.2. *The time-varying hypernetwork with multiplex formation whose dynamics are described by (3.1) possesses intralayer synchronization whenever the corresponding time-average static multiplex hypernetwork*

$$
\begin{aligned}
\dot{\mathbf{w}}_i &= F_1(\mathbf{w}_i) - \sum_{\alpha=1}^{M} \epsilon_\alpha \sum_{j=1}^{N} \bar{\mathscr{L}}_{ij}^{[\alpha]} G_\alpha^{[1]}(\mathbf{w}_j) + \lambda H_1(\mathbf{w}_i,\mathbf{z}_i), \\
\dot{\mathbf{z}}_i &= F_2(\mathbf{z}_i) - \sum_{\alpha=1}^{M} \epsilon_\alpha \sum_{j=1}^{N} \bar{\mathscr{L}}_{ij}^{[\alpha]} G_\alpha^{[2]}(\mathbf{z}_j) + \lambda H_2(\mathbf{z}_i,\mathbf{w}_i)
\end{aligned} \tag{4.3}
$$

has an asymptotically stable intralayer synchronization manifold.

Proof. We first derive the equation of motion of the error system transverse to the intralayer synchronization manifold, for both the time-varying and the time-average systems (3.1) and (4.3), respectively.

Taking the time-average intralayer networks, (4.3) is the dynamics of the time-average multiplex hypernetwork, where $\mathbf{w}_i$ ($\mathbf{z}_i$) is the state variable of the ith node in layer-1 (layer-2). This time-average system seems to be a notion of average information propagation in a network. Now it is clear that the equation of motion of the intralayer synchronization manifold for the time-varying and time-averaged networks is the same. So, without loss of generality, we can assume that when intralayer synchronization occurs, layer-1 evolves synchronously with $\mathbf{w}_i = \mathbf{x}_0$ and layer-2 with $\mathbf{z}_i = \mathbf{y}_0$ for all $i \in \mathbf{N}_1$. If $\delta\mathbf{w}(t) = \left[\delta\mathbf{w}_1(t)^{tr}, \delta\mathbf{w}_2(t)^{tr}, \ldots, \delta\mathbf{w}_N(t)^{tr}\right]^{tr}$ and $\delta\mathbf{z}(t) = \left[\delta\mathbf{z}_1(t)^{tr}, \delta\mathbf{z}_2(t)^{tr}, \ldots, \delta\mathbf{z}_N(t)^{tr}\right]^{tr}$ are the corresponding perturbations for both of the layers, then the vectorial forms of the error dynamics for intralayer synchronization states of the time-averaged system (4.3) are as follows:

$$\begin{aligned}
\delta\dot{\mathbf{w}}(t) &= I_N \otimes JF_1(\mathbf{x}_0)\delta\mathbf{w} - \sum_{\alpha=1}^{M} \epsilon_\alpha \bar{\mathscr{L}}^{[\alpha]} \otimes JG_\alpha^{[1]}(\mathbf{x}_0)\delta\mathbf{w} \\
&\quad + \lambda\Big[I_N \otimes JH_1(\mathbf{x}_0, \mathbf{y}_0)\delta\mathbf{w} + I_N \otimes DH_1(\mathbf{x}_0, \mathbf{y}_0)\delta\mathbf{z}\Big], \\
\delta\dot{\mathbf{z}}(t) &= I_N \otimes JF_2(\mathbf{y}_0)\delta\mathbf{z} - \sum_{\alpha=1}^{M} \epsilon_\alpha \bar{\mathscr{L}}^{[\alpha]} \otimes JG_\alpha^{[2]}(\mathbf{y}_0)\delta\mathbf{z} \\
&\quad + \lambda\Big[I_N \otimes JH_2(\mathbf{y}_0, \mathbf{x}_0)\delta\mathbf{z} + I_N \otimes DH_2(\mathbf{y}_0, \mathbf{x}_0)\delta\mathbf{w}\Big].
\end{aligned} \tag{4.4}$$

The linearized set of (4.4) can be decomposed into two components: one evolves along the synchronization manifold, and the other transverses to it. If the latter components are asymptotically stable, then the set of oscillators (4.3) will exhibit the stable intralayer synchronization state [35]. To find the transverse error system, we spectrally decompose $\delta\mathbf{w}(t)$ and $\delta\mathbf{z}(t)$ of the above equation and project it onto the basis of eigenvector $V^{[1]}$ corresponding to the first tier. However, the choice of the matrix of eigenvectors is arbitrary, since all of them form M equivalent bases of $\mathbb{C}^N$.

Under this Schur transformation onto the space spanned by the basis of eigenvectors of $\bar{\mathscr{L}}^{[1]}$, let $\delta\mathbf{w}(t)$ and $\delta\mathbf{z}(t)$ transform to $\eta^{(\mathbf{w})}(t) = \left[\eta_1^{(\mathbf{w})^{tr}}(t), \eta_2^{(\mathbf{w})^{tr}}(t), \ldots, \eta_N^{(\mathbf{w})^{tr}}(t)\right]^{tr}$ and $\eta^{(\mathbf{z})}(t) = \left[\eta_1^{(\mathbf{z})^{tr}}(t), \eta_2^{(\mathbf{z})^{tr}}(t), \ldots, \eta_N^{(\mathbf{z})^{tr}}(t)\right]^{tr}$, respectively, where $\eta^{(\mathbf{w})} = \left(V^{[1]} \otimes I_d\right)^{-1}\delta\mathbf{w}$ and $\eta^{(\mathbf{z})} = \left(V^{[1]} \otimes I_d\right)^{-1}\delta\mathbf{z}$. Using this Schur transformation, the linearized equation (4.4) corresponding to the time-average network becomes

$$\begin{aligned}
\dot{\eta}^{(\mathbf{w})}(t) &= I_N \otimes JF_1(\mathbf{x}_0)\eta^{(\mathbf{w})} - \sum_{\alpha=1}^{M} \epsilon_\alpha \Big(V^{[1]^{-1}} \bar{\mathscr{L}}^{[\alpha]} V^{[1]}\Big) \otimes JG_\alpha^{[1]}(\mathbf{x}_0)\eta^{(\mathbf{w})} \\
&\quad + \lambda\Big[I_N \otimes JH_1(\mathbf{x}_0, \mathbf{y}_0)\eta^{(\mathbf{w})} + I_N \otimes DH_1(\mathbf{x}_0, \mathbf{y}_0)\eta^{(\mathbf{z})}\Big], \\
\dot{\eta}^{(\mathbf{z})}(t) &= I_N \otimes JF_2(\mathbf{y}_0)\eta^{(\mathbf{z})} - \sum_{\alpha=1}^{M} \epsilon_\alpha \Big(V^{[1]^{-1}} \bar{\mathscr{L}}^{[\alpha]} V^{[1]}\Big) \otimes JG_\alpha^{[2]}(\mathbf{y}_0)\eta^{(\mathbf{z})} \\
&\quad + \lambda\Big[I_N \otimes JH_2(\mathbf{y}_0, \mathbf{x}_0)\eta^{(\mathbf{z})} + I_N \otimes DH_2(\mathbf{y}_0, \mathbf{x}_0)\eta^{(\mathbf{w})}\Big].
\end{aligned} \tag{4.5}$$

Since $\bar{\mathscr{L}}^{[\alpha]}$ is unitarily triangularizable and ${V^{[\alpha]}}^{-1}\bar{\mathscr{L}}^{[\alpha]}V^{[\alpha]} = \bar{U}^{[\alpha]}$, therefore we have

$$ {V^{[1]}}^{-1}\bar{\mathscr{L}}^{[\alpha]}V^{[1]} = {V^{[1]}}^{-1}V^{[\alpha]}\ \bar{U}^{[\alpha]}\ {V^{[\alpha]}}^{-1}V^{[1]}. \tag{4.6} $$

Consider

$$ V^{[\alpha]} = \begin{bmatrix} \frac{1}{\sqrt{N}} & v_{12}^{[\alpha]} & v_{13}^{[\alpha]} & \dots & v_{1N}^{[\alpha]} \\ \frac{1}{\sqrt{N}} & v_{22}^{[\alpha]} & v_{23}^{[\alpha]} & \dots & v_{2N}^{[\alpha]} \\ \dots & \dots & \dots & \dots & \dots \\ \frac{1}{\sqrt{N}} & v_{N2}^{[\alpha]} & v_{N3}^{[\alpha]} & \dots & v_{NN}^{[\alpha]} \end{bmatrix}. $$

Now $V^{[\alpha]}$ is the unitary matrix of orthogonal eigenvectors of $\bar{\mathscr{L}}^{[\alpha]}$, so ${V^{[\alpha]}}^{-1} = {V^{[\alpha]}}^{*}$. Hence, we can write

$$ {V^{[1]}}^{-1}V^{[\alpha]} = \begin{bmatrix} 1 & 0 & 0 & \dots & 0 \\ 0 & v_{22}^{[1,\alpha]} & v_{23}^{[1,\alpha]} & \dots & v_{2N}^{[1,\alpha]} \\ \dots & \dots & \dots & \dots & \dots \\ 0 & v_{N2}^{[1,\alpha]} & v_{N3}^{[1,\alpha]} & \dots & v_{NN}^{[1,\alpha]} \end{bmatrix} \text{ and } {V^{[\alpha]}}^{-1}V^{[1]} = \begin{bmatrix} 1 & 0 & 0 & \dots & 0 \\ 0 & v_{22}^{[\alpha,1]} & v_{23}^{[\alpha,1]} & \dots & v_{2N}^{[\alpha,1]} \\ \dots & \dots & \dots & \dots & \dots \\ 0 & v_{N2}^{[\alpha,1]} & v_{N3}^{[\alpha,1]} & \dots & v_{NN}^{[\alpha,1]} \end{bmatrix}. $$

Making the above substitutions in (4.6), we get

$$ {V^{[1]}}^{-1}\bar{\mathscr{L}}^{[\alpha]}V^{[1]} = \begin{bmatrix} 0 & \bar{U}_1^{[\alpha]} \\ O_{N-1\times 1} & \bar{U}_2^{[\alpha]} \end{bmatrix}, \tag{4.7} $$

where $\bar{U}_2^{[\alpha]} \in \mathbb{C}^{N-1\times N-1}$ and $\bar{U}_1^{[\alpha]} \in \mathbb{C}^{1\times N-1}$.

The transform variables $\eta^{(\mathbf{w})}(t)$ and $\eta^{(\mathbf{z})}(t)$ yield the decomposition $\eta^{(\mathbf{w})} = \left[\eta_P^{(\mathbf{w})}, \eta_T^{(\mathbf{w})}\right]$ and $\eta^{(\mathbf{z})} = \left[\eta_P^{(\mathbf{z})}, \eta_T^{(\mathbf{z})}\right]$, where $\eta_P^{(\mathbf{w})}, \eta_P^{(\mathbf{z})} \in \mathbb{C}^d$ and $\eta_T^{(\mathbf{w})}, \eta_T^{(\mathbf{z})} \in \mathbb{C}^{d(N-1)}$. Making these decompositions in (4.5) and with the help of (4.7), we get

(4.8a)

$$ \dot{\eta}_P^{(\mathbf{w})} = JF_1(\mathbf{x}_0)\eta_P^{(\mathbf{w})} - \sum_{\alpha=1}^{M} \epsilon_\alpha \bar{U}_1^{[\alpha]} \otimes JG_\alpha^{[1]}(\mathbf{x}_0)\eta_T^{(\mathbf{w})} + \lambda\Big[JH_1(\mathbf{x}_0,\mathbf{y}_0)\eta_P^{(\mathbf{w})} + DH_1(\mathbf{x}_0,\mathbf{y}_0)\eta_P^{(\mathbf{z})}\Big], $$

(4.8b)

$$ \begin{aligned} \dot{\eta}_T^{(\mathbf{w})} = I_{N-1} \otimes JF_1(\mathbf{x}_0)\eta_T^{(\mathbf{w})} - \sum_{\alpha=1}^{M} \epsilon_\alpha \bar{U}_2^{[\alpha]} \otimes JG_\alpha^{[1]}(\mathbf{x}_0)\eta_T^{(\mathbf{w})} \\ + \lambda\Big[I_{N-1} \otimes JH_1(\mathbf{x}_0,\mathbf{y}_0)\eta_T^{(\mathbf{w})} + I_{N-1} \otimes DH_1(\mathbf{x}_0,\mathbf{y}_0)\eta_T^{(\mathbf{z})}\Big], \end{aligned} $$

(4.8c)

$$ \dot{\eta}_P^{(\mathbf{z})} = JF_2(\mathbf{y}_0)\eta_P^{(\mathbf{z})} - \sum_{\alpha=1}^{M} \epsilon_\alpha \bar{U}_1^{[\alpha]} \otimes JG_\alpha^{[2]}(\mathbf{y}_0)\eta_T^{(\mathbf{z})} + \lambda\Big[JH_2(\mathbf{y}_0,\mathbf{x}_0)\eta_P^{(\mathbf{z})} + DH_2(\mathbf{y}_0,\mathbf{x}_0)\eta_P^{(\mathbf{w})}\Big], $$

(4.8d)

$$ \begin{aligned} \dot{\eta}_T^{(\mathbf{z})} = I_{N-1} \otimes JF_2(\mathbf{y}_0)\eta_T^{(\mathbf{z})} - \sum_{\alpha=1}^{M} \epsilon_\alpha \bar{U}_2^{[\alpha]} \otimes JG_\alpha^{[2]}(\mathbf{y}_0)\eta_T^{(\mathbf{z})} \\ + \lambda\Big[I_{N-1} \otimes JH_2(\mathbf{y}_0,\mathbf{x}_0)\eta_T^{(\mathbf{z})} + I_{N-1} \otimes DH_2(\mathbf{y}_0,\mathbf{x}_0)\eta_T^{(\mathbf{w})}\Big]. \end{aligned} $$

Note that (4.8b, d) are independent of (4.8a, c). So the former subequations are the derive subsystems, while the latter two are the response subsystems. Here $\eta_P^{(\mathbf{w})}$ and $\eta_P^{(\mathbf{z})}$ correspond to the projected perturbations within the synchronous manifold, and $\eta_T^{(\mathbf{w})}$ and $\eta_T^{(\mathbf{z})}$ are the perturbations transverse to that manifold. Thus, the synchronization stability governed by (4.8b, d) do not depend on the parallel component. However, when transverse components become stabilized, (4.8a, c) become the linearized equations for the equation of motion of the synchronous solution (4.1). So, for the stable synchronous state, (4.8a, c) asymptotically behave as the linearized equation for the synchronized dynamics. So it evolves parallel to the synchronize manifold, and those are not topical in determining the stability of the concern solution, whereas (4.8b, d) are the transverse error dynamics.

Considering $\zeta_a(t) = \left[\eta_T^{(\mathbf{w})^{tr}} \ \eta_T^{(\mathbf{z})^{tr}}\right]^{tr} \in \mathbb{C}^{2(N-1)d}$, the dynamics of the transverse error system (4.8b, d) can be rewritten in terms of $\zeta_a(t)$ as

$$\dot{\zeta}_a(t) = \left[A(t) - \sum_{\alpha=1}^{M} \epsilon_\alpha \left(\bar{E}_1^{[\alpha]} \otimes JG_\alpha^{[1]}(\mathbf{x}_0) + \bar{E}_2^{[\alpha]} \otimes JG_\alpha^{[2]}(\mathbf{y}_0)\right)\right]\zeta_a(t), \tag{4.9}$$

where

$$A(t) = \begin{bmatrix} I_{N-1} \otimes JF_1(\mathbf{x}_0) + \lambda I_{N-1} \otimes JH_1(\mathbf{x}_0, \mathbf{y}_0) & \lambda I_{N-1} \otimes DH_1(\mathbf{x}_0, \mathbf{y}_0) \\ \lambda I_{N-1} \otimes DH_2(\mathbf{y}_0, \mathbf{x}_0) & I_{N-1} \otimes JF_2(\mathbf{y}_0) + \lambda I_{N-1} \otimes JH_2(\mathbf{y}_0, \mathbf{x}_0) \end{bmatrix},$$

$$\bar{E}_1^{[\alpha]} = \begin{bmatrix} \bar{U}_2^{[\alpha]} & O_{N-1\times N-1} \\ O_{N-1\times N-1} & O_{N-1\times N-1} \end{bmatrix} \text{ and } \bar{E}_2^{[\alpha]} = \begin{bmatrix} O_{N-1\times N-1} & O_{N-1\times N-1} \\ O_{N-1\times N-1} & \bar{U}_2^{[\alpha]} \end{bmatrix}.$$

We now envisage the same change of variables applied to the error dynamics (4.2) corresponding to the temporal network. Here $\mathscr{L}^{[l,\alpha]}(t)$ is the instantaneous Laplacian matrix of tier α in layer-l. So, at each time instant, they are zero-row sum real square matrices. If $\left\{0 = \gamma_1^{[l,\alpha]}(t), \gamma_2^{[l,\alpha]}(t), \ldots, \gamma_N^{[l,\alpha]}(t)\right\}$ is the set of instantaneous eigenvalues and $V^{[l,\alpha]}(t)$ is the corresponding unitary matrix of orthogonal eigenvectors, then there exists a complex upper triangular matrix $U^{[l,\alpha]}(t)$, such that $\mathscr{L}^{[l,\alpha]}(t) = V^{[l,\alpha]}(t)\ U^{[l,\alpha]}(t)\ V^{[l,\alpha]}(t)^{-1}$. This immediately implies

$$V^{[1]^{-1}}\mathscr{L}^{[l,\alpha]}(t)V^{[1]} = V^{[1]^{-1}}V^{[l,\alpha]}(t)\ U^{[l,\alpha]}(t)\ V^{[l,\alpha]}(t)^{-1}V^{[1]}. \tag{4.10}$$

At each time instant, the columns of $V^{[l,\alpha]}(t)$ form an equivalent orthogonal basis of $\mathbb{C}^N$. So if

$$V^{[l,\alpha]}(t) = \begin{bmatrix} \frac{1}{\sqrt{N}} & v_{12}^{[l,\alpha]}(t) & v_{13}^{[l,\alpha]}(t) & \ldots & v_{1N}^{[l,\alpha]}(t) \\ \frac{1}{\sqrt{N}} & v_{22}^{[l,\alpha]}(t) & v_{23}^{[l,\alpha]}(t) & \ldots & v_{2N}^{[l,\alpha]}(t) \\ \cdots & \cdots & \cdots & \cdots & \cdots \\ \frac{1}{\sqrt{N}} & v_{N2}^{[l,\alpha]}(t) & v_{N3}^{[l,\alpha]}(t) & \ldots & v_{NN}^{[l,\alpha]}(t) \end{bmatrix}, \quad \text{then}$$

$$V^{[1]^{-1}}V^{[l,\alpha]}(t) = \begin{bmatrix} 1 & 0 & 0 & \dots & 0 \\ 0 & v_{22}^{[l,\alpha]}(t) & v_{23}^{[l,\alpha]}(t) & \dots & v_{2N}^{[l,\alpha]}(t) \\ \dots & \dots & \dots & \dots & \dots \\ 0 & v_{N2}^{[l,\alpha]}(t) & v_{N3}^{[l,\alpha]}(t) & \dots & v_{NN}^{[l,\alpha]}(t) \end{bmatrix}$$

$$\text{and} \quad V^{[l,\alpha]}(t)^{-1}V^{[1]} = \begin{bmatrix} 1 & 0 & 0 & \dots & 0 \\ 0 & v_{22}^{[l,\alpha]}(t) & v_{23}^{[l,\alpha]}(t) & \dots & v_{2N}^{[l,\alpha]}(t) \\ \dots & \dots & \dots & \dots & \dots \\ 0 & v_{N2}^{[l,\alpha]}(t) & v_{N3}^{[l,\alpha]}(t) & \dots & v_{NN}^{[l,\alpha]}(t) \end{bmatrix}.$$

Using the above expressions, (4.10) yields

$$V^{[1]^{-1}}\mathscr{L}^{[l,\alpha]}(t)V^{[1]} = \begin{bmatrix} 0 & U_1^{[l,\alpha]}(t) \\ O_{N-1\times 1} & U_2^{[l,\alpha]}(t) \end{bmatrix}, \tag{4.11}$$

where $U_2^{[l,\alpha]}(t)$ is a complex matrix of order $N-1$ and $U_1^{[l,\alpha]}(t) \in \mathbb{C}^{1\times N-1}$.

Now the change of variables $\eta^{(\mathbf{x})} = \left(V^{[1]} \otimes I_d\right)^{-1}\delta\mathbf{x}$ and $\eta^{(\mathbf{y})} = \left(V^{[1]} \otimes I_d\right)^{-1}\delta\mathbf{y}$ yields the linearized equation (4.2) corresponding to the time-average network as

$$\begin{aligned} \dot{\eta}^{(\mathbf{x})}(t) &= I_N \otimes JF_1(\mathbf{x}_0)\eta^{(\mathbf{x})} - \sum_{\alpha=1}^{M}\epsilon_\alpha\left(V^{[1]^{-1}}\mathscr{L}^{[1,\alpha]}(t)V^{[1]}\right) \otimes JG_\alpha^{[1]}(\mathbf{x}_0)\eta^{(\mathbf{x})} \\ &\quad + \lambda\Big[I_N \otimes JH_1(\mathbf{x}_0,\mathbf{y}_0)\eta^{(\mathbf{x})} + I_N \otimes DH_1(\mathbf{x}_0,\mathbf{y}_0)\eta^{(\mathbf{y})}\Big], \\ \dot{\eta}^{(\mathbf{y})}(t) &= I_N \otimes JF_2(\mathbf{y}_0)\eta^{(\mathbf{y})} - \sum_{\alpha=1}^{M}\epsilon_\alpha\left(V^{[1]^{-1}}\mathscr{L}^{[2,\alpha]}(t)V^{[1]}\right) \otimes JG_\alpha^{[2]}(\mathbf{y}_0)\eta^{(\mathbf{y})} \\ &\quad + \lambda\Big[I_N \otimes JH_2(\mathbf{y}_0,\mathbf{x}_0)\eta^{(\mathbf{y})} + I_N \otimes DH_2(\mathbf{y}_0,\mathbf{x}_0)\eta^{(\mathbf{x})}\Big]. \end{aligned} \tag{4.12}$$

To analyze the dynamics of the error system transverse to the intralayer synchronization manifold, decompose the state variable as $\eta^{(\mathbf{x})}(t) = \left[\eta_P^{(\mathbf{x})}, \eta_T^{(\mathbf{x})}\right]$ and $\eta^{(\mathbf{y})}(t) = \left[\eta_P^{(\mathbf{y})}, \eta_T^{(\mathbf{y})}\right]$, where $\eta_P^{(\mathbf{x})}, \eta_P^{(\mathbf{y})} \in \mathbb{C}^d$ and $\eta_T^{(\mathbf{x})}, \eta_T^{(\mathbf{y})} \in \mathbb{C}^{d(N-1)}$. Then we get the dynamics of the transverse system as

$$\begin{aligned} \dot{\eta}_T^{(\mathbf{x})} &= I_{N-1} \otimes JF_1(\mathbf{x}_0)\eta_T^{(\mathbf{x})} - \sum_{\alpha=1}^{M}\epsilon_\alpha U_2^{[1,\alpha]}(t) \otimes JG_\alpha^{[1]}(\mathbf{x}_0)\eta_T^{(\mathbf{x})} \\ &\quad + \lambda\Big[I_{N-1} \otimes JH_1(\mathbf{x}_0,\mathbf{y}_0)\eta_T^{(\mathbf{x})} + I_{N-1} \otimes DH_1(\mathbf{x}_0,\mathbf{y}_0)\eta_T^{(\mathbf{y})}\Big], \\ \dot{\eta}_T^{(\mathbf{y})} &= I_{N-1} \otimes JF_2(\mathbf{y}_0)\eta_T^{(\mathbf{y})} - \sum_{\alpha=1}^{M}\epsilon_\alpha U_2^{[2,\alpha]}(t) \otimes JG_\alpha^{[2]}(\mathbf{y}_0)\eta_T^{(\mathbf{y})} \\ &\quad + \lambda\Big[I_{N-1} \otimes JH_2(\mathbf{y}_0,\mathbf{x}_0)\eta_T^{(\mathbf{y})} + I_{N-1} \otimes DH_2(\mathbf{y}_0,\mathbf{x}_0)\eta_T^{(\mathbf{x})}\Big]. \end{aligned} \tag{4.13}$$

Considering $\zeta_d(t) = \left[\eta_T^{(\mathbf{x})^{tr}} \ \eta_T^{(\mathbf{y})^{tr}}\right]^{tr} \in \mathbb{C}^{2(N-1)d}$, the dynamics of the transverse error system equation (4.13) can be rewritten in terms of $\zeta_d(t)$ as

$$\dot{\zeta}_d(t) = \left[A(t) - \sum_{\alpha=1}^{M} \epsilon_\alpha \Big(E_1^{[\alpha]}(t) \otimes JG_\alpha^{[1]}(\mathbf{x}_0) + E_2^{[\alpha]}(t) \otimes JG_\alpha^{[2]}(\mathbf{y}_0) \Big) \right] \zeta_d(t), \tag{4.14}$$

$$\text{where } A(t) = \begin{bmatrix} I_{N-1} \otimes \big(JF_1(\mathbf{x}_0) + \lambda JH_1(\mathbf{x}_0, \mathbf{y}_0)\big) & \lambda I_{N-1} \otimes DH_1(\mathbf{x}_0, \mathbf{y}_0) \\ \lambda I_{N-1} \otimes DH_1(\mathbf{y}_0, \mathbf{x}_0) & I_{N-1} \otimes \big(JF_1(\mathbf{y}_0) + \lambda JH_1(\mathbf{y}_0, \mathbf{x}_0)\big) \end{bmatrix}$$

$$\text{and } E_1^{[\alpha]}(t) = \begin{bmatrix} U_2^{[1,\alpha]}(t) & O_{N-1\times N-1} \\ O_{N-1\times N-1} & O_{N-1\times N-1} \end{bmatrix}, \quad E_2^{[\alpha]}(t) = \begin{bmatrix} O_{N-1\times N-1} & O_{N-1\times N-1} \\ O_{N-1\times N-1} & U_2^{[2,\alpha]}(t) \end{bmatrix}.$$

Now $\bar{\mathscr{L}}^{[\alpha]} = \frac{1}{T}\int_t^{t+T} \mathscr{L}^{[l,\alpha]}(\tau)\, d\tau$ yields

$$V^{[1]^{-1}} \bar{\mathscr{L}}^{[\alpha]} V^{[1]} = \frac{1}{T} \int_t^{t+T} V^{[1]^{-1}} \mathscr{L}^{[l,\alpha]}(\tau) V^{[1]}\, d\tau.$$

Using (4.7) and (4.11), the above equation becomes

$$\begin{bmatrix} 0 & \bar{U}_1^{[\alpha]} \\ O_{N-1\times 1} & \bar{U}_2^{[\alpha]} \end{bmatrix} = \frac{1}{T} \int_t^{t+T} \begin{bmatrix} 0 & U_1^{[l,\alpha]}(\tau) \\ O_{N-1\times 1} & U_2^{[l,\alpha]}(\tau) \end{bmatrix} d\tau. \tag{4.15}$$

From the above expression, we can write $\bar{U}_2^{[\alpha]} = \frac{1}{T}\int_t^{t+T} U_2^{[l,\alpha]}(\tau)\, d\tau$, which implies that $\int_t^{t+T} E_m^{[\alpha]}(\tau)\, d\tau = \bar{E}_m^{[\alpha]}$ for $m = 1, 2$.

Thus, by Lemma 2.3, we conclude that systems (4.2) and (4.4) stabilize together. Hence, the time-varying network (3.1) possesses intralayer synchronization whenever the corresponding time-average static network (4.3) has an asymptotically stable intralayer synchronization manifold. ∎

Here the time constant T is assumed to be sufficiently large, which depends on the individual node dynamics $F_1(\mathbf{x})$ and $F_2(\mathbf{y})$ of both of the layers, intralayer coupling functions $G_\alpha^{[1]}(\mathbf{x})$ and $G_\alpha^{[2]}(\mathbf{y})$, interlayer coupling functions $H_{1,2}(\mathbf{x}, \mathbf{y})$, and how fast the intralayer tiers in both of the layers are switching.

4.1. Local stability of the intralayer synchronization. Theorem 4.2 tells us that the stability of the intralayer synchronization for both the time-varying and the time-average systems is equivalent. In this subsection, our main emphasis is to identify the necessary and sufficient conditions for the intralayer synchronization state. For this, we reduce the linear stability problem in the form of the MSF approach. We can investigate the stability of our original system (3.1) in terms of the time-average system (4.3). Equation (4.9) is the transverse error dynamics of the intralayer synchronous state for the averaged system. The alternative form of the error dynamics is (4.8b, d), where all the terms are block diagonal except $\bar{U}^{[\alpha]} \otimes JG_\alpha^{[l]}(\mathbf{y}_0)$. However, this is generally a very high dimensional $2d(N-1)$ equation, and the calculation of all Lyapunov exponents is very expensive.

Due to the upper triangular form of ${V^{[1]}}^{-1}\bar{\mathscr{L}}^{[1]}V^{[1]}$, $\bar{U}_2^{[1]}$is also an upper triangular complex matrix. Then the transverse error dynamics 4.8(b, d) become

$$\begin{aligned}\dot{\eta}_{T_i}^{(\mathbf{w})} &= JF_1(\mathbf{x}_0)\eta_{T_i}^{(\mathbf{w})} - \epsilon_1\sum_{j=i}^{N-1}\bar{U}_{ij}^{[1]}JG_1^{[1]}(\mathbf{x}_0)\eta_{T_j}^{(\mathbf{w})} - \sum_{\alpha=2}^{M}\epsilon_\alpha\sum_{j=1}^{N-1}\bar{U}_{ij}^{[\alpha]}JG_\alpha^{[1]}(\mathbf{x}_0)\eta_{T_j}^{(\mathbf{w})}\\ &\quad+\lambda\Big[JH_1(\mathbf{x}_0,\mathbf{y}_0)\eta_{T_i}^{(\mathbf{w})} + DH_1(\mathbf{x}_0,\mathbf{y}_0)\eta_{T_i}^{(\mathbf{z})}\Big]\\ \text{and}\\ \dot{\eta}_{T_i}^{(\mathbf{z})} &= JF_2(\mathbf{y}_0)\eta_{T_i}^{(z)} - \epsilon_1\sum_{j=i}^{N-1}\bar{U}_{ij}^{[1]}JG_1^{[2]}(\mathbf{y}_0)\eta_{T_j}^{(\mathbf{z})} - \sum_{\alpha=2}^{M}\epsilon_\alpha\sum_{j=1}^{N-1}\bar{U}_{ij}^{[\alpha]}JG_\alpha^{[2]}(\mathbf{y}_0)\eta_{T_j}^{(\mathbf{z})}\\ &\quad+\lambda\Big[JH_2(\mathbf{y}_0,\mathbf{x}_0)\eta_{T_i}^{(\mathbf{z})} + DH_2(\mathbf{y}_0,\mathbf{x}_0)\eta_{T_i}^{(\mathbf{w})}\Big].\end{aligned} \tag{4.16}$$

This is therefore our required transverse master stability equation (MSE) of the intralayer synchronization manifold. In general, this transverse error system (4.16) cannot be further reduced to a low-dimensional form. Unfortunately, we are unable to reduce these $2d(N-1)$-dimensional transverse error dynamics for the general case. If the matrices $\bar{U}^{[\alpha]}$ were diagonal, then it could be decoupled to $N-1$ independent components, but in general, there is no guarantee of this property. Such reduction is possible only if the static time-average Laplacian matrix commutes with all other time-average Laplacians. For this case, we will now try to reduce the $\mathbb{C}^{2(N-1)d}$-dimensional transverse error dynamics to the low-dimensional system. The next corollary presents this analysis in detail.

Corollary 4.3. *If all the time-average Laplacians $\bar{\mathscr{L}}^{[\alpha]}$ are symmetric, and among them one commutes with all the other time-average Laplacians, then the dynamics of the projected error system can be decoupled as*

$$\begin{aligned}\dot{\eta}_{T_i}^{(\mathbf{w})} &= JF_1(\mathbf{x}_0)\eta_{T_i}^{(\mathbf{w})} - \sum_{\alpha=1}^{M}\epsilon_\alpha\gamma_i^{[\alpha]}JG_\alpha^{[1]}(\mathbf{x}_0)\eta_{T_i}^{(\mathbf{w})} + \lambda\Big[JH_1(\mathbf{x}_0,\mathbf{y}_0)\eta_{T_i}^{(\mathbf{w})} + DH_1(\mathbf{x}_0,\mathbf{y}_0)\eta_{T_i}^{(\mathbf{z})}\Big]\\ \text{and}\\ \dot{\eta}_{T_i}^{(\mathbf{z})} &= JF_2(\mathbf{y}_0)\eta_{T_i}^{(\mathbf{z})} - \sum_{\alpha=1}^{M}\epsilon_\alpha\gamma_i^{[\alpha]}JG_\alpha^{[2]}(\mathbf{y}_0)\eta_{T_i}^{(\mathbf{z})} + \lambda\Big[JH_2(\mathbf{y}_0,\mathbf{x}_0)\eta_{T_i}^{(\mathbf{z})} + DH_2(\mathbf{y}_0,\mathbf{x}_0)\eta_{T_i}^{(\mathbf{w})}\Big],\end{aligned} \tag{4.17}$$

where $i \in N_2$.

Proof of Corollary 4.3. See Appendix A. ∎

By this dimensionality reduction, the entire $2d(N-1)$-dimensional transverse error system is reduced to $2d$-dimensional $N-1$ linear systems.

Corollary 4.4. *Let the number of tiers in each layer of the multiplex hypernetwork be two, i.e., $M=2$. Among these two tiers, the eigenvalues of the Laplacian matrix of one tier are 0 with algebraic multiplicity 1 and $\bar{a}$ with algebraic multiplicity $N-1$. Then the transverse error dynamics can be decoupled as $N-1$ numbers of $2d$-dimensional systems.*

Proof of Corollary 4.4. See Appendix A. ∎

An interesting point about the above corollary is that we can obtain the low-dimensional reduction of the transverse error system, where the two matrices $\bar{\mathscr{L}}^{[1]}$ and $\bar{\mathscr{L}}^{[2]}$ do not necessarily commute.

Remark 4.5. Consider the case where all of the off-diagonal elements of the time-average Laplacian matrix $\bar{\mathscr{L}}^{[1]}$ are equal to $-p$ (say), and diagonal elements are such that it is zero-row sum, i.e., $(N-1)p$. Then the eigenvalues of $\bar{\mathscr{L}}^{[1]}$ are 0 with algebraic multiplicity 1 and Np with algebraic multiplicity $N-1$, and furthermore the matrix is diagonalizable. This type of time-average Laplacian matrix occurs if the network architecture of the tier-1 is Erdös–Rényi (ER) random with edge joining probability p.

According to Corollary 4.4, for this type of Laplacian matrix, other ones can be chosen arbitrarily to decouple the transverse error systems.

Remark 4.6. Again consider the case of a weighted network where the weight from node j to node i is only a function of the source node j, but not of the destination node i, in other words, $\bar{\mathscr{A}}_{ij}^{[1]} = \bar{a}_j$ for all $i, j \in N_1$. Its Laplacian matrix is therefore

$$\begin{aligned} \bar{\mathscr{L}}_{ij}^{[1]} &= -\bar{a}_j && \text{for } i \neq j, \\ &= \sum_{k=1}^{N} \bar{a}_k - \bar{a}_j && \text{for } i = j. \end{aligned} \tag{4.18}$$

$\bar{\mathscr{L}}^{[1]}$ has the property that it has one eigenvalue 0 with associated eigenvector $[1, 1, \ldots, 1]^{tr}$ and the remaining $N-1$ eigenvalues are all equal to $\sum_{k=1}^{N} \bar{a}_k$. Moreover, $\bar{\mathscr{L}}^{[1]}$ can be diagonalizable by its basis of eigenvectors. Again we note that for this type of time-average Laplacian matrix, other Laplacian matrices can be chosen arbitrarily. Still we can obtain the block diagonal transverse error system.

More precisely, for the synchronous state (4.1) to be stable, it is sufficient to check the stability of the 2d-dimensional $N-1$ decoupled transverse error dynamics (4.17), instead of the $2d(N-1)$-dimensional coupled transverse error system. Hence, the intralayer synchronization manifold will be locally asymptotically stable if the maximum Lyapunov exponent of the system (4.17) becomes negative. So, sufficiently, we need only to calculate the Lyapunov exponents only for these $2d$-dimensional $N-1$ uncoupled systems.

Now we can associate an MSF with (4.17) as $\Lambda_{max}(\epsilon_1, \epsilon_2, \ldots, \epsilon_M)$ from $\mathbb{R}^M$ to $\mathbb{R}$, which returns the maximum Lyapunov exponent of (4.17) as a function of the interaction strengths of each tier. Then, given any temporal multiplex hypernetwork, the intralayer synchronization solution will be stable if $\Lambda_{max}(\epsilon_1, \epsilon_2, \ldots, \epsilon_M) < 0$. Through the maximum Lyapunov exponent of the MSE, we can predict the diversity of the special mode of stability of the intralayer synchronization manifold.

5. Stability of intralayer synchronization with multilayer hypernetwork architecture.

Now we extend our results on intralayer synchronization in multilayer hypernetwork architec-

ture. The evolution equation of the generic ith node $\left(i \in \mathbf{N}_1\right)$ can be delineated as

$$\begin{aligned}\dot{\mathbf{x}}_i &= F_1(\mathbf{x}_i) - \sum_{\alpha=1}^{M} \epsilon_\alpha \sum_{j=1}^{N} \mathscr{L}_{ij}^{[1,\alpha]}(t) G_\alpha^{[1]}(\mathbf{x}_j) + \lambda \sum_{j=1}^{N} \mathscr{B}_{ij}^{[1]} H_1(\mathbf{x}_i, \mathbf{y}_j),\\ \dot{\mathbf{y}}_i &= F_2(\mathbf{y}_i) - \sum_{\alpha=1}^{M} \epsilon_\alpha \sum_{j=1}^{N} \mathscr{L}_{ij}^{[2,\alpha]}(t) G_\alpha^{[2]}(\mathbf{y}_j) + \lambda \sum_{j=1}^{N} \mathscr{B}_{ij}^{[2]} H_2(\mathbf{y}_i, \mathbf{x}_j).\end{aligned} \tag{5.1}$$

Here $\mathscr{B}^{[l]}$ is the interlayer adjacency matrix of layer-l ($l = 1, 2$). $\mathscr{B}_{ij}^{[l]} = 1$ if the ith node in layer-l is connected to the jth node in the other layer, and zero otherwise. The interlayer degree of the ith node is denoted by $e_i^{[l]}$, which is defined as $e_i^{[l]} = \sum_{j=1}^{N} \mathscr{B}_{ij}^{[l]}$. Actually, $e_i^{[l]}$ gives how many interlayer edges are associated with the ith node in layer-l.

For this type of network architecture, intralayer synchronization may not be achieved by only tuning the coupling strengths (intra- or interlayer). A suitable network architecture is required for the existence of this type of solution. First, we derive the invariance condition, and then we will look for its stability condition.

Lemma 5.1. *For the dynamical multilayer hypernetwork* (5.1)*, the intralayer synchronization state is an invariant solution if the interlayer degree of all the nodes is equal for each layer.*

Proof of Lemma 5.1. See Appendix A. ∎

Remark 5.2. For the invariance of the intralayer synchronization state, the interlayer degree of each node in each individual layer should be equal, while they may be different for two nodes from different layers, i.e., may be $e^{[1]} \neq e^{[2]}$.

Remark 5.3. Due to the fact $\sum_{j=1}^{N} \mathscr{B}_{ij}^{[l]} = e^{[l]}$, $\mathscr{B}^{[l]}$ becomes a constant row-sum matrix for $l = 1, 2$. Therefore, $e^{[l]}$ is an eigenvalue of $\mathscr{B}^{[l]}$ with associate normalized eigenvector $\left[\frac{1}{\sqrt{N}}, \frac{1}{\sqrt{N}}, \ldots, \frac{1}{\sqrt{N}}\right]^{tr}$.

With the above invariance condition, the intralayer synchronization manifold dominates the equation of motion as

$$\begin{aligned}\dot{\mathbf{x}}_0 &= F_1(\mathbf{x}_0) + \lambda e^{[1]} H_1(\mathbf{x}_0, \mathbf{y}_0),\\ \dot{\mathbf{y}}_0 &= F_2(\mathbf{y}_0) + \lambda e^{[2]} H_2(\mathbf{y}_0, \mathbf{x}_0).\end{aligned} \tag{5.2}$$

Considering small perturbations $(\delta\mathbf{x}_i(t), \delta\mathbf{y}_i(t))$, the linearized equation in vectorial form can be written as

$$\begin{aligned}\delta\dot{\mathbf{x}} &= I_N \otimes JF_1(\mathbf{x}_0)\delta\mathbf{x} - \sum_{\alpha=1}^{M} \epsilon_\alpha \mathscr{L}^{[1,\alpha]}(t) \otimes JG_\alpha^{[1]}(\mathbf{x}_0)\delta\mathbf{x}\\ &\quad + \lambda\left[e^{[1]} I_N \otimes JH_1(\mathbf{x}_0, \mathbf{y}_0)\delta\mathbf{x} + \mathscr{B}^{[1]} \otimes DH_1(\mathbf{x}_0, \mathbf{y}_0)\delta\mathbf{y}\right],\\ \delta\dot{\mathbf{y}} &= I_N \otimes JF_2(\mathbf{y}_0)\delta\mathbf{y} - \sum_{\alpha=1}^{M} \epsilon_\alpha \mathscr{L}^{[2,\alpha]}(t) \otimes JG_\alpha^{[2]}(\mathbf{y}_0)\delta\mathbf{y}\\ &\quad + \lambda\left[e^{[2]} I_N \otimes JH_2(\mathbf{y}_0, \mathbf{x}_0)\delta\mathbf{y} + \mathscr{B}^{[2]} \otimes DH_2(\mathbf{y}_0, \mathbf{x}_0)\delta\mathbf{x}\right].\end{aligned} \tag{5.3}$$

Due to the change of variables using Schur transformations $\eta^{(\mathbf{x})} = \left(V^{[1]} \otimes I_d\right)^{-1}\delta\mathbf{x}$ and $\eta^{(\mathbf{y})} = \left(V^{[1]} \otimes I_d\right)^{-1}\delta\mathbf{y}$, the dynamics of the error systems in terms of the change of variables yield

$$\begin{aligned}
\dot{\eta}^{(\mathbf{x})} &= I_N \otimes JF_1(\mathbf{x}_0)\eta^{(\mathbf{x})} - \sum_{\alpha=1}^{M} \epsilon_\alpha \left({V^{[1]}}^{-1} \mathscr{L}^{[1,\alpha]}(t) V^{[1]}\right) \otimes JG_\alpha^{[1]}(\mathbf{x}_0)\eta^{(\mathbf{x})} \\
&\quad + \lambda\left[e^{[1]} I_N \otimes JH_1(\mathbf{x}_0, \mathbf{y}_0)\eta^{(\mathbf{x})} + \left({V^{[1]}}^{-1} \mathscr{B}^{[1]} V^{[1]}\right) \otimes DH_1(\mathbf{x}_0, \mathbf{y}_0)\eta^{(\mathbf{y})}\right], \\
\dot{\eta}^{(\mathbf{y})} &= I_N \otimes JF_2(\mathbf{y}_0)\eta^{(\mathbf{y})} - \sum_{\alpha=1}^{M} \epsilon_\alpha \left({V^{[1]}}^{-1} \mathscr{L}^{[2,\alpha]}(t) V^{[1]}\right) \otimes JG_\alpha^{[2]}(\mathbf{y}_0)\eta^{(\mathbf{y})} \\
&\quad + \lambda\left[e^{[2]} I_N \otimes JH_2(\mathbf{y}_0, \mathbf{x}_0)\eta^{(\mathbf{y})} + \left({V^{[1]}}^{-1} \mathscr{B}^{[2]} V^{[1]}\right) \otimes DH_2(\mathbf{y}_0, \mathbf{x}_0)\eta^{(\mathbf{x})}\right].
\end{aligned} \tag{5.4}$$

Here $\mathscr{B}^{[l]}$ is a real square matrix; therefore, it is unitarily triangularizable. Then there exist a unitary matrix $V_{[l]}$ of orthogonal eigenvectors of $\mathscr{B}^{[l]}$ and an upper triangular matrix $U_{[l]}$ such that $U_{[l]} = V_{[l]}^{-1}\mathscr{B}^{[l]}V_{[l]}$. Then ${V^{[1]}}^{-1}\mathscr{B}^{[l]}V^{[1]} = {V^{[1]}}^{-1}V_{[l]}U_{[l]}V_{[l]}^{-1}V^{[1]}$, which yields

$${V^{[1]}}^{-1}\mathscr{B}^{[l]}V^{[1]} = \begin{bmatrix} e^{[l]} & O_{1\times N-1} \\ O_{N-1\times 1} & U_3^{[l]} \end{bmatrix}.$$

Now decomposing the projected error components into parallel and transverse directions of the synchronization manifold, we get the respective dynamics as

(5.5a)
$$\dot{\eta}_P^{(\mathbf{x})} = JF_1(\mathbf{x}_0)\eta_P^{(\mathbf{x})} - \sum_{\alpha=1}^{M} \epsilon_\alpha U_1^{[1,\alpha]}(t) \otimes JG_\alpha^{[1]}(\mathbf{x}_0)\eta_T^{(\mathbf{x})} + \lambda e^{[1]}\left[JH_1(\mathbf{x}_0, \mathbf{y}_0)\eta_P^{(\mathbf{x})} + DH_1(\mathbf{x}_0, \mathbf{y}_0)\eta_P^{(\mathbf{y})}\right],$$

(5.5b)
$$\begin{aligned}
\dot{\eta}_T^{(\mathbf{x})} &= I_{N-1} \otimes JF_1(\mathbf{x}_0)\eta_T^{(\mathbf{x})} - \sum_{\alpha=1}^{M} \epsilon_\alpha U_2^{[1,\alpha]}(t) \otimes JG_\alpha^{[1]}(\mathbf{x}_0)\eta_T^{(\mathbf{x})} \\
&\quad + \lambda\left[e^{[1]} I_{N-1} \otimes JH_1(\mathbf{x}_0, \mathbf{y}_0)\eta_T^{(\mathbf{x})} + U_3^{[1]} \otimes DH_1(\mathbf{x}_0, \mathbf{y}_0)\eta_T^{(\mathbf{y})}\right],
\end{aligned}$$

(5.5c)
$$\dot{\eta}_P^{(\mathbf{y})} = JF_2(\mathbf{y}_0)\eta_P^{(\mathbf{y})} - \sum_{\alpha=1}^{M} \epsilon_\alpha U_1^{[2,\alpha]}(t) \otimes JG_\alpha^{[2]}(\mathbf{y}_0)\eta_T^{(\mathbf{y})} + \lambda e^{[2]}\left[JH_2(\mathbf{y}_0, \mathbf{x}_0)\eta_P^{(\mathbf{y})} + DH_2(\mathbf{y}_0, \mathbf{x}_0)\eta_P^{(\mathbf{x})}\right],$$

(5.5d)
$$\begin{aligned}
\dot{\eta}_T^{(\mathbf{y})} &= I_{N-1} \otimes JF_2(\mathbf{y}_0)\eta_T^{(\mathbf{y})} - \sum_{\alpha=1}^{M} \epsilon_\alpha U_2^{[2,\alpha]}(t) \otimes JG_\alpha^{[2]}(\mathbf{y}_0)\eta_T^{(\mathbf{y})} \\
&\quad + \lambda\left[e^{[2]} I_{N-1} \otimes JH_2(\mathbf{y}_0, \mathbf{x}_0)\eta_T^{(\mathbf{y})} + U_3^{[2]} \otimes DH_2(\mathbf{y}_0, \mathbf{x}_0)\eta_T^{(\mathbf{x})}\right].
\end{aligned}$$

Remark 5.4. Equations (5.5a, c) evolve parallel to the intralayer synchronization manifold, while (5.5b, d) are transverse to it. Interestingly, (5.5b, d) are independent of (5.5a, c), but (5.5a, c) depend on (5.5b, d). The stability of the transverse error components does not depend on the parallel components. So the parallel components do not play any role for

determining the stability of the synchronization solutions. However, when all the transverse error components $\eta_T^{(\mathbf{x})}$, $\eta_T^{(\mathbf{y})}$ die out, (5.5a, c) will become linearized equations of the intralayer synchronization manifold (5.2).

In terms of $\zeta_d(t) = \left[\eta_T^{(\mathbf{x})^{tr}} \ \eta_T^{(\mathbf{y})^{tr}}\right]^{tr}$, the dynamics of the transverse error systems can be written as

$$\dot{\zeta}_d(t) = \left[A(t) - \sum_{\alpha=1}^{M} \epsilon_\alpha \left(E_1^{[\alpha]}(t) \otimes JG_\alpha^{[1]}(\mathbf{x}_0) + E_2^{[\alpha]}(t) \otimes JG_\alpha^{[2]}(\mathbf{y}_0)\right)\right] \zeta_d(t), \tag{5.6}$$

where

$$A(t) = \begin{bmatrix} I_{N-1} \otimes \left\{JF_1(\mathbf{x}_0) + \lambda e^{[1]} JH_1(\mathbf{x}_0, \mathbf{y}_0)\right\} & \lambda U_3^{[1]} \otimes DH_1(\mathbf{x}_0, \mathbf{y}_0) \\ \lambda U_3^{[2]} \otimes DH_2(\mathbf{y}_0, \mathbf{x}_0) & I_{N-1} \otimes \left\{JF_2(\mathbf{y}_0) + \lambda e^{[2]} JH_2(\mathbf{y}_0, \mathbf{x}_0)\right\} \end{bmatrix}$$

$$\text{and} \quad E_1^{[\alpha]}(t) = \begin{bmatrix} U_2^{[1,\alpha]}(t) & O_{N-1\times N-1} \\ O_{N-1\times N-1} & O_{N-1\times N-1} \end{bmatrix}, \quad E_2^{[\alpha]}(t) = \begin{bmatrix} O_{N-1\times N-1} & O_{N-1\times N-1} \\ O_{N-1\times N-1} & U_2^{[2,\alpha]}(t) \end{bmatrix}.$$

Incorporating the time-average intralayer Laplacian matrices, the dynamics of the time-average multilayer hypernetwork can be written as

$$\begin{aligned} \dot{\mathbf{w}}_i &= F_1(\mathbf{w}_i) - \sum_{\alpha=1}^{M} \epsilon_\alpha \sum_{j=1}^{N} \bar{\mathscr{L}}_{ij}^{[\alpha]} G_\alpha^{[1]}(\mathbf{w}_j) + \lambda \sum_{j=1}^{N} \mathscr{B}_{ij}^{[1]} H_1(\mathbf{w}_i, \mathbf{z}_j), \\ \dot{\mathbf{z}}_i &= F_2(\mathbf{z}_i) - \sum_{\alpha=1}^{M} \epsilon_\alpha \sum_{j=1}^{N} \bar{\mathscr{L}}_{ij}^{[\alpha]} G_\alpha^{[2]}(\mathbf{z}_j) + \lambda \sum_{j=1}^{N} \mathscr{B}_{ij}^{[2]} H_2(\mathbf{z}_i, \mathbf{w}_i). \end{aligned} \tag{5.7}$$

For this time-average multilayer hypernetwork, the system (5.2) is also the dynamics of the intralayer synchronization manifold. Considering $\delta\mathbf{w}(t)$ and $\delta\mathbf{z}(t)$ as the perturbation components, the error dynamics for the time-average system read as

$$\begin{aligned} \delta\dot{\mathbf{w}} &= I_N \otimes JF_1(\mathbf{x}_0)\delta\mathbf{w} - \sum_{\alpha=1}^{M} \epsilon_\alpha \bar{\mathscr{L}}^{[\alpha]} \otimes JG_\alpha^{[1]}(\mathbf{x}_0)\delta\mathbf{w} \\ &\quad + \lambda\left[e^{[1]} I_N \otimes JH_1(\mathbf{x}_0, \mathbf{y}_0)\delta\mathbf{w} + \mathscr{B}^{[1]} \otimes DH_1(\mathbf{x}_0, \mathbf{y}_0)\delta\mathbf{z}\right], \\ \delta\dot{\mathbf{z}} &= I_N \otimes JF_2(\mathbf{y}_0)\delta\mathbf{z} - \sum_{\alpha=1}^{M} \epsilon_\alpha \bar{\mathscr{L}}^{[\alpha]} \otimes JG_\alpha^{[2]}(\mathbf{y}_0)\delta\mathbf{z} \\ &\quad + \lambda\left[e^{[2]} I_N \otimes JH_2(\mathbf{y}_0, \mathbf{x}_0)\delta\mathbf{z} + \mathscr{B}^{[2]} \otimes DH_2(\mathbf{y}_0, \mathbf{x}_0)\delta\mathbf{w}\right]. \end{aligned} \tag{5.8}$$

By considering the Schur transformation on these perturbed variables, we have the transformed variables as $\eta^{(\mathbf{w})} = \left(V^{[1]} \otimes I_d\right)^{-1} \delta\mathbf{w}$ and $\eta^{(\mathbf{z})} = \left(V^{[1]} \otimes I_d\right)^{-1} \delta\mathbf{z}$. Then the dynamics

of the projected system become

$$
\begin{aligned}
\dot{\eta}^{(\mathbf{w})} &= I_N \otimes JF_1(\mathbf{x}_0)\eta^{(\mathbf{w})} - \sum_{\alpha=1}^{M} \epsilon_\alpha \Big({V^{[1]}}^{-1} \bar{\mathscr{L}}^{[\alpha]} V^{[1]} \Big) \otimes JG_\alpha^{[1]}(\mathbf{x}_0)\eta^{(\mathbf{w})} \\
&\quad + \lambda \Big[e^{[1]} I_N \otimes JH_1(\mathbf{x}_0, \mathbf{y}_0)\eta^{(\mathbf{w})} + \Big({V^{[1]}}^{-1} \mathscr{B}^{[1]} V^{[1]} \Big) \otimes DH_1(\mathbf{x}_0, \mathbf{y}_0)\eta^{(\mathbf{z})} \Big], \\
\dot{\eta}^{(\mathbf{z})} &= I_N \otimes JF_2(\mathbf{y}_0)\eta^{(\mathbf{z})} - \sum_{\alpha=1}^{M} \epsilon_\alpha \Big({V^{[1]}}^{-1} \bar{\mathscr{L}}^{[\alpha]} V^{[1]} \Big) \otimes JG_\alpha^{[2]}(\mathbf{y}_0)\eta^{(\mathbf{z})} \\
&\quad + \lambda \Big[e^{[2]} I_N \otimes JH_2(\mathbf{y}_0, \mathbf{x}_0)\eta^{(\mathbf{z})} + \Big({V^{[1]}}^{-1} \mathscr{B}^{[2]} V^{[1]} \Big) \otimes DH_2(\mathbf{y}_0, \mathbf{x}_0)\eta^{(\mathbf{w})} \Big].
\end{aligned} \tag{5.9}
$$

Splitting the projected error component into parallel and transverse directions, we get the dynamics of the transverse components as

$$
\begin{aligned}
\dot{\eta}_T^{(\mathbf{w})} &= I_{N-1} \otimes JF_1(\mathbf{x}_0)\eta_T^{(\mathbf{w})} - \sum_{\alpha=1}^{M} \epsilon_\alpha \bar{U}_2^{[\alpha]} \otimes JG_\alpha^{[1]}(\mathbf{x}_0)\eta_T^{(\mathbf{w})} \\
&\quad + \lambda \Big[e^{[1]} I_{N-1} \otimes JH_1(\mathbf{x}_0, \mathbf{y}_0)\eta_T^{(\mathbf{w})} + U_3^{[1]} \otimes DH_1(\mathbf{x}_0, \mathbf{y}_0)\eta_T^{(\mathbf{z})} \Big], \\
\dot{\eta}_T^{(\mathbf{z})} &= I_{N-1} \otimes JF_2(\mathbf{y}_0)\eta_T^{(\mathbf{z})} - \sum_{\alpha=1}^{M} \epsilon_\alpha \bar{U}_2^{[\alpha]} \otimes JG_\alpha^{[2]}(\mathbf{y}_0)\eta_T^{(\mathbf{z})} \\
&\quad + \lambda \Big[e^{[2]} I_{N-1} \otimes JH_2(\mathbf{y}_0, \mathbf{x}_0)\eta_T^{(\mathbf{z})} + U_3^{[2]} \otimes DH_2(\mathbf{y}_0, \mathbf{x}_0)\eta_T^{(\mathbf{w})} \Big].
\end{aligned} \tag{5.10}
$$

In terms of $\zeta_a(t) = \big[{\eta_T^{(\mathbf{w})}}^{tr} \ {\eta_T^{(\mathbf{z})}}^{tr} \big]^{tr}$, the dynamics of the transverse error components of the time-average system can be written as

$$
\dot{\zeta}_a(t) = \left[A(t) - \sum_{\alpha=1}^{M} \epsilon_\alpha \Big(\bar{E}_1^{[\alpha]} \otimes JG_\alpha^{[1]}(\mathbf{x}_0) + \bar{E}_2^{[\alpha]}(t) \otimes JG_\alpha^{[2]}(\mathbf{y}_0) \Big) \right] \zeta_a(t), \tag{5.11}
$$

where

$$
A(t) = \begin{bmatrix} I_{N-1} \otimes \Big\{ JF_1(\mathbf{x}_0) + \lambda e^{[1]} JH_1(\mathbf{x}_0, \mathbf{y}_0) \Big\} & \lambda U_3^{[1]} \otimes DH_1(\mathbf{x}_0, \mathbf{y}_0) \\ \lambda U_3^{[2]} \otimes DH_2(\mathbf{y}_0, \mathbf{x}_0) & I_{N-1} \otimes \Big\{ JF_2(\mathbf{y}_0) + \lambda e^{[2]} JH_2(\mathbf{y}_0, \mathbf{x}_0) \Big\} \end{bmatrix}
$$

and $\bar{E}_1^{[\alpha]} = \begin{bmatrix} \bar{U}_2^{[\alpha]} & O_{N-1\times N-1} \\ O_{N-1\times N-1} & O_{N-1\times N-1} \end{bmatrix}$, $\bar{E}_2^{[\alpha]} = \begin{bmatrix} O_{N-1\times N-1} & O_{N-1\times N-1} \\ O_{N-1\times N-1} & \bar{U}_2^{[\alpha]} \end{bmatrix}$.

Due to the fact that $\int_t^{t+T} E_m^{[\alpha]}(\tau)\, d\tau = \bar{E}_m^{[\alpha]}$ for $m = 1, 2$, we can reach the conclusion that the asymptotic stability of the traverse error system (5.11) implies the traverse error system (5.6). Therefore, the asymptotic stability of the intralayer synchronization solution $(\mathbf{x}_0, \mathbf{y}_0)$ for the time-average system (5.7) implies the asymptotic stability of the intralayer synchronization solution $(\mathbf{x}_0, \mathbf{y}_0)$ for the time-varying system (5.1) for sufficiently fast switching. The equivalence of the stability of the intralayer synchronization manifold for time-varying and time-average systems is thus obtained.

Now we are interested in finding the necessary and sufficient conditions for the intralayer synchronization state. Transverse error dynamics (5.10) of the time-average system is our MSE. All of its terms are block diagonal except $\bar{U}_2^{[\alpha]} \otimes JG_\alpha^{[l]}(\mathbf{x}_0)$, $U_3^{[1]} \otimes DH_1(\mathbf{x}_0, \mathbf{y}_0)$, and $U_3^{[2]} \otimes DH_2(\mathbf{y}_0, \mathbf{x}_0)$. In component form, it can be written as

$$
\begin{aligned}
\dot{\eta}_{T_i}^{(\mathbf{w})} &= JF_1(\mathbf{x}_0)\eta_{T_i}^{(\mathbf{w})} - \epsilon_1 \sum_{j=i}^{N-1} \bar{U}_{ij}^{[1]} JG_1^{[1]}(\mathbf{x}_0)\eta_{T_j}^{(\mathbf{w})} - \sum_{\alpha=2}^{M} \epsilon_\alpha \sum_{j=1}^{N-1} \bar{U}_{ij}^{[\alpha]} JG_\alpha^{[1]}(\mathbf{x}_0)\eta_{T_j}^{(\mathbf{w})} \\
&\quad + \lambda \left[e^{[1]} JH_1(\mathbf{x}_0, \mathbf{y}_0)\eta_{T_i}^{(\mathbf{w})} + \sum_{j=1}^{N-1} U_{3ij}^{[1]} DH_1(\mathbf{x}_0, \mathbf{y}_0)\eta_{T_j}^{(\mathbf{z})} \right], \\
\dot{\eta}_{T_i}^{(\mathbf{z})} &= JF_2(\mathbf{y}_0)\eta_{T_i}^{(z)} - \epsilon_1 \sum_{j=i}^{N-1} \bar{U}_{ij}^{[1]} JG_1^{[2]}(\mathbf{y}_0)\eta_{T_j}^{(\mathbf{z})} - \sum_{\alpha=2}^{M} \epsilon_\alpha \sum_{j=1}^{N-1} \bar{U}_{ij}^{[\alpha]} JG_\alpha^{[2]}(\mathbf{y}_0)\eta_{T_j}^{(\mathbf{z})} \\
&\quad + \lambda \left[e^{[2]} JH_2(\mathbf{y}_0, \mathbf{x}_0)\eta_{T_i}^{(\mathbf{z})} + \sum_{j=1}^{N-1} U_{3ij}^{[2]} DH_2(\mathbf{y}_0, \mathbf{x}_0)\eta_{T_j}^{(\mathbf{w})} \right],
\end{aligned} \tag{5.12}
$$

which are $2d(N-1)$-dimensional coupled systems.

Now if $\bar{\mathscr{L}}^{[1]}$ commutes with all other intralayer Laplacian matrices $\bar{\mathscr{L}}^{[\alpha]}$ $(\alpha = 2, 3, \ldots, M)$ as well as interlayer adjacency matrices $\mathscr{B}^{[l]}$ $(l = 1, 2)$, then all of these matrices have a common basis of eigenvectors. Thus, they can be diagonalizable by the basis of eigenvectors $V^{[1]}$. This yields $\bar{U}_2^{[\alpha]} = \mathrm{diag}\{\gamma_2^{[\alpha]}, \gamma_3^{[\alpha]}, \ldots, \gamma_{\mathrm{N}}^{[\alpha]}\}$ and $U_3^{[l]} = \mathrm{diag}\{\Gamma_2^{[l]}, \Gamma_3^{[l]}, \ldots, \Gamma_{\mathrm{N}}^{[l]}\}$. For this special case, the block diagonal transverse equations become

$$
\begin{aligned}
\dot{\eta}_{T_i}^{(\mathbf{w})} &= JF_1(\mathbf{x}_0)\eta_{T_i}^{(\mathbf{w})} - \sum_{\alpha=1}^{M} \epsilon_\alpha \gamma_i^{[\alpha]} JG_\alpha^{[1]}(\mathbf{x}_0)\eta_{T_i}^{(\mathbf{w})} + \lambda \left[e^{[1]} JH_1(\mathbf{x}_0, \mathbf{y}_0)\eta_{T_i}^{(\mathbf{w})} + \Gamma_i^{[1]} DH_1(\mathbf{x}_0, \mathbf{y}_0)\eta_{T_i}^{(\mathbf{z})} \right], \\
\dot{\eta}_{T_i}^{(\mathbf{z})} &= JF_2(\mathbf{y}_0)\eta_{T_i}^{(\mathbf{z})} - \sum_{\alpha=1}^{M} \epsilon_\alpha \gamma_i^{[\alpha]} JG_\alpha^{[2]}(\mathbf{y}_0)\eta_{T_i}^{(\mathbf{z})} + \lambda \left[e^{[2]} JH_2(\mathbf{y}_0, \mathbf{x}_0)\eta_{T_i}^{(\mathbf{z})} + \Gamma_i^{[2]} DH_2(\mathbf{y}_0, \mathbf{x}_0)\eta_{T_i}^{(\mathbf{w})} \right],
\end{aligned} \tag{5.13}
$$

where $i \in N_2$ and these are the much reduced low-dimensional equations.

Corollary 5.5. *Consider, for a multilayer network with one tier (i.e., $M = 1$), that the eigenvalues of the intralayer Laplacian matrix are 0 with algebraic multiplicity 1 and $\bar{a}$ with algebraic multiplicity $N-1$. Also, assume that the interlayer adjacency matrices are equal and symmetric. Then the transverse error dynamics can be decoupled as $2d$-dimensional $N-1$ systems.*

Proof of Corollary 5.5. See Appendix A. ∎

Therefore, we can obtain such dimensionality reduction of the transverse error system for a multilayer network with one tier. Here intralayer Laplacian matrix does not necessarily commute with the interlayer adjacency matrix. Moreover, the interlayer adjacency matrix can be arbitrarily chosen for such decoupling. Such kind of dimensionality reduction for monolayer hypernetwork was done in [50].

Remark 5.6. Unlike for the dimensionality reduction in the multiplex network, to choose interlayer connections arbitrarily, only one tier in the intralayer network can be present. By

adding one extra tier, we again have to make the restriction that the corresponding intralayer adjacency matrix commutes with the interlayer adjacency matrices.

Remark 5.7. This type of time-average Laplacian matrix occurs if the time-varying network architecture is ER random with a certain edge joining probability. Another possibility is that $\bar{\mathscr{L}}^{[1]}$ is a weighted Laplacian matrix and the weight from node j to node i is only a function of the source node j but not of the destination node i.

6. Numerical example. To illustrate the theoretical results, we consider a 2×200 set of Rössler oscillators, with our discussed time-varying network machinery. We know that a network of chaotic Rössler oscillators can be synchronized by a suitable coupling. Here two different types of interactions are considered in the intralayer connection of each layer and which are associated with two structurally different network typologies. Intralayer synchronization is assessed by examining the local asymptotic stability of the oscillators along the synchronization manifold in each layer. To reveal the underlying mechanisms for the emergence of the synchronization state, coupled Rössler oscillators offer a generic test-bed for investigation. In this section, our main emphasis will be to identify the parameter regions for the intralayer synchronization state.

We consider the multiplex network (3.1), where each layer is composed of Rössler oscillators. We take one tier of the intralayer coupling function $G_1^{[l]}(\mathbf{x})$ as diffusive through the variable x, whose underlying network is the random network with probability p_r for $l = 1, 2$. The connectivity of the random network for layer-l is described by the Laplacian matrix $\mathscr{L}^{[l,1]}(t)$. For another tier, the coupling function $G_2^{[l]}(\mathbf{x})$ is also of diffusive type but through the variable y for $l = 1, 2$. The Laplacian matrices corresponding to these tiers in the two layers are $\mathscr{L}^{[1,2]}(t)$ and $\mathscr{L}^{[2,2]}(t)$, respectively, which was considered to be a small-world network with average degree of the network $2k_{sw}$ and edge rewiring probability p_{sw}. Each node in a layer is connected to its replica on the other layer by diffusive coupling through the y variable. So the mathematical forms of the autonomous evolution functions $F_{1,2}(\mathbf{x})$, intralayer coupling functions $G_1^{[1,2]}(\mathbf{x}), G_2^{[1,2]}(\mathbf{x})$, and interlayer coupling functions $H_{1,2}(\mathbf{x})$ are as follows:

(6.1)
$$F_{1,2}(\mathbf{x}) = \begin{bmatrix} -y - z \\ x + ay \\ b + z(x - c) \end{bmatrix}, \quad G_1^{[1,2]}(\mathbf{x}) = \begin{bmatrix} x \\ 0 \\ 0 \end{bmatrix}, \quad G_2^{[1,2]}(\mathbf{x}) = \begin{bmatrix} 0 \\ y \\ 0 \end{bmatrix}, \quad H_{1,2}(\mathbf{x}_1, \mathbf{x}_2) = \begin{bmatrix} 0 \\ y_2 - y_1 \\ 0 \end{bmatrix},$$

where $a = 0.1$, $b = 0.1$, and $c = 14.0$. With this set of parameter values, each individual oscillator retains chaotic behavior.

Here the simulations are presented by obtaining $N = 200$ oscillators in each layer. We integrate the entire network numerically using the fifth-order Runge–Kutta–Fehlberg integration algorithm scheme with a time step 0.01 up to 5×10^5 iterations. All the numerical figures are drawn after an initial transient of 2×10^5 units.

In our prescribed model, the two intralayer coupling topologies are time-varying; i.e., one is a small-world network, and the other one is an ER random network, and both are bidirectional. With probability p_r, the edges are included in the ER network independently from the other edges. The small-world networks are constructed by following the procedure proposed by Watts and Strogatz [57]. Each link in the small-world network in both of the layers is rewired

stochastically. Particularly, at any time, we rewire these two tiers by constructing a new small-world network from the initial ring, independently with probability $f\ dt$, where f is the rewiring frequency and dt is the integration time step.

Consider $E_1 = \lim_{T\to\infty} \frac{1}{T} \int_0^T \sum_{j=2}^{N} \frac{\|\mathbf{x}_j(t)-\mathbf{x}_1(t)\|}{N-1}\, dt$ to be the complete synchronization error of layer-1 and that of layer-2 to be $E_2 = \lim_{T\to\infty} \frac{1}{T} \int_0^T \sum_{j=2}^{N} \frac{\|\mathbf{y}_j(t)-\mathbf{y}_1(t)\|}{N-1}\, dt$, where $\|\cdot\|$ denotes the Euclidean norm and T is the long time interval. The asymptotic stability of E_l $(l = 1, 2)$ will imply that each oscillator in layer-l is synchronized. Then the asymptotic stability of each oscillator with respect to the intralayer synchronization solution is investigated by plotting the average synchronization error, defined as $E = \frac{E_1+E_2}{2}$. In the following numerical simulations, our main target is to investigate the intralayer synchronization state as a function of intralayer and interlayer coupling strengths $\epsilon_{1,2}$ and λ for different rewiring frequencies.

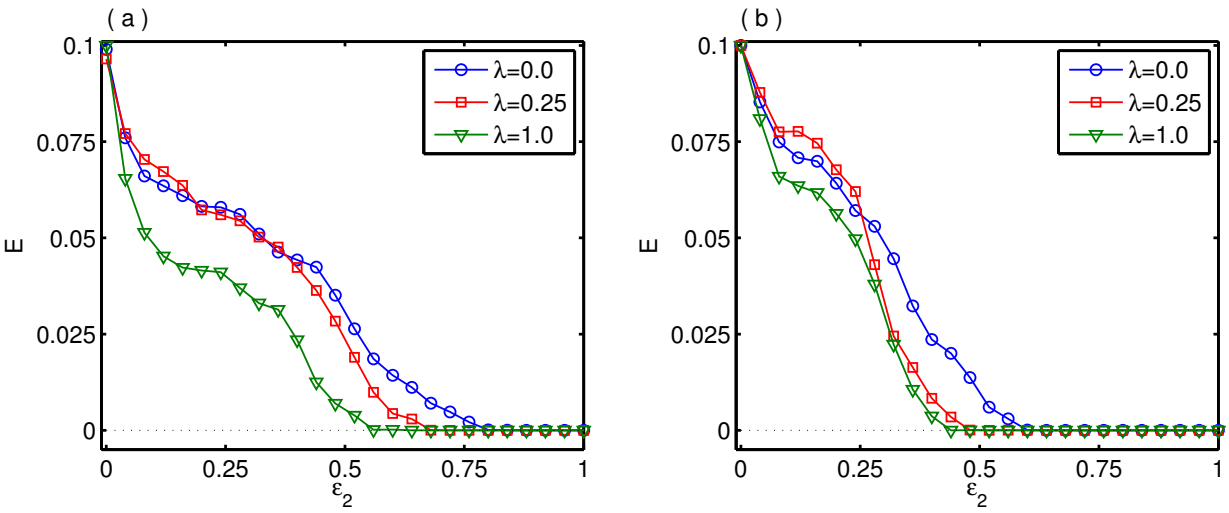

Figure 2. *Intralayer synchronization error by varying the tier-2 coupling strength ϵ_2 for a fixed value of tier-1 coupling strength:* (a) $\epsilon_1 = 0.0$, (b) $\epsilon_1 = 0.015$. *Other parameters are* $d_{sw} = 4$, $p_{sw} = 0.1$, $p_r = 0.015$, *and* $f = 0.1$.

Let us now investigate the intralayer synchronization with respect to the tier-2 coupling strength ϵ_2 in the absence and presence of tier-1 for the moderate switching case $f = 0.1$. The corresponding results are shown in Figures 2(a) and 2(b), respectively. The intralayer synchronization error E is plotted in Figure 2 by considering various values of λ and fixed values of $d_{sw} = 4$, $p_{ws} = 0.1$, and $p_r = 0.015$. The open blue circle, red square, and green triangle lines denote the results for $\lambda = 0.0,\ 0.25$, and $\lambda = 1.0$, respectively. When interlayer coupling strength and intralayer strength for tier-1 are set to zero ($\lambda = \epsilon_1 = 0.0$), then the intralayer synchronization states arrives at $\epsilon_2 = 0.8$. The corresponding result is represented by the blue open circle line in Figure 2(a). But if we introduce the layer-layer interaction strength at $\lambda = 0.25$, the intralayer synchronization is enhanced at $\epsilon_2 = 0.68$ despite the absence of ϵ_1. More enhancement of the intralayer synchrony ($\epsilon_2 = 0.56$) is observed (green line of Figure 2(a)) for even higher values of $\lambda = 1.0$. Figure 2(b) depicts these enhancement changes in the presence of tier-1 interaction. For certain values of $\epsilon_1 = 0.015$, the critical

transition appears at $\epsilon_2 = 0.6$ for $\lambda = 0.0$, and this critical threshold enhances for higher values of the λ (Figure 2(b)). Note that greater enhancements of the intralayer synchrony are shown in Figure 2(b) compared to Figure 2(a) with the same set of interlayer coupling strengths.

So in this figure it is clearly shown that the combined effect of the two types of intralayer coupling strengths leads to the enhancement of the intralayer synchrony in the slow switching case and further significant enhancing is taking place for the intercoupling strength λ.

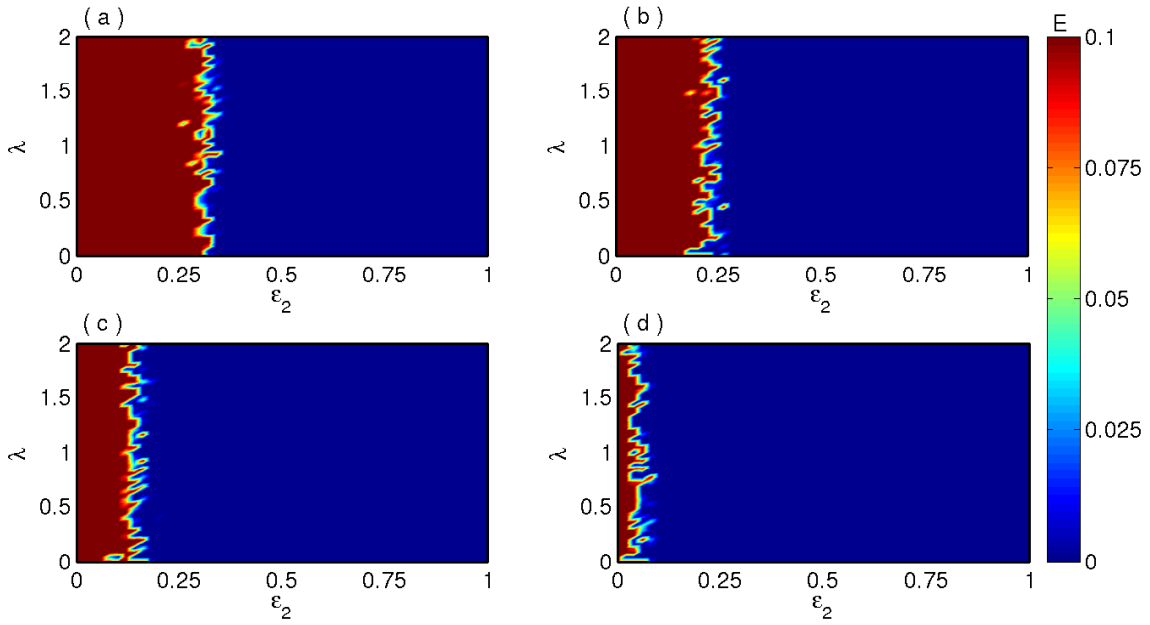

Figure 3. *Intralayer synchronization error in the (ϵ_2, λ) plane for* (a) $\epsilon_1 = 0.0$, (b) $\epsilon_1 = 0.015$, (c) $\epsilon_1 = 0.03$, *and* (d) $\epsilon_1 = 0.045$. *Other parameters are $d_{sw} = 4$, $p_{ws} = 0.1$, $p_r = 0.015$, and $f = 100.0$. The color bar denotes the variation of the intralayer synchronization error E of the multiplex temporal hypernetworks where the deep red and blue correspond to the desynchronized and synchronized domains, respectively.*

For fast switching ($f = 100.0$), the intralayer synchronization regions are plotted in Figure 3 for different values of tier-1 intralayer coupling strength ϵ_1 in the plane of intralayer coupling strength ϵ_2 of tier-2 and interlayer coupling strength λ. The color bar denotes the variation of the intralayer synchronization error E of the multiplex temporal hypernetworks where the deep red and blue correspond to the desynchronized and synchronized domains, respectively. In the absence of tier-1 (i.e., $\epsilon_1 = 0.0$), the coherent and incoherent domains are plotted in Figure 3(a), and by introducing the ϵ_1 at $\epsilon_1 = 0.015$, the enhancement of the synchrony is shown in Figure 3(b). Also, by considering the several exemplified values of ϵ_1 as $\epsilon_1 = 0.03$ and 0.045, the enhancing phenomena are delineated in Figures 3(c) and 3(d), respectively. However, in all these figures, the critical transition point against the ϵ_2 is almost vertical. This means that the transition point is only affected by the intralayer coupling strengths $\epsilon_{1,2}$ and interlayer interaction strength λ has no effect on the intralayer synchronization transition in the fast rewiring case.

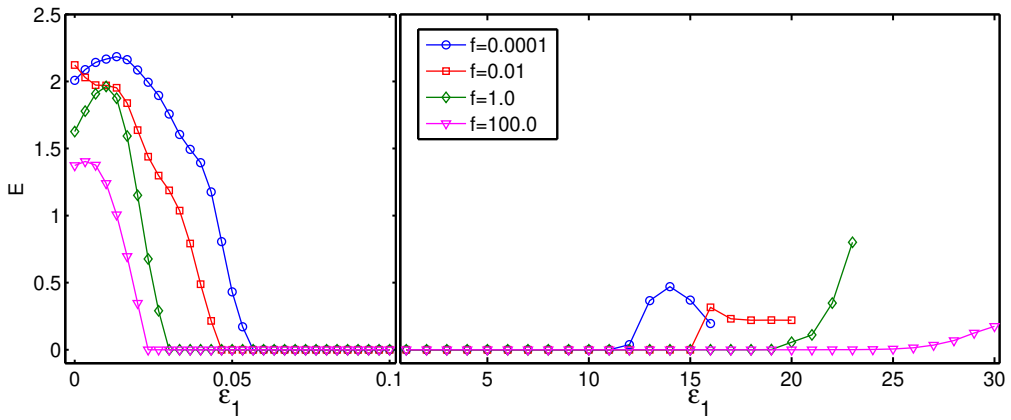

Figure 4. *Variation of the intralayer synchronization error E with respect to ϵ_1 for several values of the rewiring frequencies $f = 0.0001$ (blue circle line), $f = 0.01$ (red square line), $f = 1.0$ (green diamond line), and $f = 100.0$ (magenta triangle line). Other parameters are $d_{sw} = 4$, $p_{ws} = 0.1$, $p_r = 0.015$, $\epsilon_2 = 0.2$, and $\lambda = 0.5$.*

Figure 4 represents the variation of the intralayer synchronization error E with respect to ϵ_1 for four different values of the rewiring frequencies $f = 0.0001$ (blue circle line), $f = 0.01$ (red square line), $f = 1.0$ (green diamond line), and $f = 100.0$ (magenta triangle line). For these rewiring frequencies, the critical values of ϵ_1 for the intralayer synchronization are $\epsilon_1^{(1)} = 0.057$, $\epsilon_1^{(1)} = 0.047$, $\epsilon_1^{(1)} = 0.03$, and $\epsilon_1^{(1)} = 0.023$, respectively. Here the superscript (1) denotes the critical threshold for the first transition from desynchrony to synchrony, while the second transition (from synchrony to desynchrony) is represented by the superscript (2). This layerwise synchrony persists up to a certain value of ϵ_1 but depending on the rewiring frequency f. For $f = 0.0001$, the transition from synchronization to desynchronization occurs at $\epsilon_1^{(2)} \simeq 11.0$. For the slow-switching case, the range of synchronization is $[0.057, 11.0]$. For other values of f, these transitions occur respectively at $\epsilon_1^{(2)} \simeq 15.0$, $\epsilon_1^{(2)} \simeq 19.0$, and $\epsilon_1^{(2)} \simeq 21.0$. So the intralayer synchronization state appears in $\left[\epsilon_1^{(1)}, \epsilon_1^{(2)}\right]$ and the length of this interval increases on both sides by increasing the rewiring frequency of each temporal intralayer network. The stability of the synchronization regime loses at increasing the x-coupling strength due to the short wavelength bifurcation [24]. Additionally, for $f = 0.0001$, the system becomes unbounded for $\epsilon_1 \geq 16.1$. By increasing the rewiring frequency, this unboundedness can be de-enhanced. For $f = 0.01$ and $f = 1.0$, the system becomes unbounded at $\epsilon_1 = 19.8$ and $\epsilon_1 = 22.7$, respectively. Interestingly, for very fast switching, the dynamical network possesses a bounded solution up to $\epsilon_1 = 30$.

Next, we find the low-dimensional MSE based on the approach discussed in section 4. If $\bar{\mathscr{L}}^{[1]}$ is the time-average Laplacian matrix for tier-1 (random network) in both of the layers, then

$$\bar{\mathscr{L}}_{ij}^{[1]} \begin{array}{ll} = -p_r & \text{for } i \neq j \\ = (N-1)p_r & \text{for } i = j. \end{array} \tag{6.2}$$

Also, if $\bar{\mathscr{L}}^{[2]}$ is chosen by tier-2 (small-world network), then

$$\begin{aligned}\bar{\mathscr{L}}_{ij}^{(2)} &= -(1-p_{sw}) \quad \text{for } i-k_{sw}\le j\le i+k_{sw} \text{ and } i\neq j\\ &= 2k_{sw} \qquad\qquad \text{for } i=j\\ &= -\frac{k_{sw}\ p_{sw}}{N-k_{sw}-1} \qquad \text{otherwise.}\end{aligned} \tag{6.3}$$

It is clear that the two matrices $\bar{\mathscr{L}}^{[1]}$ and $\bar{\mathscr{L}}^{[2]}$ are commutative with respect to each other, and eigenvalues of these two matrices are all real. Then the transverse MSEs can be written as

$$\begin{aligned}\delta\dot{x}_{1i} &= -\delta y_1 - \delta z_1 - \epsilon_1\gamma_i^{[1]}\delta x_1,\\ \delta\dot{y}_{1i} &= \delta x_1 + a\ \delta y_1 - \epsilon_2\gamma_i^{[2]}\delta y_1 + \lambda(\delta y_2 - \delta y_1),\\ \delta\dot{z}_{1i} &= z_1\delta x_1 + (x_1 - c)\delta z_1,\\ \delta\dot{x}_{2i} &= -\delta y_2 - \delta z_2 - \epsilon_1\gamma_i^{[1]}\delta x_2,\\ \delta\dot{y}_{2i} &= \delta x_2 + a\ \delta y_2 - \epsilon_2\gamma_i^{[2]}\delta y_2 + \lambda(\delta y_1 - \delta y_2),\\ \delta\dot{z}_{2i} &= z_2\delta x_2 + (x_2 - c)\delta z_2.\end{aligned} \tag{6.4}$$

Here $i\in\mathbf{N}_2$ and (x_1,y_1,z_1), (x_2,y_2,z_2) are the state variables of the synchronization manifolds for layer-1 and layer-2, respectively, satisfying

$$\begin{aligned}\dot{x}_1 &= -y_1 - z_1,\\ \dot{y}_1 &= x_1 + a\ y_1 + \lambda(y_2 - y_1),\\ \dot{z}_1 &= b + z_1(x_1 - c),\\ \dot{x}_2 &= -y_2 - z_2,\\ \dot{y}_2 &= x_2 + a\ y_2 + \lambda(y_1 - y_2),\\ \dot{z}_2 &= b + z_2(x_2 - c).\end{aligned} \tag{6.5}$$

We calculate all the Lyapunov exponents of the above six-dimensional system for each $i\in\mathbf{N}_2$. The transition from desynchrony to synchrony is characterized through a maximum Lyapunov exponent (MLE) Λ_{max} of the transverse master stability equation (6.4). The MLE of each of these $N-1$ transverse error systems is drawn in the color-coded Figure 5(a) with respect to the interaction strength ϵ_2 in the x-axis, and the y-axis depicts the index of transverse error dynamics; the color bar shows the variation of the MLE of the transverse systems. The interaction strength of the other tier is kept fixed at $\epsilon_1 = 0.03$ and the interlayer coupling strength at $\lambda = 1.0$. Figure 5(a) describes that the critical coupling strength required to stabilize the error systems (6.4) monotonically decreases as i increases. That is, as ϵ_2 gradually increases, 200th error dynamics first stabilize and then second error dynamics stabilize after stabilization of all other subsystems. Hence, the variation of MLE in the most unstable direction corresponding to the subsystem $i = 2$ signifies the transition from synchronization to desynchronization states of the layer in the network. For the coherent oscillation, all error dynamics stabilize at the origin. Therefore, they all stabilize at the critical coupling strength where the intralayer coherence stabilizes when oscillation of the transverse systems vanishes.

To gauge this transition scenario, we plot the bifurcation diagram of δx_2 against the coupling strength ϵ_2 in Figure 5(b). The black dot, red dot, and open circle denote the unstable fixed point, stable steady state, and stable oscillation states, respectively.

Here the transition from the oscillatory to the steady state appears through the Hopf bifurcation (HB) and the critical transition point of this least stable error system is also reflected in Figure 5(a). The vanishing of δx_2 versus ϵ_2 refers to the synchronized states in each layer.

So this numerical experiment confirms our theoretical prediction that the transverse direction corresponding to the smallest nonzero eigenvalue of the average Laplacian matrices for each tier determines the intralayer synchronization transition in the whole network.

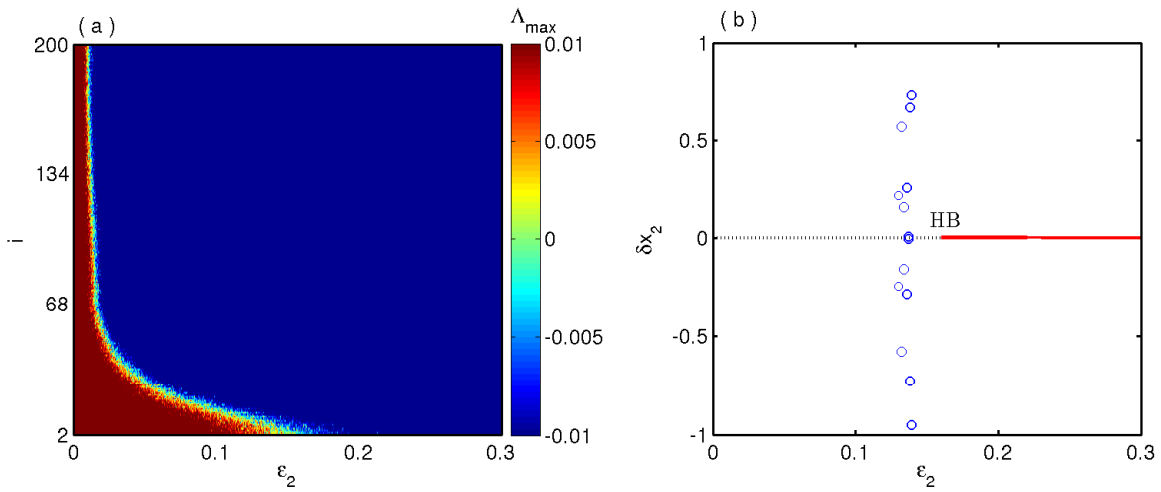

Figure 5. (a) *Maximum Lyapunov exponent of each transverse component of the error system with respect to ϵ_2, which enunciates that system (6.4) corresponds to the least unstable direction for $i = 2$.* (b) *Bifurcation diagram of the least unstable direction with respect to ϵ_2. Other parameters are $\epsilon_1 = 0.03$ and $\lambda = 1.0$.*

Thus by Corollary 4.3 we calculate the MLE of the block-diagonal transverse error dynamics to analyze the stability of the synchronization states. The intralayer synchronization assimilates with respect to the stability of the transverse error dynamics. Among all the Lyapunov exponents, let Λ_{max} be the maximum one. The variation of Λ_{max} as a function of the system parameters and network parameters yields the necessary and sufficient conditions for the intralayer synchronization state when $\Lambda_{max} < 0$. Then the perturbations transverse to the synchronization die out and both of the layers evolve in unison. So the negativity of Λ_{max} obtained from linearized equation (6.4) together with nonlinear equation (6.5) implies stable intralayer coherence.

The variation of Λ_{max} corresponding to Figure 3 is plotted in color-coded Figure 6 for the parameter space of (ϵ_2, λ). The color bar shows the variation of Λ_{max}, where colors below 0 value signify the intralayer synchronous state. The variation of Λ_{max} as a function of ϵ_2 and λ are plotted in Figures 6(a), 6(b), 6(c), and 6(d) respectively for $\epsilon_1 = 0.0$, $\epsilon_1 = 0.015$, $\epsilon_1 = 0.03$, and $\epsilon_1 = 0.045$. In these figures, the regions of the negative MLE of the transverse error systems and the region of the zero synchronization error in Figure 3 of

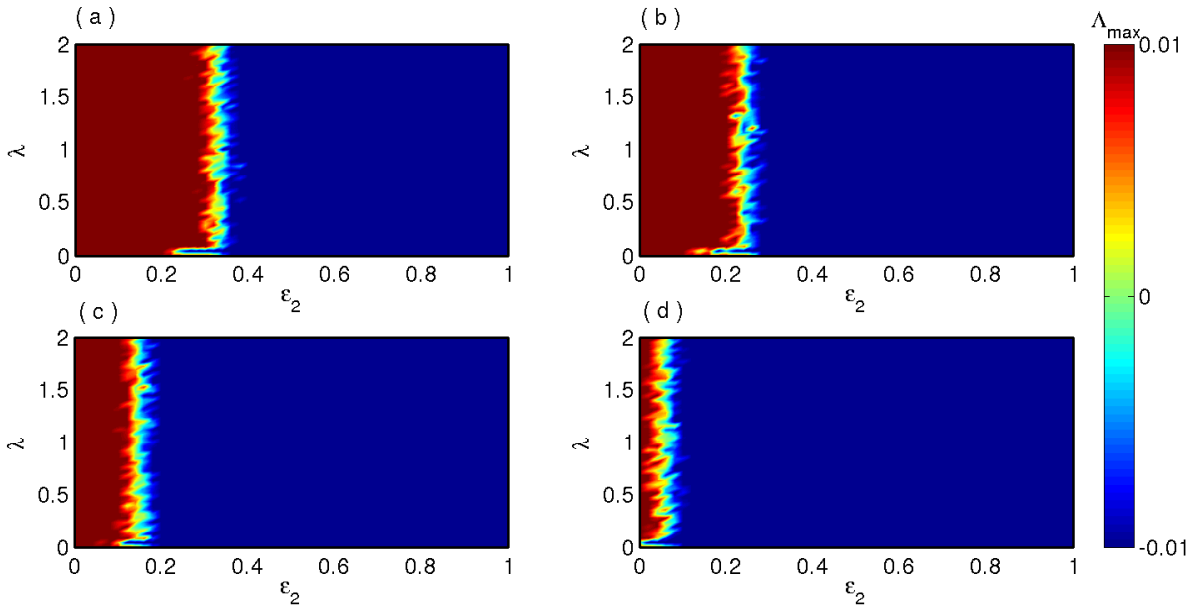

Figure 6. *MLE of the transverse error system for* (a) $\epsilon_1 = 0.0$, (b) $\epsilon_1 = 0.015$, (c) $\epsilon_1 = 0.03$, *and* (d) $\epsilon_1 = 0.045$. *Other parameters are* $d_{sw} = 4$, $p_{ws} = 0.1$, *and* $p_r = 0.015$.

the dynamic network for $f = 100.0$ are exactly identical. So the linear stability analysis of the time-average network exactly matches the numerical results of the time-varying networks for sufficiently fast switching. Hence, our analytical results are verified by taking multiplex temporal hypernetworks of Rössler oscillators.

Next, we investigate the simultaneous effect of the network probability p_r and the coupling strength ϵ_1 corresponding to tier-1 interaction on the intralayer synchronization for the fast-switching case. Here the synchronization transitions are characterized through the variation of the MLE of the error systems in the transverse direction delineated in the color-coded Figure 7. The deep red and blue regions in Figure 7 correspond to the desynchronized and synchronized states, respectively. The desynchronization and synchronization regions are plotted for various values of the intralayer coupling values ϵ_2 with fixed values of $d_{sw} = 4$ and $p_{ws} = 0.1$. For small values of the $\epsilon_2 = 0.15$ (Figure 7(a)), higher ER probability p_r is required of each individual layer to attain the synchrony and the critical transition point of p_r decreases with the increasing values of ϵ_1. In Figure 7(b), when ϵ_2 is increased at $\epsilon_2 = 0.2$, a slight enhancement of synchrony is observed in the (ϵ_1, p_r) plane compared to the previous one. However, for a greater increment of $\epsilon_2 = 0.25$ and $\epsilon_2 = 0.3$, the significant enhancement of the intralayer synchrony is observed in Figures 7(c) and 7(d), respectively. Here the enlargement of the synchronization regions occurs due to the increased values of the intralayer coupling strength of one layer.

Note that the combined effect of the speedy rewiring links and the higher values of the intralayer coupling strength leads to the enlargement of the intralayer synchrony domains and shrinking the desynchronized regions.

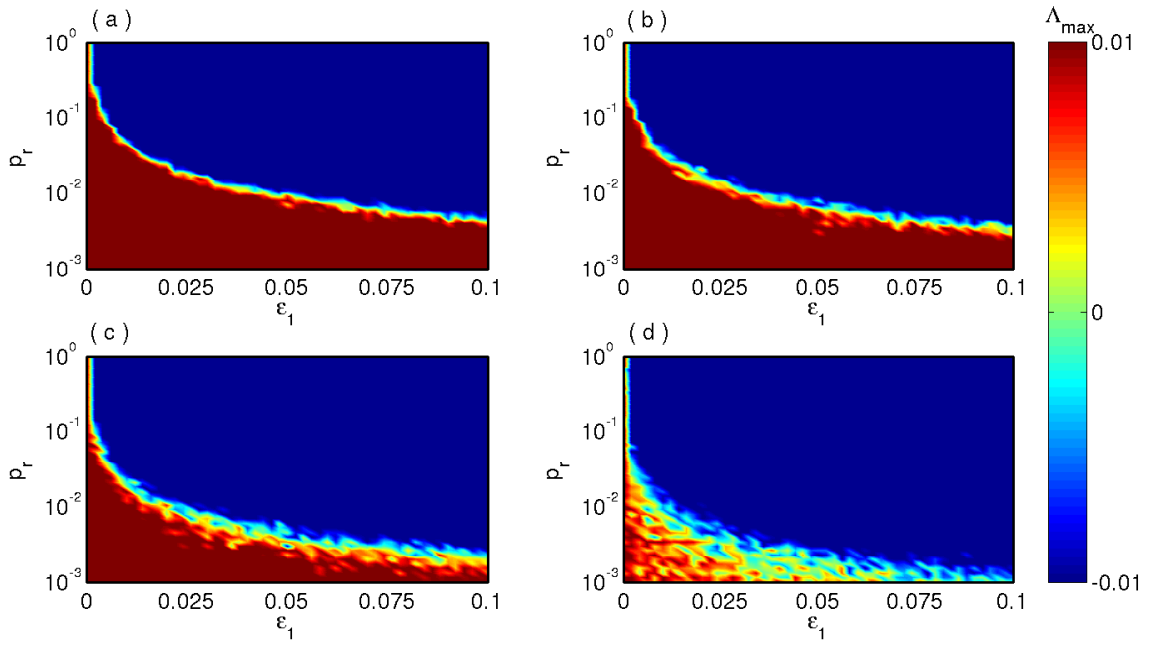

Figure 7. *MLE of the transverse error system in the* (ϵ_1, p_r) *parameter plane for* (a) $\epsilon_2 = 0.15$, (b) $\epsilon_2 = 0.2$, (c) $\epsilon_2 = 0.25$, *and* (d) $\epsilon_2 = 0.3$. *Other parameters are* $d_{sw} = 4$, $p_{ws} = 0.1$, *and* $\lambda = 1.0$.

Similarly, in Figure 8, we investigate the influence of the probability p_{sw} of the small-world network and its interaction strength ϵ_2 on the emergence of the intralayer synchronization states. The synchronized and desynchronized regions in Figure 8 are measured through the MSF characterization by considering several specific values of the intralayer coupling constants $\epsilon_1 = 0.0,\ 0.015,\ 0.03$, and 0.045 in Figures 8(a)–(d). Here also the synchronization region is dominated for higher values of the intralayer coupling values. Also, for sufficiently fast rewiring, links in the hypernetwork and larger values of $\epsilon_{1,2}$ give rise to reducing the small-world probability against the intralayer coupling strength for the intralayer synchronization states.

7. Conclusions and future problems. In this paper, we have carried out a detailed analysis of the stability of the complete intralayer synchronization properties in a time-varying multiplex hypernetwork. The main result of this paper specifically builds on the concept of the fast-switching stability criterion and the MSF approach. Using the fast-switching stability criterion, we show the following.

If a dynamical hypernetwork in a multiplex structure possesses intralayer synchronization in the static time-average network topology, then for a sufficiently fast switching case, each layer of the time-varying multiplex hypernetwork will also be synchronized.

So the stability of intralayer synchronization for a specific averaged system implies the stability of original systems for sufficiently fast switching. Using the master stability framework, the stability condition of this state is derived analytically and we generalize the results in the time-varying network architecture in terms of a time-average network.

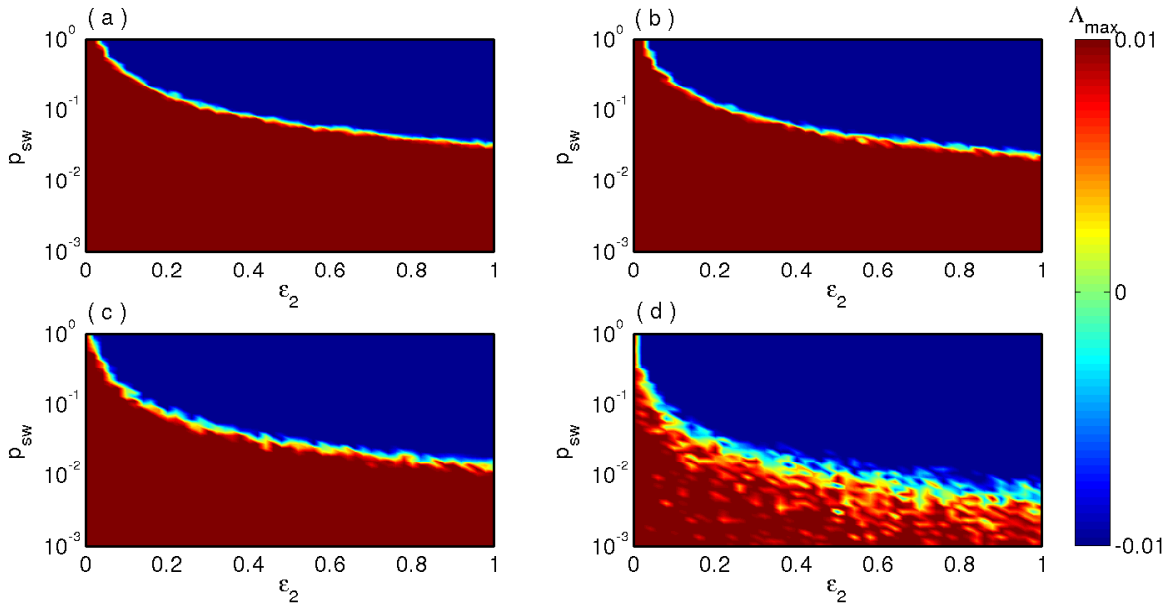

Figure 8. *Variation of the MLE of the transverse error system for* (a) $\epsilon_1 = 0.0$, (b) $\epsilon_1 = 0.015$, (c) $\epsilon_1 = 0.03$, *and* (d) $\epsilon_1 = 0.045$. *Other parameters are* $d_{sw} = 4$, $p_r = 0.015$, *and* $\lambda = 1.0$.

For verification of the analytical results, we have considered the paradigmatic chaotic Rössler oscillator as nodal dynamics of the hypernetwork and found that our numerical results are perfectly matched with our obtained analytical conditions. Finally, we have explored our proposed mechanism on the effect of the coupling strength after the existence of the synchronization manifold. The stability of intralayer synchronization in the time-varying multilayer hypernetwork is also derived. We try to make progress towards developing a general approach to study the stability of intralayer synchronization of time-varying multilayer hypernetwork architecture. Further, by numerical experiments, we have shown that the spectrum of the time-average graph Laplacian together with the MSF formalism works well to accurately predict intralayer synchronization. The synchrony concept of this multiplex hypernetwork offers studying a large variety of complex systems, including mobile networks, ecological networks, neural networks, and many natural phenomena, where the time-varying features are typical.

The interplay between multilayer structure and dynamics still remains unexplored. Especially the study of synchronization under temporal network architecture remains in infancy. In the future, the stability of the intralayer synchronization state in temporal multilayer hypernetworks for nonfast rewiring may be studied. For this, the nonfast stability criterion which was recently developed [18, 37] can be used. The global stability of the intralayer synchronization in the temporal multilayer networks in the presence of different interaction tiers is also an interesting problem and may be studied further.

Appendix A. Proof of corollaries.

Proof of Corollary 4.3. Since the time-average Laplacian matrices $\bar{\mathscr{L}}^{[\alpha]}$, $\alpha = 1, 2, \ldots, M$, are real symmetric, their eigenvalues are all real and each of them can be diagonalizable over

the field $\mathbb{R}$ by the orthogonal basis of eigenvectors $V^{[\alpha]}$.

Additionally, there exists a time-average Laplacian (say $\bar{\mathscr{L}}^{[1]}$) which commutes with all other time-average Laplacians. So $\bar{\mathscr{L}}^{[1]}$ and $\bar{\mathscr{L}}^{[\alpha]}$ share a common eigenspace. In other words, they have the common orthogonal basis of eigenvectors, i.e., $V^{[1]} = V^{[\alpha]}$ for all $\alpha = 1, 2, \ldots, M$. Hence, all the matrices $\bar{\mathscr{L}}^{[\alpha]}$ can be simultaneously diagonalizable by $V^{[1]}$. So from (4.7), we obtain ${V^{[1]}}^{-1}\bar{\mathscr{L}}^{[\alpha]}V^{[1]} = \operatorname{diag}\{0 < \gamma_2^{[\alpha]} \le \gamma_3^{[\alpha]} \le \cdots \le \gamma_N^{[\alpha]}\}$.

Therefore, all the terms of the transverse equations (4.8b), (4.8d) become block-diagonal. So their stability is equivalent to the stability of the uncoupled systems,

(A.1)
$$\begin{aligned}
\dot{\eta}_{T_i}^{(\mathbf{w})} &= JF_1(\mathbf{x}_0)\eta_{T_i}^{(\mathbf{w})} - \sum_{\alpha=1}^{M} \epsilon_\alpha \gamma_i^{[\alpha]} JG_\alpha^{[1]}(\mathbf{x}_0)\eta_{T_i}^{(\mathbf{w})} + \lambda\Big[JH_1(\mathbf{x}_0, \mathbf{y}_0)\eta_{T_i}^{(\mathbf{w})} + DH_1(\mathbf{x}_0, \mathbf{y}_0)\eta_{T_i}^{(\mathbf{z})}\Big],\\
\dot{\eta}_{T_i}^{(\mathbf{z})} &= JF_2(\mathbf{y}_0)\eta_{T_i}^{(\mathbf{z})} - \sum_{\alpha=1}^{M} \epsilon_\alpha \gamma_i^{[\alpha]} JG_\alpha^{[2]}(\mathbf{y}_0)\eta_{T_i}^{(\mathbf{z})} + \lambda\Big[JH_2(\mathbf{y}_0, \mathbf{x}_0)\eta_{T_i}^{(\mathbf{z})} + DH_2(\mathbf{y}_0, \mathbf{x}_0)\eta_{T_i}^{(\mathbf{w})}\Big],
\end{aligned}$$

$i \in \mathbf{N}_2$. So we are now able to decouple the effect of the coupling function from the structure of the network. Since the Jacobians of the functions are evaluated at the synchronization state, they are the same for each block. For each i, the form of the entire equation is the same but only differs by the scalar multiplier $\epsilon_\alpha \gamma_i^{[\alpha]}$. ∎

Proof of Corollary 4.4. From the hypothesis, we have each layer of the multiplex hypernetwork consisting of two tiers. Between these two tiers, the eigenvalues of the Laplacian matrix of one tier (say $\bar{\mathscr{L}}^{[1]}$) are 0 with algebraic multiplicity 1 and $\bar{a}$ with algebraic multiplicity $N-1$. In addition, $\bar{\mathscr{L}}^{[1]}$ is diagonalizable, i.e.,

$$ {V^{[1]}}^{-1}\bar{\mathscr{L}}^{[1]}V^{[1]} = \operatorname{diag} = \{0, \underbrace{\bar{a}, \bar{a}, \ldots, \bar{a}}_{(N-1)\text{ times}}\}. $$

We have

$$ {V^{[1]}}^{-1}\bar{\mathscr{L}}^{[2]}V^{[1]} = \begin{bmatrix} 0 & \bar{U}_1^{[2]} \\ O_{N-1\times 1} & \bar{U}_2^{[2]} \end{bmatrix}. $$

Now the transverse error dynamics can be rewritten as

(A.2)
$$\begin{aligned}
\dot{\eta}_T^{(\mathbf{w})} &= I_{N-1} \otimes JF_1(\mathbf{x}_0)\eta_T^{(\mathbf{w})} - \Big[\epsilon_1 \bar{a} I_{N-1} \otimes JG_1^{[1]}(\mathbf{x}_0) + \epsilon_2 \bar{U}_2^{[2]} \otimes JG_2^{[1]}(\mathbf{x}_0)\Big]\eta_T^{(\mathbf{w})}\\
&\quad + \lambda\Big[I_{N-1} \otimes JH_1(\mathbf{x}_0, \mathbf{y}_0)\eta_T^{(\mathbf{w})} + I_{N-1} \otimes DH_1(\mathbf{x}_0, \mathbf{y}_0)\eta_T^{(\mathbf{z})}\Big],\\
\dot{\eta}_T^{(\mathbf{z})} &= I_{N-1} \otimes JF_2(\mathbf{y}_0)\eta_T^{(\mathbf{z})} - \Big[\epsilon_1 \bar{a} I_{N-1} \otimes JG_1^{[2]}(\mathbf{y}_0) + \epsilon_2 \bar{U}_2^{[2]} \otimes JG_2^{[2]}(\mathbf{y}_0)\Big]\eta_T^{(\mathbf{z})}\\
&\quad + \lambda\Big[I_{N-1} \otimes JH_2(\mathbf{y}_0, \mathbf{x}_0)\eta_T^{(\mathbf{z})} + I_{N-1} \otimes DH_2(\mathbf{y}_0, \mathbf{x}_0)\eta_T^{(\mathbf{w})}\Big].
\end{aligned}$$

Here $\bar{U}_2^{[2]}$ is a square matrix of order $N-1$. Let $V_2^{[2]}$ be a matrix of eigenvectors of the matrix $\bar{U}_2^{[2]}$. Also, ${V_2^{[2]}}^{-1}\bar{U}_2^{[2]}V_2^{[2]} = S^{[2]}$ is an upper triangular matrix. Now, again projecting the transverse error components onto the eigenspace of $\bar{U}_2^{[2]}$, we have $\zeta_T^{(\mathbf{w})} = \big(V_2^{[2]} \otimes I_d\big)^{-1}\eta_T^{(\mathbf{w})}$

and $\zeta_T^{(\mathbf{z})} = \left(V_2^{[2]} \otimes I_d\right)^{-1} \eta_T^{(\mathbf{z})}$. Then the new projected transverse error system can be written as

$$\begin{aligned}
\dot{\zeta}_{T_i}^{(\mathbf{w})} &= JF_1(\mathbf{x}_0)\zeta_{T_i}^{(\mathbf{w})} - \Big[\epsilon_1 \bar{a} JG_1^{[1]}(\mathbf{x}_0)\zeta_{T_i}^{(\mathbf{w})} + \epsilon_2 \sum_{j=i}^{N-1} S^{[2]} JG_2^{[1]}(\mathbf{x}_0)\zeta_{T_j}^{(\mathbf{w})}\Big] \\
&\quad + \lambda\Big[JH_1(\mathbf{x}_0, \mathbf{y}_0)\zeta_{T_i}^{(\mathbf{w})} + DH_1(\mathbf{x}_0, \mathbf{y}_0)\zeta_{T_i}^{(\mathbf{z})}\Big], \\
\dot{\zeta}_{T_i}^{(\mathbf{z})} &= JF_2(\mathbf{y}_0)\zeta_{T_i}^{(\mathbf{z})} - \Big[\epsilon_1 \bar{a} JG_1^{[2]}(\mathbf{y}_0)\zeta_{T_i}^{(\mathbf{z})} + \epsilon_2 \sum_{j=i}^{N-1} S^{[2]} JG_2^{[2]}(\mathbf{y}_0)\zeta_{T_j}^{(\mathbf{z})}\Big] \\
&\quad + \lambda\Big[JH_2(\mathbf{y}_0, \mathbf{x}_0)\zeta_{T_i}^{(\mathbf{z})} + DH_2(\mathbf{y}_0, \mathbf{x}_0)\zeta_{T_i}^{(\mathbf{w})}\Big],
\end{aligned} \tag{A.3}$$

$i = 1, 2, \ldots, N-1$. Again, if $\bar{U}_2^{[2]}$ is a real symmetric matrix, $S^{[2]}$ will become a diagonal matrix whose diagonal elements are the eigenvalues of $\bar{U}_2^{[2]}$, say $\nu_1, \nu_2, \ldots, \nu_{N-1}$. Accordingly, (A.3) becomes $N-1$ decoupled equations

$$\begin{aligned}
\dot{\zeta}_{T_i}^{(\mathbf{w})} &= JF_1(\mathbf{x}_0)\zeta_{T_i}^{(\mathbf{w})} - \Big[\epsilon_1 \bar{a} JG_1^{[1]}(\mathbf{x}_0) + \epsilon_2 \nu_i JG_2^{[1]}(\mathbf{x}_0)\Big]\zeta_{T_i}^{(\mathbf{w})} + \lambda\Big[JH_1(\mathbf{x}_0, \mathbf{y}_0)\zeta_{T_i}^{(\mathbf{w})} + DH_1(\mathbf{x}_0, \mathbf{y}_0)\zeta_{T_i}^{(\mathbf{z})}\Big], \\
\dot{\zeta}_{T_i}^{(\mathbf{z})} &= JF_2(\mathbf{y}_0)\zeta_{T_i}^{(\mathbf{z})} - \Big[\epsilon_1 \bar{a} JG_1^{[2]}(\mathbf{y}_0) + \epsilon_2 \nu_i JG_2^{[2]}(\mathbf{y}_0)\Big]\zeta_{T_i}^{(\mathbf{z})} + \lambda\Big[JH_2(\mathbf{y}_0, \mathbf{x}_0)\zeta_{T_i}^{(\mathbf{z})} + DH_2(\mathbf{y}_0, \mathbf{x}_0)\zeta_{T_i}^{(\mathbf{w})}\Big]
\end{aligned} \tag{A.4}$$

for $i = 1, 2, \ldots, N-1$. ∎

Proof of Lemma 5.1. If the multilayer hypernetwork (5.1) starts evolving with the intralayer synchronization state at time $t = t_0$, then $\mathbf{x}_i(t_0) = \mathbf{x}_0$ and $\mathbf{y}_i(t_0) = \mathbf{y}_0$ for all $i \in N_1$. Then the velocities of the node i in both of the layers at $t = t_0$ are

$$\begin{aligned}
\dot{\mathbf{x}}_i(t_0) &= F_1(\mathbf{x}_0) - \sum_{\alpha=1}^{M} \epsilon_\alpha \sum_{j=1}^{N} \mathscr{L}_{ij}^{[1,\alpha]}(t_0) G_\alpha^{[1]}(\mathbf{x}_0) + \lambda \sum_{j=1}^{N} \mathscr{B}_{ij}^{[1]} H_1(\mathbf{x}_0, \mathbf{y}_0) \\
&= F_1(\mathbf{x}_0) + \lambda e_i^{[1]} H_1(\mathbf{x}_0, \mathbf{y}_0), \\
\dot{\mathbf{y}}_i(t_0) &= F_2(\mathbf{y}_0) - \sum_{\alpha=1}^{M} \epsilon_\alpha \sum_{j=1}^{N} \mathscr{L}_{ij}^{[2,\alpha]}(t_0) G_\alpha^{[2]}(\mathbf{y}_0) + \lambda \sum_{j=1}^{N} \mathscr{B}_{ij}^{[2]} H_2(\mathbf{y}_0, \mathbf{x}_0) \\
&= F_2(\mathbf{y}_0) + \lambda e_i^{[2]} H_2(\mathbf{y}_0, \mathbf{x}_0).
\end{aligned} \tag{A.5}$$

To maintain the intralayer synchronization state, each individual layer should evolve synchronously. Therefore, the velocities of any two different nodes in layer-1 should be equal, i.e., $\dot{\mathbf{x}}_i(t_0) = \dot{\mathbf{x}}_k(t_0)$ for all $i, k \in N_1$. This yields $e_i^{[1]} = e_k^{[1]}$ for each $i, k \in N_1$. Hence, the interlayer degree of each node in layer-1 should be equal (say $e^{[1]}$).

Similarly, for the complete synchronous evolution of layer-2, we should have $\dot{\mathbf{y}}_i(t_0) = \dot{\mathbf{y}}_k(t_0)$ for all $i, k \in N_1$. These yield $e_i^{[2]} = e_k^{[2]}$. Therefore, the interlayer degree of each node in layer-2 should be identical (say $e^{[2]}$). ∎

Proof of Corollary 5.5. By hypothesis, in the multilayer network architecture, the number of tiers in each layer is one. The corresponding intralayer adjacency matrix $\bar{\mathscr{L}}^{[1]}$ has the set of eigenvalues

$$\{0, \underbrace{\bar{a}, \bar{a}, \ldots, \bar{a}}_{(N-1) \text{ times}}\}.$$

Thus,

$$\bar{U}_2^{[1]} = \mathrm{diag}\{\underbrace{\bar{a}, \bar{a}, \ldots, \bar{a}}_{(N-1) \text{ times}}\},$$

also given that the interlayer adjacency matrices are equal, i.e., $\mathscr{B}^{[1]} = \mathscr{B}^{[2]}$. Therefore, we have that the constant interlayer degree of the nodes in both of the two layers are equal, i.e., $e^{[1]} = e^{[2]} = e$ (say). The eigenvalues of this common interlayer adjacency matrix are $e, \Gamma_2, \Gamma_3, \ldots, \Gamma_N$. Moreover, we have $U_3^{[1]} = U_3^{[2]} = U_3$ (say).

Then, in vectorial form, the transverse error system reduces as

$$\begin{aligned}
\dot{\eta}_T^{(\mathbf{w})} &= I_{N-1} \otimes JF_1(\mathbf{x}_0)\eta_T^{(\mathbf{w})} - \epsilon_1 \bar{a} I_{N-1} \otimes JG_1^{[1]}(\mathbf{x}_0)\eta_T^{(\mathbf{w})} \\
&\quad + \lambda\Big[eI_{N-1} \otimes JH_1(\mathbf{x}_0, \mathbf{y}_0)\eta_T^{(\mathbf{w})} + U_3 \otimes DH_1(\mathbf{x}_0, \mathbf{y}_0)\eta_T^{(\mathbf{z})}\Big], \\
\dot{\eta}_T^{(\mathbf{z})} &= I_{N-1} \otimes JF_2(\mathbf{y}_0)\eta_T^{(\mathbf{z})} - \epsilon_1 \bar{a} I_{N-1} \otimes JG_1^{[2]}(\mathbf{y}_0)\eta_T^{(\mathbf{z})} \\
&\quad + \lambda\Big[eI_{N-1} \otimes JH_2(\mathbf{y}_0, \mathbf{x}_0)\eta_T^{(\mathbf{z})} + U_3 \otimes DH_2(\mathbf{y}_0, \mathbf{x}_0)\eta_T^{(\mathbf{w})}\Big].
\end{aligned} \tag{A.6}$$

As the interlayer adjacency matrices are symmetric, thus U_3 is also a real symmetric matrix of order $N-1$. Then it can be diagonalizable by its basis of eigenvectors. If V_3 is the matrix of eigenvectors of U_3, then we can write $V_3^{-1} U_3 V_3 = \mathrm{diag}\{\Gamma_2, \Gamma_3, \ldots, \Gamma_N\}$.

Again, by projecting the error components $\eta_T^{(\mathbf{w})}$ and $\eta_T^{(\mathbf{z})}$ on the eigenspace of U_3, we have the reprojected transverse error components $\zeta_T^{(\mathbf{w})} = \big(V_2^{[2]} \otimes I_d\big)^{-1}\eta_T^{(\mathbf{w})}$ and $\zeta_T^{(\mathbf{z})} = \big(V_2^{[2]} \otimes I_d\big)^{-1}\eta_T^{(\mathbf{z})}$.

Observe that all the components of (A.6) are block-diagonal except the last one for both of the subequations. But due to this projection that component for the first subequation of (A.6) becomes

$$\begin{aligned}
\big(V_3 \otimes I_d\big)^{-1}\big(U_3 \otimes DH_1(\mathbf{x}_0, \mathbf{y}_0)\big)\big(V_3 \otimes I_d\big) &= V_3^{-1} U_3 V_3 \otimes DH_1(\mathbf{x}_0, \mathbf{y}_0) \\
&= \mathrm{diag}\{\Gamma_2, \Gamma_3, \ldots, \Gamma_N\} \otimes \mathrm{DH}_1(\mathbf{x}_0, \mathbf{y}_0).
\end{aligned}$$

Similarly, after this projection, the corresponding term for the second subequation of (A.6) can be written as $\mathrm{diag}\{\Gamma_2, \Gamma_3, \ldots, \Gamma_N\} \otimes \mathrm{DH}_2(\mathbf{y}_0, \mathbf{x}_0)$.

Now all the coupling terms of (A.6) are decoupled. The required $N-1$ decoupled transverse error system can be written in component form as

$$\begin{aligned}
\dot{\zeta}_{T_i}^{(\mathbf{w})} &= JF_1(\mathbf{x}_0)\zeta_{T_i}^{(\mathbf{w})} - \epsilon_1 \bar{a} JG_1^{[1]}(\mathbf{x}_0)\zeta_{T_i}^{(\mathbf{w})} + \lambda\Big[eJH_1(\mathbf{x}_0, \mathbf{y}_0)\zeta_{T_i}^{(\mathbf{w})} + \Gamma_i DH_1(\mathbf{x}_0, \mathbf{y}_0)\zeta_{T_i}^{(\mathbf{z})}\Big], \\
\dot{\zeta}_{T_i}^{(\mathbf{z})} &= JF_2(\mathbf{y}_0)\zeta_{T_i}^{(\mathbf{z})} - \epsilon_1 \bar{a} JG_1^{[2]}(\mathbf{y}_0)\zeta_{T_i}^{(\mathbf{z})} + \lambda\Big[eJH_2(\mathbf{y}_0, \mathbf{x}_0)\zeta_{T_i}^{(\mathbf{w})} + \Gamma_i DH_2(\mathbf{y}_0, \mathbf{x}_0)\zeta_{T_i}^{(\mathbf{w})}\Big],
\end{aligned} \tag{A.7}$$

where $i = 2, 3, \ldots, N$. ∎

Appendix B. Nonlinear intralayer coupling function with multiplex hypernetwork architecture. The dynamics of the multiplex temporal hypernetwork with a nonlinear intralayer

coupling function can be written as

$$\begin{aligned}\dot{\mathbf{x}}_i &= F_1(\mathbf{x}_i) + \sum_{\alpha=1}^{M} \epsilon_\alpha \sum_{j=1}^{N} \mathscr{A}_{ij}^{[1,\alpha]}(t) G_\alpha^{[1]}(\mathbf{x}_i, \mathbf{x}_j) + \lambda H_1(\mathbf{x}_i, \mathbf{y}_i),\\ \dot{\mathbf{y}}_i &= F_2(\mathbf{y}_i) + \sum_{\alpha=1}^{M} \epsilon_\alpha \sum_{j=1}^{N} \mathscr{A}_{ij}^{[2,\alpha]}(t) G_\alpha^{[2]}(\mathbf{y}_i, \mathbf{y}_j) + \lambda H_2(\mathbf{y}_i, \mathbf{x}_i),\end{aligned} \tag{B.1}$$

where $i \in \mathbf{N}_1$. $G_\alpha^{[l]} : \mathbb{R}^d \times \mathbb{R}^d \to \mathbb{R}^d$ is the vector field of the output vectorial function within the layers for tier α.

Lemma B.1. *For the dynamical multiplex hypernetwork* (B.1) *with nonlinear intralayer coupling, the intralayer synchronization state will be an invariant state if the intralayer degrees of each node in a particular layer are equal.*

Proof. To find the condition of the invariance of the intralayer synchronization state, we will determine in what condition if all oscillators in a particular layer start evolving with identical initial conditions (i.e., $\mathbf{x}_i(t_0) = \mathbf{x}_0$ and $\mathbf{y}_i(t_0) = \mathbf{y}_0$ for $i \in N_1$), their velocities will also be identical (i.e., $\dot{\mathbf{x}}_i(t_0) = \dot{\mathbf{x}}_k(t_0)$ and $\dot{\mathbf{y}}_i(t_0) = \dot{\mathbf{y}}_k(t_0)$ for all $i \neq k$).

At the initial time $t = t_0$ with layerwise identical initial conditions, the velocity of the ith node for both of the layers becomes

$$\begin{aligned}\dot{\mathbf{x}}_i(t_0) &= F_1(\mathbf{x}_0) + \sum_{\alpha=1}^{M} \epsilon_\alpha \sum_{j=1}^{N} \mathscr{A}_{ij}^{[1,\alpha]}(t_0) G_\alpha^{[1]}(\mathbf{x}_0, \mathbf{x}_0) + \lambda H_1(\mathbf{x}_0, \mathbf{y}_0)\\ &= F_1(\mathbf{x}_0) + \sum_{\alpha=1}^{M} \epsilon_\alpha d_i^{[1,\alpha]}(t_0) G_\alpha^{[1]}(\mathbf{x}_0, \mathbf{x}_0) + \lambda H_1(\mathbf{x}_0, \mathbf{y}_0),\\ \dot{\mathbf{y}}_i(t_0) &= F_2(\mathbf{y}_0) + \sum_{\alpha=1}^{M} \epsilon_\alpha \sum_{j=1}^{N} \mathscr{A}_{ij}^{[2,\alpha]}(t_0) G_\alpha^{[2]}(\mathbf{y}_0, \mathbf{y}_0) + \lambda H_2(\mathbf{y}_0, \mathbf{x}_0)\\ &= F_2(\mathbf{y}_0) + \sum_{\alpha=1}^{M} \epsilon_\alpha d_i^{[2,\alpha]}(t_0) G_\alpha^{[2]}(\mathbf{y}_0, \mathbf{y}_0) + \lambda H_2(\mathbf{y}_0, \mathbf{x}_0).\end{aligned} \tag{B.2}$$

Therefore, for two different nodes i and k in layer-1, their velocities will follow $\dot{\mathbf{x}}_i(t_0) = \dot{\mathbf{x}}_k(t_0)$ if and only if $d_i^{[1,\alpha]}(t_0) = d_k^{[1,\alpha]}(t_0)$ for arbitrary intralayer coupling function $G_\alpha^{[1]}(\mathbf{x}_i, \mathbf{x}_j)$.

Similarly, due to the arbitrary intralayer coupling function $G_\alpha^{[2]}(\mathbf{y}_i, \mathbf{y}_j)$ in layer-2, $\dot{\mathbf{y}}_i(t_0) = \dot{\mathbf{y}}_k(t_0)$ holds if and only if $d_i^{[2,\alpha]}(t_0) = d_k^{[2,\alpha]}(t_0)$.

Therefore, for the invariance of the intralayer synchrony, the intralayer degree of each node should be identical for the nonlinear-type coupling functions. However, the intralayer degree of each node in two different layers may differ. ∎

So, for the intralayer synchronization to exist, the in-degree for each node corresponding to each tier in both of the layers should be equal for all time instants t. Diverse in-degree of the nodes is unfavorable for complete synchronization when the coupling function is nonlinear.

We will further assume that the in-degree of the node under tier-α is time-invariant, i.e.,

$$\sum_{j=1}^{N} \mathscr{A}_{ij}^{[l\alpha]}(t) = d^{[\alpha]}, \quad l = 1, 2, \ \alpha = 1, 2, \ldots, M \ \forall \ t \in \mathbb{R}^{+}. \tag{B.3}$$

Let $\mathbf{x}_0$ and $\mathbf{y}_0$ be the state vectors for intralayer synchronous solutions for layer-1 and layer-2, respectively. The dynamics of this synchronization manifold become

$$\begin{aligned} \dot{\mathbf{x}}_0 &= F_1(\mathbf{x}_0) + \sum_{\alpha=1}^{M} \epsilon_\alpha d^{[\alpha]} G_\alpha^{[1]}(\mathbf{x}_0, \mathbf{x}_0) + \lambda H_1(\mathbf{x}_0, \mathbf{y}_0), \\ \dot{\mathbf{y}}_0 &= F_2(\mathbf{y}_0) + \sum_{\alpha=1}^{M} \epsilon_\alpha d^{[\alpha]} G_\alpha^{[2]}(\mathbf{y}_0, \mathbf{y}_0) + \lambda H_2(\mathbf{y}_0, \mathbf{x}_0). \end{aligned} \tag{B.4}$$

If $\delta\mathbf{x}_i(t)$ and $\delta\mathbf{y}_i(t)$ are the small perturbations of the ith node, respectively, for layer-1 and layer-2 around intralayer synchronous solutions, then the dynamics of the error system can be written in vectorial form as

(B.5)

$$\begin{aligned} \delta\dot{\mathbf{x}} &= I_N \otimes JF_1(\mathbf{x}_0)\delta\mathbf{x} + \sum_{\alpha=1}^{M} \epsilon_\alpha d^{[\alpha]} \Big[I_N \otimes JG_\alpha^{[1]}(\mathbf{x}_0, \mathbf{x}_0) + I_N \otimes DG_\alpha^{[1]}(\mathbf{x}_0, \mathbf{x}_0) \Big] \delta\mathbf{x} \\ &\quad - \sum_{\alpha=1}^{M} \epsilon_\alpha \mathscr{L}^{[1,\alpha]}(t) \otimes DG_\alpha^{[1]}(\mathbf{x}_0, \mathbf{x}_0)\delta\mathbf{x} + \lambda \Big[I_N \otimes JH_1(\mathbf{x}_0, \mathbf{y}_0)\delta\mathbf{x} + I_N \otimes DH_1(\mathbf{x}_0, \mathbf{y}_0)\delta\mathbf{y} \Big], \\ \delta\dot{\mathbf{y}} &= I_N \otimes JF_2(\mathbf{y}_0)\delta\mathbf{y} + \sum_{\alpha=1}^{M} \epsilon_\alpha d^{[\alpha]} \Big[I_N \otimes JG_\alpha^{[2]}(\mathbf{y}_0, \mathbf{y}_0) + I_N \otimes DG_\alpha^{[2]}(\mathbf{y}_0, \mathbf{y}_0) \Big] \delta\mathbf{y} \\ &\quad - \sum_{\alpha=1}^{M} \epsilon_\alpha \mathscr{L}^{[2,\alpha]}(t) \otimes DG_\alpha^{[2]}(\mathbf{y}_0, \mathbf{y}_0)\delta\mathbf{y} + \lambda \Big[I_N \otimes JH_2(\mathbf{y}_0, \mathbf{x}_0)\delta\mathbf{y} + I_N \otimes DH_2(\mathbf{y}_0, \mathbf{x}_0)\delta\mathbf{x} \Big], \end{aligned}$$

where $JG_\alpha^{[l]}(\mathbf{x}_0, \mathbf{x}_0) = \frac{\partial G_\alpha^{[l]}(\mathbf{x},\mathbf{y})}{\partial \mathbf{x}}|_{(\mathbf{x},\mathbf{y})=(\mathbf{x}_0,\mathbf{x}_0)}$, $DG_\alpha^{[l]}(\mathbf{x}_0, \mathbf{x}_0) = \frac{\partial G_\alpha^{[l]}(\mathbf{x},\mathbf{y})}{\partial \mathbf{y}}|_{(\mathbf{x},\mathbf{y})=(\mathbf{x}_0,\mathbf{x}_0)}$ and $\delta\mathbf{x}(t) = [\delta\mathbf{x}_1(t)^{tr}, \delta\mathbf{x}_2(t)^{tr}, \ldots, \delta\mathbf{x}_N(t)^{tr}]^{tr}$ and $\delta\mathbf{y}(t) = [\delta\mathbf{y}_1(t)^{tr}, \delta\mathbf{y}_2(t)^{tr}, \ldots, \delta\mathbf{y}_N(t)^{tr}]^{tr}$ are the collection of perturbations of all oscillators. Then $\bar{\mathscr{L}}^{[\alpha]}$ is the time-average matrix of the temporal Laplacian matrix $\mathscr{L}^{[l,\alpha]}(t)$, $l = 1, 2$, $\alpha = 1, 2, \ldots, M$.

Lemma B.2. *If $d^{[\alpha]}$ is the constant in-degree of each node for tier-α for all times t in both of the layers, then $\bar{\mathscr{L}}_{ii}^{[\alpha]} = d^{[\alpha]}$.*

Although the proof of this lemma is trivial, we provide it nonetheless for the reader's guidance.

Proof. Here $d^{[\alpha]}$ is the constant in-degree of each node for the tier-α for all times t in both of the layers. Therefore,

$$\sum_{j=1}^{N} \mathscr{A}_{ij}^{[l\alpha]}(t) = d^{[\alpha]} \quad \Rightarrow \quad \mathscr{L}_{ii}^{[l,\alpha]}(t) = d^{[\alpha]}.$$

Now $\bar{\mathscr{L}}_{ii}^{[\alpha]} = \frac{1}{T}\int_t^{t+T} \mathscr{L}_{ii}^{[l,\alpha]}(\tau)\, d\tau = d^{[\alpha]}$. So $d^{[\alpha]}$ is the average in-degree of each node in tier-α. ∎

Lemma B.3. *The time-average adjacency matrix for tier-α in layer-l is*

$$\frac{1}{T}\int_t^{t+T} \mathscr{A}^{[l,\alpha]}(\tau)\, d\tau = d^{[\alpha]} I_N - \bar{\mathscr{L}}^{[\alpha]}.$$

We denote it by $\bar{\mathscr{A}}^{[\alpha]}$.

Proof. Each component of the time-average adjacency matrix is

$$\begin{aligned}\frac{1}{T}\int_t^{t+T} \mathscr{A}_{ij}^{[l,\alpha]}(\tau)\, d\tau &= \frac{1}{T}\int_t^{t+T} \left[d^{[\alpha]}\delta_j^i - \mathscr{L}_{ij}^{[l,\alpha]}(\tau)\right] d\tau \\ &= d^{[\alpha]}\delta_j^i - \frac{1}{T}\int_t^{t+T} \mathscr{L}_{ij}^{[l,\alpha]}(\tau)\, d\tau \\ &= d^{[\alpha]}\delta_j^i - \bar{\mathscr{L}}_{ij}^{[\alpha]}.\end{aligned}$$

Hence, we have $\bar{\mathscr{A}}^{[\alpha]} = d^{[\alpha]} I_N - \bar{\mathscr{L}}^{[\alpha]}$. ∎

It is clear that like average Laplacian matrices, the adjacency matrices are also independent of the layers due to the same topological structure of a particular tier for both of the layers.

The equation of motion of the time-static multiplex hypernetwork with these averaged Laplacian matrices can be written as

$$\begin{aligned}\dot{\mathbf{w}}_i &= F_1(\mathbf{w}_i) + \sum_{\alpha=1}^{M} \epsilon_\alpha \sum_{j=1}^{N} \bar{\mathscr{A}}_{ij}^{[\alpha]} G_\alpha^{[1]}(\mathbf{w}_i, \mathbf{w}_j) + \lambda H_1(\mathbf{w}_i, \mathbf{z}_i), \\ \dot{\mathbf{z}}_i &= F_2(\mathbf{z}_i) + \sum_{\alpha=1}^{M} \epsilon_\alpha \sum_{j=1}^{N} \bar{\mathscr{A}}_{ij}^{[\alpha]} G_\alpha^{[2]}(\mathbf{z}_i, \mathbf{z}_j) + \lambda H_2(\mathbf{z}_i, \mathbf{w}_i).\end{aligned} \tag{B.6}$$

It is clear that the equation of motions of the intralayer synchronous manifolds for time-varying and time-average networks are same. Therefore, for the time-average system (B.6), the state vectors for the intralayer synchronization are $\mathbf{x}_0(t)$ and $\mathbf{y}_0(t)$, respectively, for layer-1 and layer-2, with equation of motion (B.4).

Considering the error vectors $\delta\mathbf{w}$ and $\delta\mathbf{z}$ for layer-1 and layer-2, respectively, their dynamics can be written as

(B.7)

$$\begin{aligned}\delta\dot{\mathbf{w}} &= I_N \otimes JF_1(\mathbf{x}_0)\delta\mathbf{w} + \sum_{\alpha=1}^{M} \epsilon_\alpha d^{[\alpha]} \left[I_N \otimes JG_\alpha^{[1]}(\mathbf{x}_0, \mathbf{x}_0) + I_N \otimes DG_\alpha^{[1]}(\mathbf{x}_0, \mathbf{x}_0)\right]\delta\mathbf{w} \\ &\quad - \sum_{\alpha=1}^{M} \epsilon_\alpha \bar{\mathscr{L}}^{[\alpha]} \otimes DG_\alpha^{[1]}(\mathbf{x}_0, \mathbf{x}_0)\delta\mathbf{w} + \lambda\left[I_N \otimes JH_1(\mathbf{x}_0, \mathbf{y}_0)\delta\mathbf{w} + I_N \otimes DH_1(\mathbf{x}_0, \mathbf{y}_0)\delta\mathbf{z}\right], \\ \delta\dot{\mathbf{z}} &= I_N \otimes JF_2(\mathbf{y}_0)\delta\mathbf{z} + \sum_{\alpha=1}^{M} \epsilon_\alpha d^{[\alpha]} \left[I_N \otimes JG_\alpha^{[2]}(\mathbf{y}_0, \mathbf{y}_0) + I_N \otimes DG_\alpha^{[2]}(\mathbf{y}_0, \mathbf{y}_0)\right]\delta\mathbf{z} \\ &\quad - \sum_{\alpha=1}^{M} \epsilon_\alpha \bar{\mathscr{L}}^{[\alpha]} \otimes DG_\alpha^{[2]}(\mathbf{y}_0, \mathbf{y}_0)\delta\mathbf{z} + \lambda\left[I_N \otimes JH_2(\mathbf{y}_0, \mathbf{x}_0)\delta\mathbf{z} + I_N \otimes DH_2(\mathbf{y}_0, \mathbf{x}_0)\delta\mathbf{w}\right].\end{aligned}$$

To decompose the error vectors $\delta\mathbf{w}(t)$ and $\delta\mathbf{z}(t)$ into parallel and transverse modes, we project the error vectors onto the matrix of the eigenvectors $V^{[1]}$ of $\bar{\mathscr{L}}^{[1]}$ corresponding to tier-1. Then the Schur transformations $\eta^{(\mathbf{w})} = \left(V^{[1]} \otimes I_d\right)^{-1}\delta\mathbf{w}$ and $\eta^{(\mathbf{z})} = \left(V^{[1]} \otimes I_d\right)^{-1}\delta\mathbf{z}$ yield (B.7) as

(B.8)

$$\begin{aligned}
\dot{\eta}^{(\mathbf{w})} &= I_N \otimes JF_1(\mathbf{x}_0)\eta^{(\mathbf{w})} + \sum_{\alpha=1}^{M} \epsilon_\alpha d^{[\alpha]} \Big[I_N \otimes JG_\alpha^{[1]}(\mathbf{x}_0,\mathbf{x}_0) + I_N \otimes DG_\alpha^{[1]}(\mathbf{x}_0,\mathbf{x}_0)\Big]\eta^{(\mathbf{w})} \\
&\quad - \sum_{\alpha=1}^{M} \epsilon_\alpha \Big(V^{(1)^{-1}} \bar{\mathscr{L}}^{[\alpha]} V^{(1)}\Big) \otimes DG_\alpha^{[1]}(\mathbf{x}_0,\mathbf{x}_0)\eta^{(\mathbf{w})} + \lambda\Big[I_N \otimes JH_1(\mathbf{x}_0,\mathbf{y}_0)\eta^{(\mathbf{w})} + I_N \otimes DH_1(\mathbf{x}_0,\mathbf{y}_0)\eta^{(\mathbf{z})}\Big], \\
\dot{\eta}^{(\mathbf{z})} &= I_N \otimes JF_2(\mathbf{y}_0)\eta^{(\mathbf{z})} + \sum_{\alpha=1}^{M} \epsilon_\alpha d^{[\alpha]} \Big[I_N \otimes JG_\alpha^{[2]}(\mathbf{y}_0,\mathbf{y}_0) + I_N \otimes DG_\alpha^{[2]}(\mathbf{y}_0,\mathbf{y}_0)\Big]\eta^{(\mathbf{z})} \\
&\quad - \sum_{\alpha=1}^{M} \epsilon_\alpha \Big(V^{(1)^{-1}} \bar{\mathscr{L}}^{[\alpha]} V^{(1)}\Big) \otimes DG_\alpha^{[2]}(\mathbf{y}_0,\mathbf{y}_0)\eta^{(\mathbf{z})} + \lambda\Big[I_N \otimes JH_2(\mathbf{y}_0,\mathbf{x}_0)\eta^{(\mathbf{z})} + I_N \otimes DH_2(\mathbf{y}_0,\mathbf{x}_0)\eta^{(\mathbf{w})}\Big].
\end{aligned}$$

Considering the transverse components $\eta_T^{(\mathbf{w})}, \eta_T^{(\mathbf{z})} \in \mathbb{C}^{(N-1)d}$ for $\eta^{(\mathbf{w})}$ and $\eta^{(\mathbf{z})}$, respectively, and using the relation (4.7), the transverse components yield

(B.9)

$$\begin{aligned}
\dot{\eta}_T^{(\mathbf{w})} &= I_{N-1} \otimes JF_1(\mathbf{x}_0)\eta_T^{(\mathbf{w})} + \sum_{\alpha=1}^{M} \epsilon_\alpha d^{[\alpha]} \Big[I_{N-1} \otimes JG_\alpha^{[1]}(\mathbf{x}_0,\mathbf{x}_0) + I_{N-1} \otimes DG_\alpha^{[1]}(\mathbf{x}_0,\mathbf{x}_0)\Big]\eta_T^{(\mathbf{w})} \\
&\quad - \sum_{\alpha=1}^{M} \epsilon_\alpha \bar{U}_2^{[\alpha]} \otimes DG_\alpha^{[1]}(\mathbf{x}_0,\mathbf{x}_0)\eta_T^{(\mathbf{w})} + \lambda\Big[I_{N-1} \otimes JH_1(\mathbf{x}_0,\mathbf{y}_0)\eta_T^{(\mathbf{w})} + I_{N-1} \otimes DH_1(\mathbf{x}_0,\mathbf{y}_0)\eta_T^{(\mathbf{z})}\Big], \\
\dot{\eta}_T^{(\mathbf{z})} &= I_{N-1} \otimes JF_2(\mathbf{y}_0)\eta_T^{(\mathbf{z})} + \sum_{\alpha=1}^{M} \epsilon_\alpha d^{[\alpha]} \Big[I_{N-1} \otimes JG_\alpha^{[2]}(\mathbf{y}_0,\mathbf{y}_0) + I_{N-1} \otimes DG_\alpha^{[2]}(\mathbf{y}_0,\mathbf{y}_0)\Big]\eta_T^{(\mathbf{z})} \\
&\quad - \sum_{\alpha=1}^{M} \epsilon_\alpha \bar{U}_2^{[\alpha]} \otimes DG_\alpha^{[2]}(\mathbf{y}_0,\mathbf{y}_0)\eta_T^{(\mathbf{z})} + \lambda\Big[I_{N-1} \otimes JH_2(\mathbf{y}_0,\mathbf{x}_0)\eta_T^{(\mathbf{z})} + I_{N-1} \otimes DH_2(\mathbf{y}_0,\mathbf{x}_0)\eta_T^{(\mathbf{w})}\Big].
\end{aligned}$$

Considering $\zeta_a(t) = \left[\eta_T^{(\mathbf{w})^{tr}}\ \eta_T^{(\mathbf{z})^{tr}}\right]^{tr}$, the above equation can be written as

$$\dot{\zeta}_a(t) = \left[A(t) + \sum_{\alpha=1}^{M} \epsilon_\alpha \Big(\bar{E}_1^{[\alpha]} \otimes DG_\alpha^{[1]}(\mathbf{x}_0,\mathbf{x}_0) + \bar{E}_2^{[\alpha]} \otimes DG_\alpha^{[2]}(\mathbf{y}_0,\mathbf{y}_0)\Big)\right]\zeta_a(t), \tag{B.10}$$

where

$$A(t) = \begin{bmatrix} A_{11}(t) & \lambda I_{N-1} \otimes DH_1(\mathbf{x}_0,\mathbf{y}_0) \\ \lambda I_{N-1} \otimes DH_2(\mathbf{y}_0,\mathbf{x}_0) & A_{22}(t) \end{bmatrix},$$

$$\begin{aligned}
A_{11}(t) &= I_{N-1} \otimes JF_1(\mathbf{x}_0) + \sum_{\alpha=1}^{M} \epsilon_\alpha d^{[\alpha]} \Big\{I_{N-1} \otimes JG_\alpha^{[1]}(\mathbf{x}_0,\mathbf{x}_0) + I_{N-1} \otimes DG_\alpha^{[1]}(\mathbf{x}_0,\mathbf{x}_0)\Big\} \\
&\quad + \lambda I_{N-1} \otimes JH_1(\mathbf{x}_0,\mathbf{y}_0), \\
A_{22}(t) &= I_{N-1} \otimes JF_2(\mathbf{y}_0) + \sum_{\alpha=1}^{M} \epsilon_\alpha d^{[\alpha]} \Big\{I_{N-1} \otimes JG_\alpha^{[2]}(\mathbf{y}_0,\mathbf{y}_0) + I_{N-1} \otimes DG_\alpha^{[2]}(\mathbf{y}_0,\mathbf{y}_0)\Big\} \\
&\quad + \lambda I_{N-1} \otimes JH_2(\mathbf{y}_0,\mathbf{x}_0),
\end{aligned}$$

and $\bar{E}_1^{[\alpha]} = \begin{bmatrix} \bar{U}_2^{[\alpha]} & O_{N-1\times N-1} \\ O_{N-1\times N-1} & O_{N-1\times N-1} \end{bmatrix}$, $\bar{E}_2^{[\alpha]} = \begin{bmatrix} O_{N-1\times N-1} & O_{N-1\times N-1} \\ O_{N-1\times N-1} & \bar{U}_2^{[\alpha]} \end{bmatrix}$.

Considering the same change of variables for the error dynamics (B.5) corresponding to the temporal network, the error vector $(\delta\mathbf{x}, \delta\mathbf{y})$ transforms as $\eta^{(\mathbf{x})} = \left(V^{[1]} \otimes I_d\right)^{-1}\delta\mathbf{x}$ and $\eta^{(\mathbf{y})} = \left(V^{[1]} \otimes I_d\right)^{-1}\delta\mathbf{y}$, and its equation of motion transforms as

(B.11)

$$\begin{aligned}
\dot{\eta}_T^{(\mathbf{x})} &= I_{N-1} \otimes JF_1(\mathbf{x}_0)\eta_T^{(\mathbf{x})} + \sum_{\alpha=1}^{M} \epsilon_\alpha d^{[\alpha]} \Big[I_{N-1} \otimes JG_\alpha^{[1]}(\mathbf{x}_0, \mathbf{x}_0) + I_{N-1} \otimes DG_\alpha^{[1]}(\mathbf{x}_0, \mathbf{x}_0) \Big] \eta_T^{(\mathbf{x})} \\
&\quad - \sum_{\alpha=1}^{M} \epsilon_\alpha U_2^{[1,\alpha]}(t) \otimes DG_\alpha^{[1]}(\mathbf{x}_0, \mathbf{x}_0)\eta_T^{(\mathbf{x})} + \lambda \Big[I_{N-1} \otimes JH_1(\mathbf{x}_0, \mathbf{y}_0)\eta_T^{(\mathbf{x})} + I_{N-1} \otimes DH_1(\mathbf{x}_0, \mathbf{y}_0)\eta_T^{(\mathbf{y})} \Big], \\
\dot{\eta}_T^{(\mathbf{y})} &= I_{N-1} \otimes JF_2(\mathbf{y}_0)\eta_T^{(\mathbf{y})} + \sum_{\alpha=1}^{M} \epsilon_\alpha d^{[\alpha]} \Big[I_{N-1} \otimes JG_\alpha^{[2]}(\mathbf{y}_0, \mathbf{y}_0) + I_{N-1} \otimes DG_\alpha^{[2]}(\mathbf{y}_0, \mathbf{y}_0) \Big] \eta_T^{(\mathbf{y})} \\
&\quad - \sum_{\alpha=1}^{M} \epsilon_\alpha U_2^{[2,\alpha]}(t) \otimes DG_\alpha^{[2]}(\mathbf{y}_0, \mathbf{y}_0)\eta_T^{(\mathbf{y})} + \lambda \Big[I_{N-1} \otimes JH_2(\mathbf{y}_0, \mathbf{x}_0)\eta_T^{(y)} + I_{N-1} \otimes DH_2(\mathbf{y}_0, \mathbf{x}_0)\eta_T^{(\mathbf{x})} \Big].
\end{aligned}$$

Now decomposing these transformed error dynamics into parallel and transverse directions, the dynamics of the transverse error components $\zeta_d(t) = \left[\eta_T^{(x)^{tr}} \ \eta_T^{(y)^{tr}}\right]^{tr}$ become

$$\dot{\zeta}_d(t) = \left[A(t) + \sum_{\alpha=1}^{M} \epsilon_\alpha \Big(E_1^{[\alpha]}(t) \otimes DG_\alpha^{[1]}(\mathbf{x}_0, \mathbf{x}_0) + E_2^{[\alpha]}(t) \otimes DG_\alpha^{[2]}(\mathbf{y}_0, \mathbf{y}_0) \Big) \right] \zeta_a(t), \tag{B.12}$$

where

$$A(t) = \begin{bmatrix} A_{11}(t) & \lambda I_{N-1} \otimes DH_1(\mathbf{x}_0, \mathbf{y}_0) \\ \lambda I_{N-1} \otimes DH_2(\mathbf{y}_0, \mathbf{x}_0) & A_{22}(t) \end{bmatrix},$$

$$\begin{aligned}
A_{11}(t) &= I_{N-1} \otimes JF_1(\mathbf{x}_0) + \sum_{\alpha=1}^{M} \epsilon_\alpha d^{[\alpha]} \Big\{ I_{N-1} \otimes JG_\alpha^{[1]}(\mathbf{x}_0, \mathbf{x}_0) + I_{N-1} \otimes DG_\alpha^{[1]}(\mathbf{x}_0, \mathbf{x}_0) \Big\} \\
&\quad + \lambda I_{N-1} \otimes JH_1(\mathbf{x}_0, \mathbf{y}_0), \\
A_{22}(t) &= I_{N-1} \otimes JF_2(\mathbf{y}_0) + \sum_{\alpha=1}^{M} \epsilon_\alpha d^{[\alpha]} \Big\{ I_{N-1} \otimes JG_\alpha^{[2]}(\mathbf{y}_0, \mathbf{y}_0) + I_{N-1} \otimes DG_\alpha^{[2]}(\mathbf{y}_0, \mathbf{y}_0) \Big\} \\
&\quad + \lambda I_{N-1} \otimes JH_2(\mathbf{y}_0, \mathbf{x}_0),
\end{aligned}$$

$$\text{and} \quad E_1^{[\alpha]}(t) = \begin{bmatrix} U_2^{[1,\alpha]}(t) & O_{N-1\times N-1} \\ O_{N-1\times N-1} & O_{N-1\times N-1} \end{bmatrix}, \quad E_2^{[\alpha]}(t) = \begin{bmatrix} O_{N-1\times N-1} & O_{N-1\times N-1} \\ O_{N-1\times N-1} & U_2^{[2,\alpha]}(t) \end{bmatrix}.$$

Now clearly $\frac{1}{T}\int_t^{t+T} E_l^{[\alpha]}(\tau)\, d\tau = \bar{E}_l^{[\alpha]}$, $l = 1, 2$.

Therefore, by Lemma 2.3, the time-varying network (B.1) possesses the intralayer synchronization whenever the corresponding time-average static network (B.6) has an asymptotically stable intralayer synchronization solution. So the stability of the intralayer synchronization for both the time-varying and the time-average systems is also equivalent for nonlinear intralayer coupling functions.

In this context, our required transverse MSE being (B.9), it cannot be further reduced to a low-dimensional form. To find the necessary and sufficient conditions for the local stability of the intralayer coherence, we have to calculate all the Lyapunov exponents of this $2d(N-1)$-dimensional equation. The negative Lyapunov exponents give the signature of the stable intralayer coherence state.

Remark B.4. For this multiplex time-varying hypernetwork with a nonlinear intralayer coupling function, the linearized equation parallel to the synchronization manifold can be written as

$$\begin{aligned}
\dot{\eta}_P^{(\mathbf{w})} &= JF_1(\mathbf{x}_0)\eta_P^{(\mathbf{w})} + \sum_{\alpha=1}^{M} \epsilon_\alpha d^{[\alpha]} \Big[JG_\alpha^{[1]}(\mathbf{x}_0, \mathbf{x}_0) + DG_\alpha^{[1]}(\mathbf{x}_0, \mathbf{x}_0) \Big] \eta_P^{(\mathbf{w})} \\
&\quad + \lambda \Big[JH_1(\mathbf{x}_0, \mathbf{y}_0)\eta_P^{(\mathbf{w})} + DH_1(\mathbf{x}_0, \mathbf{y}_0)\eta_P^{(\mathbf{z})} \Big], \\
\dot{\eta}_P^{(\mathbf{z})} &= JF_2(\mathbf{y}_0)\eta_P^{(\mathbf{z})} + \sum_{\alpha=1}^{M} \epsilon_\alpha d^{[\alpha]} \Big[JG_\alpha^{[2]}(\mathbf{y}_0, \mathbf{y}_0) + DG_\alpha^{[2]}(\mathbf{y}_0, \mathbf{y}_0) \Big] \eta_P^{(\mathbf{z})} \\
&\quad + \lambda \Big[JH_2(\mathbf{y}_0, \mathbf{x}_0)\eta_P^{(\mathbf{z})} + DH_2(\mathbf{y}_0, \mathbf{x}_0)\eta_P^{(\mathbf{w})} \Big],
\end{aligned} \tag{B.13}$$

where $\eta_P^{(\mathbf{w})}, \eta_P^{(\mathbf{z})} \in \mathbb{R}^d$.

The dimensional reduction of the transverse error components can further be possible for a few special cases. We illustrate these in the next two corollaries.

Corollary B.5. *Among all the time-average intralayer Laplacians, if one commutes with all others and all are symmetric, then the transverse error dynamics can be decoupled as a $2d$-dimensional $N-1$ number of systems.*

Proof. Without loss of any generality, first assume that $\bar{\mathscr{L}}^{[1]}$ commutes with $\bar{\mathscr{L}}^{[\alpha]}$ for all $\alpha = 2, 3, \ldots, M$. Moreover, by hypothesis, $\bar{\mathscr{L}}^{[\alpha]}$ is real symmetric for all α.

Then there exists a matrix $V^{[1]}$ that consists of a common orthogonal basis of eigenvectors, such that $\bar{\mathscr{L}}^{[\alpha]}$ can be simultaneously diagonalizable by $V^{[1]}$. Therefore, we have ${V^{[1]}}^{-1}\bar{\mathscr{L}}^{[\alpha]}V^{[1]} = \operatorname{diag}\{0, \gamma_2^{[\alpha]}, \gamma_3^{[\alpha]}, \ldots, \gamma_{\mathrm{N}}^{[\alpha]}\}$. Thus, commutative and symmetric Laplacians make $\bar{U}^{[\alpha]}$ a diagonal matrix for all α. Consequently, we have $\bar{U}_2^{[\alpha]} = \operatorname{diag}\{\gamma_2^{[\alpha]}, \gamma_3^{[\alpha]}, \ldots, \gamma_{\mathrm{N}}^{[\alpha]}\}$.

Hence, all the terms of the transverse error system (see (B.9)) of the time-average system become block-diagonal. So its stability is equivalent to the stability of the $2d$-dimensional $N-1$ independent systems

$$\begin{aligned}
\dot{\eta}_{T_i}^{(\mathbf{w})} &= JF_1(\mathbf{x}_0)\eta_{T_i}^{(\mathbf{w})} + \sum_{\alpha=1}^{M} \epsilon_\alpha d^{[\alpha]} \Big[JG_\alpha^{[1]}(\mathbf{x}_0, \mathbf{x}_0) + DG_\alpha^{[1]}(\mathbf{x}_0, \mathbf{x}_0) \Big] \eta_{T_i}^{(\mathbf{w})} \\
&\quad - \sum_{\alpha=1}^{M} \epsilon_\alpha \gamma_i^{[\alpha]} DG_\alpha^{[1]}(\mathbf{x}_0, \mathbf{x}_0)\eta_{T_i}^{(\mathbf{w})} + \lambda \Big[JH_1(\mathbf{x}_0, \mathbf{y}_0)\eta_{T_i}^{(\mathbf{w})} + DH_1(\mathbf{x}_0, \mathbf{y}_0)\eta_{T_i}^{(\mathbf{z})} \Big], \\
\dot{\eta}_{T_i}^{(\mathbf{z})} &= JF_2(\mathbf{y}_0)\eta_{T_i}^{(\mathbf{z})} + \sum_{\alpha=1}^{M} \epsilon_\alpha d^{[\alpha]} \Big[JG_\alpha^{[2]}(\mathbf{y}_0, \mathbf{y}_0) + DG_\alpha^{[2]}(\mathbf{y}_0, \mathbf{y}_0) \Big] \eta_{T_i}^{(\mathbf{z})} \\
&\quad - \sum_{\alpha=1}^{M} \epsilon_\alpha \gamma_i^{[\alpha]} DG_\alpha^{[2]}(\mathbf{y}_0, \mathbf{y}_0)\eta_{T_i}^{(\mathbf{z})} + \lambda \Big[JH_2(\mathbf{y}_0, \mathbf{x}_0)\eta_{T_i}^{(\mathbf{z})} + DH_2(\mathbf{y}_0, \mathbf{x}_0)\eta_{T_i}^{(\mathbf{w})} \Big]
\end{aligned} \tag{B.14}$$

for $i \in \mathbf{N}_2$. ∎

Among these $(N-1)$ transverse equations, the least stable eigendirection becomes

$$\begin{aligned}
\dot{\eta}_{T_2}^{(\mathbf{w})} &= JF_1(\mathbf{x}_0)\eta_{T_2}^{(\mathbf{w})} + \sum_{\alpha=1}^{M} \epsilon_\alpha d^{[\alpha]} \Big[JG_\alpha^{[1]}(\mathbf{x}_0,\mathbf{x}_0) + DG_\alpha^{[1]}(\mathbf{x}_0,\mathbf{x}_0) \Big] \eta_{T_2}^{(\mathbf{w})} \\
&\quad - \sum_{\alpha=1}^{M} \epsilon_\alpha \gamma_2^{[\alpha]} DG_\alpha^{[1]}(\mathbf{x}_0,\mathbf{x}_0)\eta_{T_2}^{(\mathbf{w})} + \lambda \Big[JH_1(\mathbf{x}_0,\mathbf{y}_0)\eta_{T_2}^{(\mathbf{w})} + DH_1(\mathbf{x}_0,\mathbf{y}_0)\eta_{T_2}^{(\mathbf{z})} \Big], \\
\dot{\eta}_{T_2}^{(\mathbf{z})} &= JF_2(\mathbf{y}_0)\eta_{T_2}^{(\mathbf{z})} + \sum_{\alpha=1}^{M} \epsilon_\alpha d^{[\alpha]} \Big[JG_\alpha^{[2]}(\mathbf{y}_0,\mathbf{y}_0) + DG_\alpha^{[2]}(\mathbf{y}_0,\mathbf{y}_0) \Big] \eta_{T_2}^{(\mathbf{z})} \\
&\quad - \sum_{\alpha=1}^{M} \epsilon_\alpha \gamma_2^{[\alpha]} DG_\alpha^{[2]}(\mathbf{y}_0,\mathbf{y}_0)\eta_{T_2}^{(\mathbf{z})} + \lambda \Big[JH_2(\mathbf{y}_0,\mathbf{x}_0)\eta_{T_2}^{(\mathbf{z})} + DH_2(\mathbf{y}_0,\mathbf{x}_0)\eta_{T_2}^{(\mathbf{w})} \Big].
\end{aligned} \tag{B.15}$$

So for the bidirectional intralayer network, if the family of average Laplacian matrices commutes, then the MSE becomes $2d$-dimensional equations.

Corollary B.6. *Let the multiplex hypernetwork consist of two bidirectional tiers in each layer. Among the two corresponding time-average Laplacian matrices, one has eigenvalue zero with algebraic multiplicity one and $\bar{a}$ with algebraic multiplicity $N-1$. Then the transverse error system can be decoupled as $2d$-dimensional $N-1$ systems.*

Proof. Given that $M = 2$, $\bar{\mathscr{L}}^{[1]}$ and $\bar{\mathscr{L}}^{[2]}$ are both symmetric. Without loss of any generality, assume that the set of eigenvalues of $\bar{\mathscr{L}}^{[1]}$ is

$$\{0, \underbrace{\bar{a}, \bar{a}, \ldots, \bar{a}}_{(N-1)\text{ times}}\}.$$

Then we have

$$V^{[1]^{-1}} \bar{\mathscr{L}}^{[1]} V^{[1]} = \operatorname{diag}\{0, \underbrace{\bar{a}, \bar{a}, \ldots, \bar{a}}_{(N-1)\text{ times}}\},$$

which yields

$$\bar{U}_2^{[2]} = \{\underbrace{\bar{a}, \bar{a}, \ldots, \bar{a}}_{(N-1)\text{ times}}\}.$$

Then, in vectorial form, the transverse error dynamics can be written as

$$\begin{aligned}
\dot{\eta}_T^{(\mathbf{w})} &= I_{N-1} \otimes JF_1(\mathbf{x}_0)\eta_T^{(\mathbf{w})} + \sum_{\alpha=1}^{2} \epsilon_\alpha d^{[\alpha]} \Big[I_{N-1} \otimes JG_\alpha^{[1]}(\mathbf{x}_0,\mathbf{x}_0) + I_{N-1} \otimes DG_\alpha^{[1]}(\mathbf{x}_0,\mathbf{x}_0) \Big] \eta_T^{(\mathbf{w})} \\
&\quad - \Big[\epsilon_1 \bar{a} I_{N-1} \otimes DG_1^{[1]}(\mathbf{x}_0,\mathbf{x}_0) + \epsilon_2 \bar{U}_2^{[2]} \otimes DG_2^{[1]}(\mathbf{x}_0,\mathbf{x}_0) \Big] \eta_T^{(\mathbf{w})} \\
&\quad + \lambda \Big[I_{N-1} \otimes JH_1(\mathbf{x}_0,\mathbf{y}_0)\eta_T^{(\mathbf{w})} + I_{N-1} \otimes DH_1(\mathbf{x}_0,\mathbf{y}_0)\eta_T^{(\mathbf{z})} \Big], \\
\dot{\eta}_T^{(\mathbf{z})} &= I_{N-1} \otimes JF_2(\mathbf{y}_0)\eta_T^{(\mathbf{z})} + \sum_{\alpha=1}^{2} \epsilon_\alpha d^{[\alpha]} \Big[I_{N-1} \otimes JG_\alpha^{[2]}(\mathbf{y}_0,\mathbf{y}_0) + I_{N-1} \otimes DG_\alpha^{[2]}(\mathbf{y}_0,\mathbf{y}_0) \Big] \eta_T^{(\mathbf{z})} \\
&\quad - \Big[\epsilon_1 \bar{a} I_{N-1} \otimes DG_1^{[2]}(\mathbf{y}_0,\mathbf{y}_0) + \epsilon_2 \bar{U}_2^{[2]} \otimes DG_2^{[2]}(\mathbf{y}_0,\mathbf{y}_0) \Big] \eta_T^{(\mathbf{z})} \\
&\quad + \lambda \Big[I_{N-1} \otimes JH_2(\mathbf{y}_0,\mathbf{x}_0)\eta_T^{(\mathbf{z})} + I_{N-1} \otimes DH_2(\mathbf{y}_0,\mathbf{x}_0)\eta_T^{(\mathbf{w})} \Big].
\end{aligned} \tag{B.16}$$

Here $\bar{U}_2^{[2]}$ is a real symmetric matrix of order $N-1$. Let $V_2^{[2]}$ be the matrix of orthogonal eigenvectors and $\{\nu_1, \nu_2, \ldots, \nu_{N-1}\}$ be the set of eigenvalues of the matrix $\bar{U}_2^{[2]}$. Then ${V_2^{[2]}}^{-1}\bar{U}_2^{[2]}V_2^{[2]} = \text{diag}\{\nu_1, \nu_2, \ldots, \nu_{\text{N}-1}\}$.

Again, projecting the transverse error components on the eigenspace of $\bar{U}_2^{[2]}$, we have the further projected components $\zeta_T^{(\mathbf{w})} = \left(V_2^{[2]} \otimes I_d\right)^{-1}\eta_T^{(\mathbf{w})}$ and $\zeta_T^{(\mathbf{z})} = \left(V_2^{[2]} \otimes I_d\right)^{-1}\eta_T^{(\mathbf{z})}$. This transformation yields our required block-diagonal transverse error system as

(B.17)

$$\begin{aligned}
\dot{\zeta}_{T_i}^{(\mathbf{w})} &= JF_1(\mathbf{x}_0)\zeta_{T_i}^{(\mathbf{w})} + \sum_{\alpha=1}^{2}\epsilon_\alpha d^{[\alpha]}\Big[JG_\alpha^{[1]}(\mathbf{x}_0,\mathbf{x}_0) + DG_\alpha^{[1]}(\mathbf{x}_0,\mathbf{x}_0)\Big]\zeta_{T_i}^{(\mathbf{w})} \\
&\quad - \Big[\epsilon_1\bar{a}DG_1^{[1]}(\mathbf{x}_0,\mathbf{x}_0) + \epsilon_2\nu_i DG_2^{[1]}(\mathbf{x}_0,\mathbf{x}_0)\Big]\zeta_{T_i}^{(\mathbf{w})} + \lambda\Big[JH_1(\mathbf{x}_0,\mathbf{y}_0)\zeta_{T_i}^{(\mathbf{w})} + DH_1(\mathbf{x}_0,\mathbf{y}_0)\zeta_{T_i}^{(\mathbf{z})}\Big], \\
\dot{\zeta}_{T_i}^{(\mathbf{z})} &= JF_2(\mathbf{y}_0)\zeta_{T_i}^{(\mathbf{z})} + \sum_{\alpha=1}^{2}\epsilon_\alpha d^{[\alpha]}\Big[JG_\alpha^{[2]}(\mathbf{y}_0,\mathbf{y}_0) + DG_\alpha^{[2]}(\mathbf{y}_0,\mathbf{y}_0)\Big]\zeta_{T_i}^{(\mathbf{z})} \\
&\quad - \Big[\epsilon_1\bar{a}DG_1^{[2]}(\mathbf{y}_0,\mathbf{y}_0) + \epsilon_2\nu_i DG_2^{[2]}(\mathbf{y}_0,\mathbf{y}_0)\Big]\zeta_{T_i}^{(\mathbf{z})} + \lambda\Big[JH_2(\mathbf{y}_0,\mathbf{x}_0)\zeta_{T_i}^{(\mathbf{z})} + DH_2(\mathbf{y}_0,\mathbf{x}_0)\zeta_{T_i}^{(\mathbf{w})}\Big],
\end{aligned}$$

where $i = 1, 2, \ldots, N-1$. ■

The possible applications of the above corollary are similar to Remarks 4.5 and 4.6.

REFERENCES

[1] N. Abaid and M. Porfiri, *Fish in a ring: Spatio-temporal pattern formation in one-dimensional animal groups*, J. R. Soc. Interface, 7 (2010), pp. 1441–1453, https://doi.org/10.1098/rsif.2010.0175.

[2] B. M. Adhikari, A. Prasad, and M. Dhamala, *Time-delay-induced phase-transition to synchrony in coupled bursting neurons*, Chaos, 21 (2011), 023116, https://doi.org/10.1063/1.3584822.

[3] R. Albert and A. L. Barabási, *Statistical mechanics of complex networks*, Rev. Modern Phys., 74 (2002), pp. 47–94, https://doi.org/10.1103/RevModPhys.74.47.

[4] M. S. Baptista, F. M. Moukam Kakmeni, and C. Grebogi, *Combined effect of chemical and electrical synapses in Hindmarsh-Rose neural networks on synchronization and the rate of information*, Phys. Rev. E (3), 82 (2010), 036203, https://doi.org/10.1103/PhysRevE.82.036203.

[5] I. Belykh, D. Carter, and R. Jeter, *Synchronization in multilayer networks: When good links go bad*, SIAM J. Appl. Dyn. Syst., 18 (2019), pp. 2267–2302, https://doi.org/10.1137/19M1257123.

[6] I. V. Belykh, V. N. Belykh, and M. Hasler, *Blinking model and synchronization in small-world networks with a time-varying coupling*, Phys. D, 195 (2004), pp. 188–206, https://doi.org/10.1016/j.physd.2004.03.013.

[7] V. N. Belykh, I. V. Belykh, and M. Hasler, *Connection graph stability method for synchronized coupled chaotic systems*, Phys. D, 195 (2004), pp. 159–187, https://doi.org/10.1016/j.physd.2004.03.012.

[8] G. Bianconi and S. N. Dorogovtsev, *Multiple percolation transitions in a configuration model of a network of networks*, Phys. Rev. E (3), 89 (2014), 062814, https://doi.org/10.1103/PhysRevE.89.062814.

[9] K. A. Blaha, K. Huang, F. Della Rossa, L. Pecora, M. Hossein-Zadeh, and F. Sorrentino, *Cluster synchronization in multilayer networks: A fully analog experiment with LC oscillators with physically dissimilar coupling*, Phys. Rev. Lett., 122 (2019), 014101, https://doi.org/10.1103/PhysRevLett.122.014101.

[10] S. Boccaletti, G. Bianconi, R. Criado, C. I. D. Genio, J. Gómez-Gardeñes, M. Romance, I. Sendiña Nadal, Z. Wang, and M. Zanin, *The structure and dynamics of multilayer networks*, Phys. Rep., 544 (2014), pp. 1–122, https://doi.org/10.1016/j.physrep.2014.07.001.

[11] S. Boccaletti, V. Latora, Y. Moreno, M. Chavez, and D.-U. Hwang, *Complex networks: Structure and dynamics*, Phys. Rep., 424 (2006), pp. 175–308, https://doi.org/10.1016/j.physrep.2005.10.009.

[12] S. V. Buldyrev, R. Parshani, G. Paul, H. E. Stanley, and S. Havlin, *Catastrophic cascade of failures in interdependent networks*, Nature, 464 (2010), pp. 1025–1028, https://doi.org/10.1038/nature08932.

[13] C. Buono, L. G. Alvarez-Zuzek, P. A. Macri, and L. A. Braunstein, *Epidemics in partially overlapped multiplex networks*, PLOS ONE, 9 (2014), e92200, https://doi.org/10.1371/journal.pone.0092200.

[14] A. Cardillo, J. Gómez-Gardeñes, M. Zanin, M. Romance, D. Papo, F. del Pozo, and S. Boccaletti, *Emergence of network features from multiplexity*, Sci. Rep., 3 (2013), 1344, https://doi.org/10.1038/srep01344.

[15] A. Cardillo, M. Zanin, J. Gómez-Gardeñes, M. Romance, A. García del Amo, and S. Boccaletti, *Modeling the multi-layer nature of the European air transport network: Resilience and passengers re-scheduling under random failures*, Eur. Phys. J. Spec. Top., 215 (2013), pp. 23–33, https://doi.org/10.1140/epjst/e2013-01712-8.

[16] R. Criado, M. Romance, and M. Vela-Pérez, *Hyperstructures, a new approach to complex systems*, Internat. J. Bifur. Chaos Appl. Sci. Engrg., 20 (2010), pp. 877–883, https://doi.org/10.1142/S0218127410026162.

[17] L. V. Gambuzza, M. Frasca, and J. Gómez-Gardeñes, *Intra-layer synchronization in multiplex networks*, Europhys. Lett., 110 (2015), 20010, https://doi.org/10.1209/0295-5075/110/20010.

[18] O. Golovneva, R. Jeter, I. Belykh, and M. Porfiri, *Windows of opportunity for synchronization in stochastically coupled maps*, Phys. D, 340 (2017), pp. 1–13, https://doi.org/10.1016/j.physd.2016.08.005.

[19] G. H. Golub and C. F. Van Loan, *Matrix Computations*, Johns Hopkins University Press, Baltimore, London, 1996.

[20] S. Gómez, A. Díaz-Guilera, J. Gómez-Gardeñes, C. J. Pérez-Vicente, Y. Moreno, and A. Arenas, *Diffusion dynamics on multiplex networks*, Phys. Rev. Lett., 110 (2013), 028701, https://doi.org/10.1103/PhysRevLett.110.028701.

[21] C. Granell, S. Gómez, and A. Arenas, *Dynamical interplay between awareness and epidemic spreading in multiplex networks*, Phys. Rev. Lett., 111 (2013), 128701, https://doi.org/10.1103/PhysRevLett.111.128701.

[22] M. Hasler, V. Belykh, and I. Belykh, *Dynamics of stochastically blinking systems. Part* I: *Finite time properties*, SIAM J. Appl. Dyn. Syst., 12 (2013), pp. 1007–1030, https://doi.org/10.1137/120893409.

[23] M. Hasler, V. Belykh, and I. Belykh, *Dynamics of stochastically blinking systems. Part* II: *Asymptotic properties*, SIAM J. Appl. Dyn. Syst., 12 (2013), pp. 1031–1084, https://doi.org/10.1137/120893410.

[24] J. F. Heagy, L. M. Pecora, and T. L. Carroll, *Short wavelength bifurcations and size instabilities in coupled oscillator systems*, Phys. Rev. Lett., 74 (1995), pp. 4185–4188, https://doi.org/10.1103/PhysRevLett.74.4185.

[25] P. Holme and J. Saramäki, *Temporal networks*, Phys. Rep., 519 (2012), pp. 97–125, https://doi.org/10.1016/j.physrep.2012.03.001.

[26] D. Irving and F. Sorrentino, *Synchronization of dynamical hypernetworks: Dimensionality reduction through simultaneous block-diagonalization of matrices*, Phys. Rev. E (3), 86 (2012), 056102, https://doi.org/10.1103/PhysRevE.86.056102.

[27] E. M. Izhikevich, *The Dynamical Systems in Neuroscience: Geometry of Excitability and Bursting*, MIT Press, Cambridge, MA, 2007.

[28] R. Jeter and I. Belykh, *Synchronization in on-off stochastic networks: Windows of opportunity*, IEEE Trans. Circuits Syst. I, Reg. Papers, 62 (2015), pp. 1260–1269, https://doi.org/10.1109/TCSI.2015.2415172.

[29] M. Kivelä, A. Arenas, M. Barthelemy, J. P. Gleeson, Y. Moreno, and M. A. Porter, *Multilayer networks*, J. Complex Netw., 2 (2014), pp. 203–271, https://doi.org/10.1093/comnet/cnu016.

[30] M. Kurant and P. Thiran, *Layered complex networks*, Phys. Rev. Lett., 96 (2006), 138701, https://doi.org/10.1103/PhysRevLett.96.138701.

[31] P. J. Mucha, T. Richardson, K. Macon, M. A. Porter, and J. P. Onnela, *Community structure*

in time-dependent, multiscale, and multiplex networks, Science, 328 (2010), pp. 876–878, https://doi.org/10.1126/science.1184819.

[32] J. P. Onnela, J. Saramäki, J. Hyvönen, G. Szabo, D. Lazer, K. Kaski, J. Kertész, and A. L. Barabási, *Structure and tie strengths in mobile communication networks*, Proc. Natl. Acad. Sci. USA, 104 (2007), pp. 7332–7336, https://doi.org/10.1073/pnas.0610245104.

[33] B. L. Partridge and T. J. Pitcher, *The sensory basis of fish schools: Relative roles of lateral line and vision*, J. Comp. Physiol., 135 (1980), pp. 315–325.

[34] R. Pastor-Satorras and A. Vespignani, *Evolution and Structure of the Internet: A Statistical Physics Approach*, Cambridge University Press, Cambridge, UK, 2004.

[35] L. Pecora, T. Carroll, G. Johnson, D. Mar, and K. S. Fink, *Synchronization stability in coupled oscillator arrays: Solution for arbitrary configurations*, Internat. J. Bifur. Chaos Appl. Sci. Engrg., 10 (2000), pp. 273–290, https://doi.org/10.1142/S0218127400000189.

[36] L. M. Pecora and T. L. Carroll, *Master stability functions for synchronized coupled systems*, Phys. Rev. Lett., 80 (1998), pp. 2109–2112, https://doi.org/10.1103/PhysRevLett.80.2109.

[37] M. Porfiri and I. Belykh, *Memory matters in synchronization of stochastically coupled maps*, SIAM J. Appl. Dyn. Syst., 16 (2017), pp. 1372–1396, https://doi.org/10.1137/17M111136X.

[38] M. Porfiri and F. Fiorilli, *Global pulse synchronization of chaotic oscillators through fast-switching: Theory and experiments*, Chaos Solitons Fractals, 41 (2009), pp. 245–262, https://doi.org/10.1016/j.chaos.2007.11.033.

[39] M. Porfiri and R. Pigliacampo, *Master-slave global stochastic synchronization of chaotic oscillators*, SIAM J. Appl. Dyn. Syst., 7 (2008), pp. 825–842, https://doi.org/10.1137/070688973.

[40] M. Porfiri, D. J. Stilwell, and E. M. Bollt, *Synchronization in random weighted directed networks*, IEEE Trans. Circuits Syst. I, Reg. Papers, 55 (2008), pp. 3170–3177, https://doi.org/10.1109/TCSI.2008.925357.

[41] M. Porfiri, D. J. Stilwell, E. M. Bollt, and J. D. Skufca, *Random talk: Random walk and synchronizability in a moving neighborhood network*, Phys. D, 224 (2006), pp. 102–113, https://doi.org/10.1016/j.physd.2006.09.016.

[42] S. Rakshit, B. K. Bera, and D. Ghosh, *Synchronization in a temporal multiplex neuronal hypernetwork*, Phys. Rev. E (3), 98 (2018), 032305, https://doi.org/10.1103/PhysRevE.98.032305.

[43] S. Rakshit, B. K. Bera, D. Ghosh, and S. Sinha, *Emergence of synchronization and regularity in firing patterns in time-varying neural hypernetworks*, Phys. Rev. E (3), 97 (2018), 052304, https://doi.org/10.1103/PhysRevE.97.052304.

[44] S. Rakshit, S. Majhi, B. K. Bera, S. Sinha, and D. Ghosh, *Time-varying multiplex network: Intralayer and interlayer synchronization*, Phys. Rev. E (3), 96 (2017), 062308, https://doi.org/10.1103/PhysRevE.96.062308.

[45] D. G. Roberson and D. J. Stilwell, *Control of an autonomous underwater vehicle platoon with a switched communication network*, in Proceedings of the American Control Conference, 2005, pp. 4333–4338, https://doi.org/10.1109/ACC.2005.1470661.

[46] J. Sanz, C. Y. Xia, S. Meloni, and Y. Moreno, *Dynamics of interacting diseases*, Phys. Rev. X, 4 (2014), 041005, https://doi.org/10.1103/PhysRevX.4.041005.

[47] A. Saumell-Mendiola, M. A. Serrano, and M. Boguñá, *Epidemic spreading on interconnected networks*, Phys. Rev. E (3), 86 (2012), 026106, https://doi.org/10.1103/PhysRevE.86.026106.

[48] R. Sevilla-Escoboza, I. Sendiña Nadal, I. Leyva, R. Gutiérrez, J. M. Buldú, and S. Boccaletti, *Inter-layer synchronization in multiplex networks of identical layers*, Chaos, 26 (2016), 065304, https://doi.org/10.1063/1.4952967.

[49] J. D. Skufca and E. M. Bollt, *Communication and synchronization in disconnected networks with dynamic topology: Moving neighborhood networks*, Math. Biosci. Eng., 1 (2004), pp. 347–359, https://doi.org/10.3934/mbe.2004.1.347.

[50] F. Sorrentino, *Synchronization of hypernetworks of coupled dynamical systems*, New J. Phys., 14 (2012), 033035, https://doi.org/10.1088/1367-2630/14/3/033035.

[51] F. Sorrentino and E. Ott, *Network synchronization of groups*, Phys. Rev. E (3), 76 (2007), 056114, https://doi.org/10.1103/PhysRevE.76.056114.

[52] D. J. Stilwell, E. M. Bollt, and D. G. Roberson, *Sufficient conditions for fast switching synchronization in time-varying network topologies*, SIAM J. Appl. Dyn. Syst., 5 (2006), pp. 140–156,

https://doi.org/10.1137/050625229.

[53] J. Sun, E. M. Bollt, and T. Nishikawa, *Master stability functions for coupled nearly identical dynamical systems*, Europhys. Lett., 85 (2009), 60011, https://doi.org/10.1209/0295-5075/85/60011.

[54] M. Szell, R. Lambiotte, and S. Thurner, *Multirelational organization of large-scale social networks in an online world*, Proc. Natl. Acad. Sci. USA, 107 (2010), pp. 13636–13641, https://doi.org/10.1073/pnas.1004008107.

[55] Z. Wang, A. Szolnoki, and M. Perc, *Rewarding evolutionary fitness with links between populations promotes cooperation*, J. Theoret. Biol., 349 (2014), pp. 50–56, https://doi.org/10.1016/j.jtbi.2014.01.037.

[56] S. Wasserman and K. Faust, *Social Network Analysis: Methods and Applications*, Cambridge University Press, Cambridge, UK, 1994.

[57] D. J. Watts and S. H. Strogatz, *Collective dynamics of "small-world" networks*, Nature, 393 (1998), pp. 440–442, https://doi.org/10.1038/30918.